The NreABC system of *Staphylococcus carnosus* combines nitrate and oxygen sensing by an NreA/NreB sensor complex

Dissertation
Zur Erlangung des Grades
Doktor der Naturwissenschaften

Am Fachbereich Biologie
Der Johannes Gutenberg-Universität Mainz

Stephanie Nilkens
geb. am 24.06.1986 in El Paso, Texas

Mainz, September 2013

Dekan:

1. Berichterstatter:

2. Berichterstatter:

Tag der mündlichen Prüfung:

Content

1. Abstract

Staphylococcus carnosus is a facultative anaerobic bacterium which features the cytoplasmic NreABC system. It is necessary for regulation of nitrate respiration and the nitrate reductase gene *narG* in response to oxygen and nitrate availability. NreB is a sensor kinase of a two-component system and represents the oxygen sensor of the system. It binds an oxygen labile $[4Fe\text{-}4S]^{2+}$ cluster under anaerobic conditions. NreB autophosphorylates and phosphoryl transfer activates the response regulator NreC which induces *narG* expression. The third component of the Nre system is the nitrate receptor NreA. In this study the role of the nitrate receptor protein NreA in nitrate regulation and its functional and physiological effect on oxygen regulation and interaction with the NreBC two-component system were detected.

In vivo, a reporter gene assay for measuring expression of the NreABC regulated nitrate reductase gene *narG* was used for quantitative evaluation of NreA function. Maximal *narG* expression in wild type *S. carnosus* required anaerobic conditions and the presence of nitrate. Deletion of *nreA* allowed expression of *narG* under aerobic conditions, and under anaerobic conditions nitrate was no longer required for maximal induction. This indicates that NreA is a nitrate regulated inhibitor of *narG* expression. Purified NreA and variant NreA(Y95A) inhibited the autophosphorylation of anaerobic NreB in part and completely, respectively. Neither NreA nor NreA(Y95A) stimulated dephosphorylation of NreB-phosphate, however. Inhibition of phosphorylation was relieved completely when NreA with bound nitrate (NreA·$[NO_3^-]$) was used. The same effects of NreA were monitored with aerobically isolated Fe-S-less NreB, which indicates that NreA does not have an influence on the iron-sulfur cluster of NreB. In summary, the data of this study show that NreA interacts with the oxygen sensor NreB and controls its phosphorylation level in a nitrate dependent manner. This modulation of NreB-function by nitrate and NreA results in nitrate/oxygen co-sensing by an NreA/NreB sensory unit. It transmits the regulatory signal from O_2 and nitrate in a joint signal to target promoters. Therefore, nitrate and oxygen regulation of nitrate dissimilation follows a new mode of regulation not present in other facultative anaerobic bacteria.

2. Introduction

2.1 Oxygen sensing in bacteria

Facultative anaerobic bacteria, like the gram positive bacterium *Staphylococcus carnosus*, are capable of growing under aerobic and under anaerobic conditions. Energy conservation by oxygen respiration presents the pathway of highest adenosine triphosphate (ATP) production because oxygen has a high reduction potential of E_0' 820 mV. In the electron transport chain oxygen presents the terminal electron acceptor. Oxygen regulates a wide range of energy metabolisms and presents one of the most important signal molecules. When the oxygen concentration in the medium is depleted, the microorganisms switch to anaerobic respiration. Molecules like nitrate (E_0' 420 mV) serve as alternative electron acceptors in the anaerobic respiration. When there are no exogenous electron acceptors present then the metabolism is adjusted to energy conservation by fermentation, an oxidation of endogenous, organic compounds that generates ATP by the process of substrate-level phosphorylation.

To detect the oxygen availability in the medium, bacteria possess oxygen sensors. These sensors are often part of two-component systems. They control the activity of associated response regulators for the regulation of target genes. The sensor of a two-component system is a histidine kinase that senses a specific environmental stimulus via its sensor domain (Stock *et al*., 2000; Mascher *et al*., 2006). Two-component systems with direct oxygen sensors control the expression of genes in response to the actual oxygen concentration. Cofactors of the sensor domains which are used for the reaction with oxygen are, for example, HemeB or $[4Fe\text{-}4S]^{2+}$ (Unden *et al*., 1995; Green and Paget 2004). The presence of oxygen leads to binding of O_2 or oxidation and disintegration of the cofactor. Indirect sensors respond to components of the respiratory chain, like the redox state of the quinones (Georgellis *et al*., 2001), or cytoplasmic factors like $NADH/NAD^+$ (McLaughlin *et al*., 2010; Green and Paget, 2004).

Signal transduction from the sensor occurs by transfer of a phosphoryl group to the response regulator. Phosphorylation causes a conformational change of the response regulator (Birck *et al*., 1999; Gao *et al*., 2006), usually activating its function as a transcription factor, stimulating or repressing the expression of target

genes. Two-component systems enable the bacteria to sense, respond, and adapt to a wide range of environmental conditions.

2.2 *Staphylococcus carnosus*

The apathogenic microorganism *Staphylococcus carnosus* was used in this study for research on the two-component system NreBC. It is a coagulase-negative (Zell *et al*., 2008), gram positive bacterium and belongs to the phylum of Firmicutes. *S. carnosus* consists of single and paired cocci and has the highest GC content of 36.4 % of all sequenced staphylococcal species (Rosenstein *et al*., 2009). *S. carnosus* is used as a food grade bacterium: Because of its ability to reduce nitrate to nitrite it is used as a starter culture in the industrial production of raw fermented sausages and dry cured ham (Neubauer and Götz, 1996). The reaction of nitrite with myoglobin, which contains heme as prosthetic group, produces nitrosomyoglobin. It is responsible for the bright red color of the meat (Hammes, 2012).

S. carnosus features the two-component system NreBC. It is composed of the direct oxygen sensor NreB (Müllner *et al*., 2008) and response regulator NreC. In the absence of oxygen this system regulates the expression of genes for anaerobic nitrate respiration (Fedtke *et al*., 2002).

2.3 Nitrate respiration of *Staphylococcus carnosus*

Under aerobic conditions *Staphylococcus carnosus* grows by aerobic respiration, using O_2 as terminal electron acceptor in the electron transport chain. Under anaerobic conditions *S. carnosus* is able to switch to nitrate respiration using NO_3^- as an alternative electron acceptor and nitrate is reduced to ammonium with nitrite as an intermediate (Fig. 1). In the first step nitrate is transported into the cell by the nitrate transporter NarT (*narT* gene) and is then reduced to nitrite by the membrane bound, dissimilatory nitrate reductase of the NarG type (*narGHJI* genes). This contributes to the formation of a proton motive force for respiratory energy conservation. It has been shown for *S. aureus* that electron transfer to the nitrate reductase is performed by menaquinone (Sasarman *et al*., 1974). After nitrate reduction nitrite is transported out of the cell. Nitrite reduction is inhibited by nitrate and only when all nitrate is reduced to nitrite, then nitrite is transported back into the cell and is reduced to ammonium (Neubauer and Götz, 1996). Nitrite reduction is performed by the cytoplasmic, NADH-dependent nitrite reductase (*nirRBDsirAB*

genes) (Neubauer and Götz, 1996; Fedtke *et al*., 2002; Schlag *et al*., 2008). Anaerobic conditions and the presence of nitrate lead to a full induction of nitrate respiration (Fedtke *et al*., 2002).

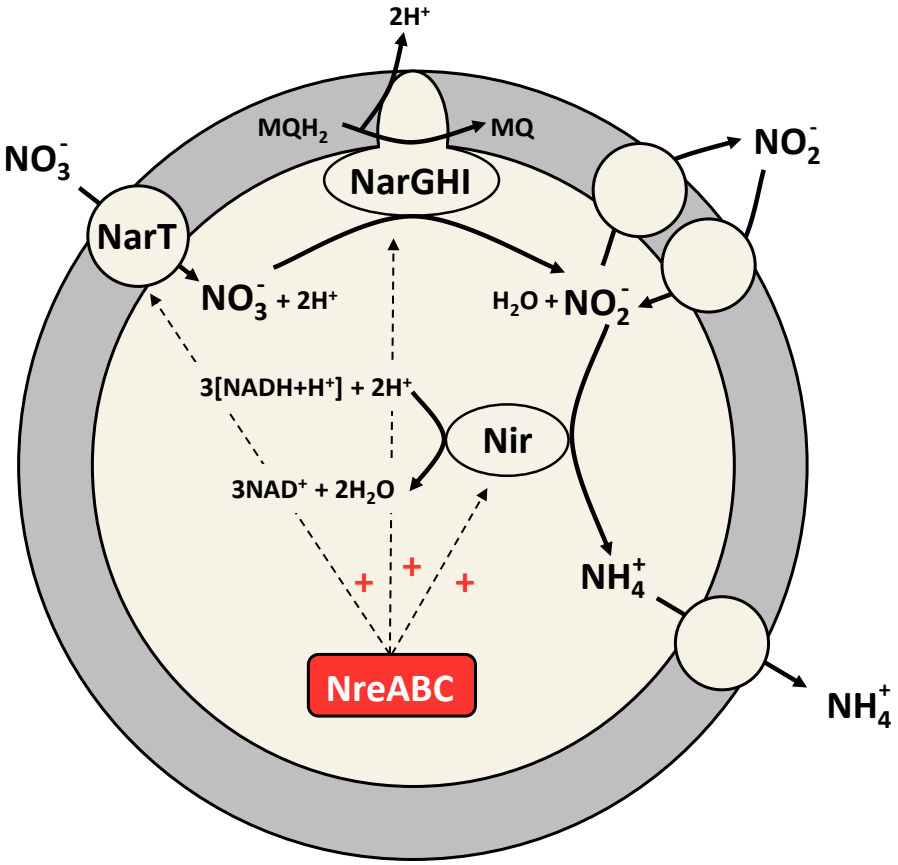

Figure 1: Nitrate respiration in *Staphylococcus carnosus.* In the absence of oxygen nitrate is transported into the cell by the nitrate transporter NarT. Nitrate is reduced to nitrite by the membrane bound, dissimilatory nitrate reductase NarGHI which plays a role in energy conservation. It contributes to the formation of a proton motive force by oxidation of menachinol (MQH_2) and reduction of nitrate by transfer of two electrons. Two protons from menachinol are transferred into the periplasm and two protons from the cytoplasm and O^{2-} (from nitrate) form H_2O. Nitrite is transported out of the cell. When all nitrate is reduced to nitrite then nitrite is transported back into the cell and is reduced to ammonium by the cytosolic nitrite reductase NirBD which is involved in NADH reoxidation. The genes for nitrate respiration *narGHJI*, *nirRBD, sirAB,* and *narT* stand under the transcriptional control of NreABC.

The nitrate reductase of *S. carnosus* is encoded in the *narGHJI* operon which lies downstream of the genes for the nitrate reductase (*nirRBDsirAB*) and upstream of the *nreABC*-operon and the *narT* gene. It consists of three subunits. Sequence alignments of *narGHJI* showed similarities to genes of the dissimilatory nitrate reductases of *B. subtilis* and *E. coli*, as described by Pantel *et al*., 1998. The nitrate reductase of *S. carnosus* consists of three subunits NarGHI. The α-subunit NarG

(138.4 kDa) consists of five conserved regions which feature properties of molybdenum cofactor binding sites (Blasco *et al*., 1990). The NarH subdomain (59.9 kDa) of *S. carnosus* is similar to the β-subdomain in *E. coli* which is responsible for electron transfer between NarG and NarI (Blasco *et al*., 1989). NarH of *S. carnosus* features an array of cysteine residues, typical for the binding of an Fe-S cluster (Pantel *et al*., 1998). NarJ (22.6 kDa) only has a small similarity to the proteins from *E*. *coli* and *B*. *subtilis* but is still essential. In *E. coli* and *B. subtilis* it is necessary for assembly of the protein (Blasco *et al*., 1992). NarI presents the γ-subunit. Structure predictions indicate a membrane protein with five transmembrane segments. It is supposed that NarI anchors the α- and β-subunits in the membrane (Pantel *et al*., 1998).

Studies on the regulation of *narGHJI* were performed. An expression of *narGHJI* is strongly reduced in an *nreABC* deletion strain of *S. carnosus*, even under aerobic conditions in the presence of nitrate. It was shown that the expression of the nitrate reductase NarGHI is regulated by the NreBC two-component system (Fedtke *et al*., 2002).

2.4 The NreBC two-component system

In *Staphylococcus carnosus* regulation of nitrate respiration by oxygen is effected by the NreBC two-component system (Kamps *et al.,* 2004; Fedtke *et al.,* 2002). NreB is the sensor histidine kinase of the system and possesses an N-terminal PAS domain with four conserved cysteine residues (C59, C62, C74, and C77) (Unden *et al*., 2013). PAS domains are present in many eukaryotic and prokaryotic sensor proteins. They feature sensory functions and are named after proteins where the structure was initially discovered: Per (periodic clock protein of *Drosophila*), Arnt (acryl hydrocarbon receptor nuclear translocator, vertebrates), and Sim (single-minded protein, *Drosophila*) (Zhulin *et al*., 1997; Ponting and Aravind, 1997). PAS domains function as input modules for stimuli like oxygen, redox potential, and light (Taylor *et al*., 1999). The cytoplasmic sensor kinase NreB is a direct O_2 sensor and uses the oxygen labile $[4Fe\text{-}4S]^{2+}$ cluster which is coordinated by the cysteine residues of the PAS domain for O_2 sensing and controlling kinase activity (Müllner *et al*., 2008; Reinhart *et al*., 2010).

The C-terminus of NreB features a kinase domain with a conserved histidine residue (H159). Under anoxic conditions NreB binds a $[4Fe\text{-}4S]^{2+}$ cluster and the pro-

tein is then in the active state with high autophosphorylation activity. In the presence of oxygen the $[4Fe\text{-}4S]^{2+}$ cluster is degraded to a $[2Fe\text{-}2S]^{2+}$ cluster and the kinase activity of NreB is reduced. Further oxygen exposure leads to the formation of apo-NreB (Müllner *et al*., 2008).

When NreB is in its $[4Fe\text{-}4S]^{2+}$ containing active state then NreB autophosphorylates and the phosphoryl group is transferred from the conserved histidine residue (H159) of NreB to the conserved aspartate residue (D53) of the response regulator NreC. Like other DNA binding proteins, the response regulator NreC presents a helix-turn-helix motif in the transmitter domain (Fedtke *et al*., 2002). Phosphorylated NreC (NreC-P) is activated and binds to the DNA as a transcription factor and stimulates the expression of genes for nitrate respiration. It binds to GC-rich palindromic consensus sequences of the promoters of its target genes. Binding sites for NreC are present in the promoter of the *narGHJI* operon and *narT* gene in the -35 region and in the -60 to -70 regions. In the *nir* promoter, the sequence motif is found upstream in the -90 region. An additional, different palindromic sequence was found in the -35 region of *nir* which indicates that another transcription factor is involved in the expression of the nitrite reductase (Fedtke *et al*., 2002). The *nreABC* promoter of *S. aureus* resembles a typical σ^A promoter (Schlag *et al*., 2008). However, it has been shown that the regulator AirR (anaerobic iron-sulfur cluster-containing redox regulator) binds to the promoter of the *nreABC*-operon (Yan *et al*., 2011). AirR is part of the AirSR two-component system of *S. aureus* and the sensor AirS senses the oxygen and redox state of the cell via [2Fe-2S] cluster, which binds at a GAF domain of the protein (Sun *et al*., 2012). Expression of AirSR is enhanced in the presence of nitrate under anaerobic conditions. Also gel shifts showed binding of AirR to the promoter of *narG*. Therefore, AirSR presents an additional system for regulation of *narG* expression in *S. aureus* (Yan *et al*., 2011). AirSR is a key regulator that affects transcription of more than 350 genes under anaerobic conditions (Sun *et al*., 2011). A homolog system is present in *S. carnosus*.

An additional protein encoded in the *nreABC*-operon is NreA. The function of the protein was unknown, but it was believed to play a role in nitrate regulation (Fedtke *et al*., 2002). It was subject of this study to identify the function of NreA and its effect on *narGHJI* expression and interaction with the NreBC two-component system (Figure 2).

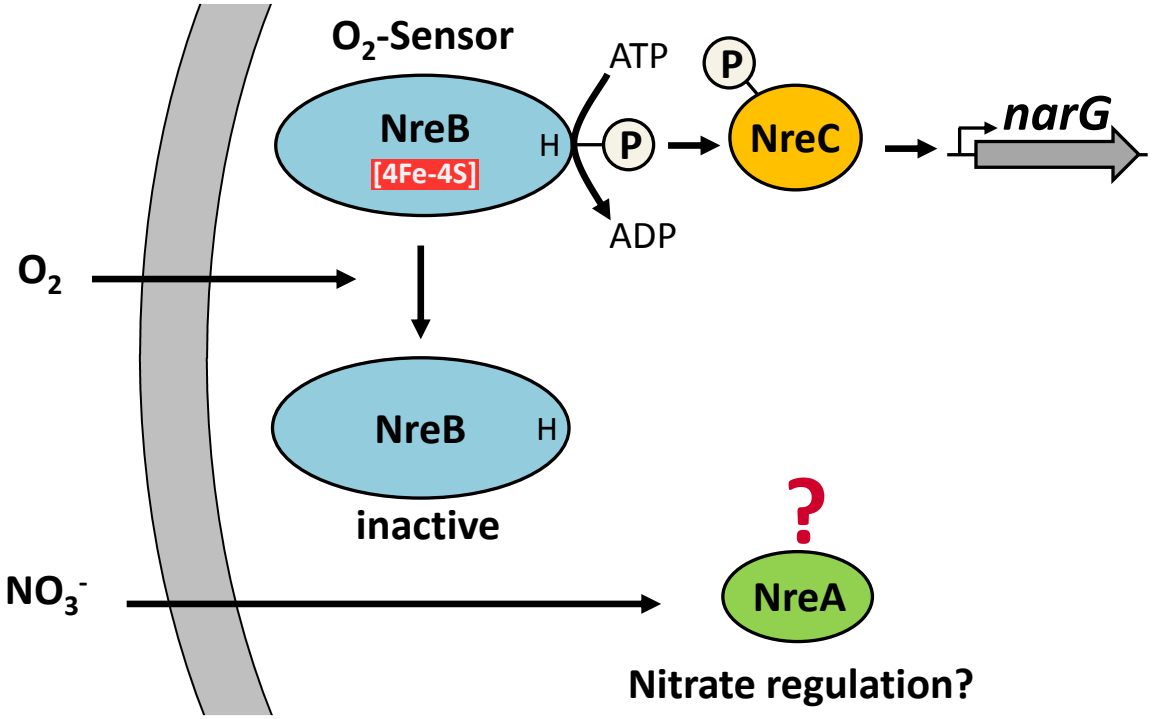

Figure 2: Model for oxygen and nitrate sensing in *Staphylococcus carnosus*. Under anaerobic conditions the oxygen sensor NreB binds a $[4Fe\text{-}4S]^{2+}$ cluster at the N-terminal sensory PAS domain. This leads to a high autophosphorylation activity of the C-terminal kinase domain. The phosphate is transferred to the response regulator NreC at a conserved aspartate residue and activated NreC-P controls genes for nitrate respiration (*narGHJI*, *narT*, *nirRBD*, and *sirAB*). The third component of the system is NreA. The structure of NreA was solved by Niemann *et al*., 2013 and revealed a GAF domain protein which binds nitrate. This suggested that NreA plays a role in nitrate regulation. The function of NreA and interaction with the NreBC system were tested in this study.

2.5 NreA, a GAF domain protein

The crystal structure of NreA has been solved recently (Niemann *et al*., 2013). It shows that NreA is a small cytoplasmic GAF domain protein. GAF domains define a large protein family and are named after some proteins where they have originally been identified: cGMP-specific phosphodiesterases, adenylyl cyclases, and FhlA (Aravind and Ponting, 1997). GAF domains are involved in signal transduction pathways and signaling is commonly performed by binding of small, regulatory molecules (Anantharaman *et al*., 2001; Ho *et al*., 2000; Martinez *et al*., 2002; Schultz *et al*., 1998; Zoraghi *et al*., 2004). The NreA crystal structure revealed that the protein binds one molecule of nitrate at the binding site of the GAF domain. *In vivo* the function was seriously affected by mutations at the nitrate binding site. This suggests that NreA is directly involved in nitrate dependent regulation (Nie-

mann *et al*., 2013). NreA is a new type of nitrate receptor using a GAF domain for nitrate perception.

NreA shows no resemblance to nitrate receptors or sensors from other bacteria as, for example, to the periplasmic nitrate binding protein NrtA from *Synechocystis sp*. (Koropatkin *et al*., 2006), the cytoplasmic RNA binding protein and translational regulator NasR (Boudes *et al*., 2012), or the membrane bound sensor kinase NarX of proteobacteria (Williams and Stewart, 1997; Cheung and Hendrickson, 2009). Additionally, these types of nitrate receptors or sensors are not encoded in the genome of *S. carnosus*. This and the physiological effect of *nreA* deletion indicated that NreA is responsible for nitrate sensing and regulation (Schlag, 2008).

2.6 Oxygen and nitrate regulated *narGHJI* expression in *E. coli*

Escherichia coli features the NarXL system for nitrate regulation and the FNR system for oxygen regulation (Fig. 3). NarXL presents a classical two-component system with the membrane bound sensor NarX and the cytoplasmic regulator NarL, whereas FNR is a one-component system that combines the sensor and regulator in one protein.

The oxygen sensor FNR of *E. coli* is a global regulator which mediates the transfer from aerobic to anaerobic metabolism on a transcriptional level (Green *et al*., 1991; Green and Guest, 1993; Unden and Schirawski, 1997; Kiley and Beinert 1998). Under anaerobic conditions FNR is in its active state and carries a [4Fe-4S]$^{2+}$ cluster via four conserved cysteine residues (C20, C23, C29, and C122) (Melville and Gunsalus, 1990; Six *et al*., 1996). In the presence of oxygen, FNR is inactivated by oxidation of the [4Fe-4S]$^{2+}$ to a [2Fe-2S]$^{2+}$ cluster (Jordan *et al*., 1997; Khoroshilova *et al*., 1997). Further oxygen exposure leads to a loss of the [2Fe-2S]$^{2+}$ cluster and monomeric apo-FNR is formed (Unden and Schirawski, 1997). The binding of the [4Fe-4S]$^{2+}$ cluster under anaerobic conditions leads to a dimerization of the FNR proteins (Green *et al*., 1996; Melville and Gunsalus, 1996; Lazazzera *et al*., 1996). In comparison to monomeric apo-FNR the dimer shows high sequence specific DNA-binding (Lazazzaera *et al*., 1996). In its active form FNR activates genes for anaerobic growth, like the nitrate reductase operon *narGHJI* (Lamberg *et al*., 2000) and the NADH-dependent nitrite reductase operon *nirBDC* (Wu *et al*., 1998), and represses genes for aerobic growth (Gunsalus and Park, 1994; Melville and Gunsalus, 1990; Meng *et al*., 1997).

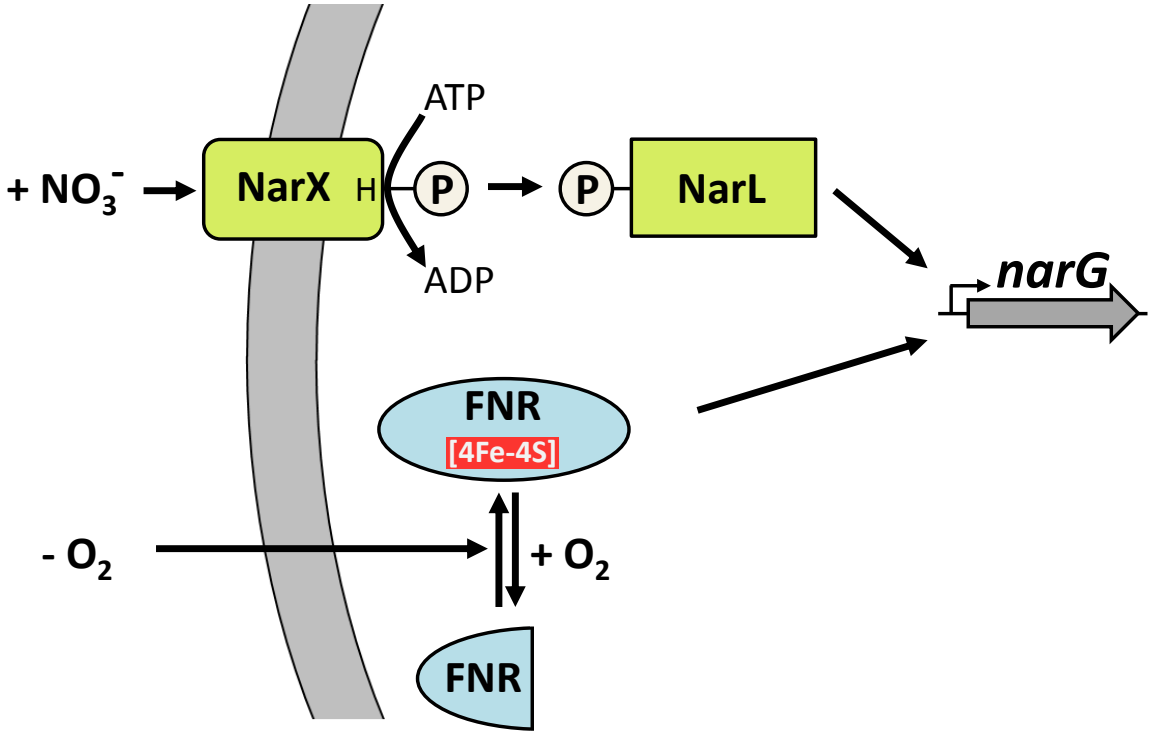

Figure 3: Nitrate and oxygen sensing in *Escherichia coli* for regulation of *narG* expression. Nitrate sensing is performed by the NarXL system. NarX, the membrane bound sensor, detects nitrate in the periplasm. The presence of nitrate leads to autophosphorylation in the cytoplasm and phosphotransfer to the response regulator NarL. Oxygen sensing is performed via FNR. Under anaerobic conditions (- O_2) FNR forms a dimer, binds a $[4Fe\text{-}4S]^{2+}$ cluster and is activated for regulation of *narG*. FNR presents a one-component system and acts as a transcription factor for gene regulation. In the presence of oxygen (+ O_2) FNR is inactivated by degradation of the Fe-S cluster and monomerizes. Binding of the two transcriptional regulators NarL and FNR causes maximal *narGHJI* transcription activation.

The nitrate and nitrite dependent gene expression in *E. coli* is controlled by the regulatory two-component systems NarXL. It consists of the membrane bound sensor NarX and the cytoplasmic response regulator NarL (Stewart, 1982; Rabin and Stewart, 1993; Darwin *et al*., 1996). NarX senses the presence of nitrate and nitrite in the periplasm of the cell (Kalman and Gunsalus, 1989). The signal transduction contains the autophosphorylation of the kinase of NarX in the cytoplasm and a subsequent phosphoryl transfer to the aspartate residue of the response regulator NarL (Schröder *et al*., 1994; Caviccioli *et al*., 1995). Activated NarL-P binds to the promoters of target genes via C-terminal helix-turn-helix-motif, (Baikalov *et al*., 1996) and regulates gene expression by activation or repression.

NarPQ is a homologous system which is also involved in nitrate and nitrite sensing. NarXL and NarPQ control the expression of different genes. NarL, and not NarP, is necessary for the *narGHJI* expression (Darwin *et al*., 1996). Both NarL and NarP activate expression of the *nir*-operon (Browning *et al*., 2000).

The promoter of the nitrate reductase *narGHJI* in *E. coli* features binding sites for regulation by FNR and NarXL. Regulation of gene expression is often performed by a combination of different transcription factors which allows a precise control. Here the presence of oxygen and nitrate in the surrounding environment is sensed by two systems which regulate the expression of one operon. FNR and NarXL present two distinct and independent transcriptional regulators which are both required for maximal induction of the *narGHJI* expression in *E. coli* (Stewart, 1982).

2.7 Lipase *lip* from *Staphylococcus hyicus* as a reporter gene

To identify the function of the three components NreA, NreB, and NreC in *narGHJI* expression, a reporter gene system was established. The contribution of anaerobic conditions and nitrate to the induction of nitrate respiration had not been quantified in detail due to the lack of a suitable reporter gene system. Therefore, the lipase gene *lip* from *Staphylococcus hyicus* was used as a reporter gene in this study to determine the expression of the nitrate reductase *narG*. The lipase gene *lip* was fused to the promoter of *narG* resulting in the plasmid-encoded reporter gene fusion *narG-lip*. Additionally, the plasmid also encoded the *nreABC*-operon, which allowed a mutagenesis on the system. This made it possible to get an insight on the function of the different components of the system.

The lipase gene *lip* from *S. hyicus* codes a pre-pro-protein of 641 amino acids which consists of a signal peptide of 38 amino acids, a pro-peptide of 207 amino acids and the mature lipase of 396 amino acids (van Oort *et al*., 1989). The pro-lipase is secreted by the common secretory pathway of the cells (Drouault *et al*., 2000). This is followed by cleavage of the pro-lipase (86 kDa) by the metalloprotease ShpII in the surrounding medium which leads to the formation of the mature lipase (48 kDa) (Ayora *et al*., 1994). In S. *carnosus*, only the 86 kDa pro-lipase is produced, because it lacks the ShpII protease and the secreted pro-lipase is not further processed. Although the pro-lipase only reaches 50 % of the activity of the mature lipase (van Oort *et al*., 1989), it is still a suitable, convenient reporter in *S. carnosus*.

The biochemical properties of the lipase are well characterized. The lipase shows broad substrate specificity and features lipase activity, high phospholipase A and lysophopholipase activity (van Oort *et al*., 1989) and is not influenced by adverse parameters like oxygen. In this study the chromogenic substrate p-nitrophenyl caprylate was used for the quantification of expression.

2.8 The combination of NreA and NreB as a sensor complex

S. carnosus features the NreBC two-component system which regulates *narG* expression in response to oxygen. Additionally, NreA is also encoded in the *nreABC*-operon. The structural data show that NreA is a nitrate binding GAF domain and it seemed likely that NreA is involved in nitrate sensing and nitrate regulation. There were indications that nitrate regulation is effected by NreA but the data did not give an insight on the function of NreA and the effect of nitrate. Not only has the concentrated organization of the *nre* genes in the *nreABC*-operon, but also the effects of *nreA* deletion on *narG* expression indicated that NreA is closely linked to the NreB-NreC two-component system in function. The aim of this study was to physiologically and biochemically confirm NreA as a nitrate regulator. In order to describe the function of NreA and to analyze how nitrate regulation is achieved, here *in vivo* and *in vitro* studies were performed. The *in vivo* studies should demonstrate that NreA regulates the expression of *narG* in response to nitrate and differentiate the role of NreA and NreB in nitrate and oxygen regulation. The NreA, NreB, and NreC proteins were purified to identify the effect of NreA and nitrate on the function of NreB as an oxygen sensor. This was done by monitoring the autophosphorylation activity and state of NreB *in vitro*.

These studies were performed to assess the possibility of a joint regulation of two different sensors, NreA and NreB. Other than in *E. coli*, where oxygen and nitrate sensing are performed by the two independent FNR and NarXL systems, in *S. carnosus* the signal of two sensors would be transmitted via one response regulator to the DNA. This study shows that NreA interacts with NreB and modulates the kinase activity of NreB in response to nitrate, indicating that NreA/NreB form a new type of sensor complex responding to nitrate and oxygen.

3. Experimental procedures

3.1 Bacterial strains and plasmids

In the course of this study the following strains and plasmids were used:

3.1.1 *Staphylococcus carnosus* strains and plasmids

Strain	Genotype	Reference
TM300	WT	Schleifer and Fischer,1982
m1	Δ*nreABC*::*ermB*	Fedtke *et al*., 2002
Δ*nreA*	Δ*nreA*	Schlag, 2008

Plasmid	Genotype	Reference
pPS44	Staphylococcal promoter probe vector, *lip* (*Staphylococcus hyicus*), pC194 origin, cam^R	Peschel *et al*., 1993
pMW1001	pPS44 derivative with *narG* promoter introduced into the single BamHI site in front of lipase gene	This study
pRB473	*E. coli*/*S. carnosus* shuttle vector with amp^R for *E. coli* and cam^R for *S. carnosus*	Brückner, 1992
pRB473nreABC	pRB473 with *nreABC* and native promoter	Müllner *et al*., 2008
pCQE1nreB	pCQE1 derivative carrying *nreB*, staphylococcal His_6-tag (C-terminal) expression vector, xylose inducible, glucose repressible *xylA* promoter, cam^R	Fedtke *et al*., 2002
pMW1040	*narG-lip* in SbfI/NheI of site of pRB473nreABC, cam^R	This study
pMW1393	pMW1040 derivative with *nreA* deletion	This study

Plasmid	Genotype	Reference
pMW1532	pMW1040 derivative with *nreBC* deletion	Koch-Singenstreu, 2013
pMW1298	pMW1040 derivative with *nreA* coding NreA(Y95A)	Koch-Singenstreu, 2013
pMW1083	pMW1040 derivative with *nreB* coding NreB(C62S)	This study
pMW1897	pMW1393 (Δ*nreA*) derivative with *nreB* coding NreB(C62S)	This study
pMW1951	pMW1040 derivative with *xylR*, *xylA*-*nreA*, Δ*nreBC*, for overproduction of NreA	This study

3.1.2 *Escherichia coli* strains and plasmids

Strain	Genotype	Reference
JM109	*recA1*, *supE44*, *endA1*, *hsdR17*, *gyrA96*, *relA1*, *thi-1, Δ(lac-proAB)*, [F', *traD36*, *proAB*, *lacIqZ⊿M15*]	Yanisch-Perron *et al*., 1985
XL1-Blue	*recA1*, *supE44*, *endA1, hsdR17*, *gyrA96*, *relA1*, *thi-1*, *lac*, [*F'*, *proAB*, *lacIqZΔM15*, *Tn10 (Tet^R)*]	Stratagene
M15	[pREP4], *Nal^S*, *Str^S*, *Rif^S*, *Thi$^-$*, *Lac$^-$*, *Ara$^+$*, *Gal$^+$*, *Mtl$^-$*, *F$^-$*, *RecA$^+$*, *Uvr$^+$*, *Lon$^+$*	Qiagen

Plasmids	Genotype	Reference
pQE31nreA	*nreA* with N-terminal His_6-tag, cloning by insertion of BamHI/HindIII restriction sites, *kan^R*, *amp^R*, IPTG inducible promoter	Schlag, 2008
pMW1733	pQE31nreA derivative with *nreA* coding NreA(Y95A)	This study
pMW1613	pQE31nreA derivative with *nreA* coding NreA(F28A)	This study
pMW1614	pQE31nreA derivative with *nreA* coding NreA(W45A)	This study
pMW1615	pQE31nreA derivative with *nreA* coding NreA(L67N)	This study

Plasmid	Genotype	Reference
pMW1801	pQE31nreA derivative with *nreA* coding NreA(E101Q)	This study
pASK-IBA3plus	Strep-tag (C-terminal) expression vector, anhydrotetracycline inducible, *tet*-promoter, amp^R	IBA
pMW1617	pASK-IBA3plus derivative with *nreC* introduced into the single BsaI site, C-terminal Strep-tag, amp^R	This study
pASK-IBA13plus	Strep-tag (N-terminal) expression vector, anhydrotetracycline inducible, *tet*-promoter, amp^R	IBA
pMW1243	pASK-IBA13plus derivative with *nreA* introduced into XhoI and EcoRV site, N-terminal Step-tag, amp^R	This study

3.2 Media and growth

3.2.1 Media for growth of *Staphylococcus carnosus*

B (basic)-broth (BM) pH 7.2	(Götz and Schumacher 1987)
Tryptone/peptone from casein	10 g/l
Yeast extract	5 g/l
NaCl	5 g/l
Na_2HPO_4*	1 g/l
Glucose	1 g/l
Agar (addition for agar plates)	15 g/l
Tween-20** (addition for agar plates)	1 g/l

All components were dissolved in $H_2O_{dest.}$ and were autoclaved.

* Na_2HPO_4 was not added for studies on lipase activity, because it leads to formation of precipitation during lipase assay which interferes with photometrical measurements.

** Tween-20 was used in agar plates for qualitative detection of lipase activity.

Yeast extract production medium (YEP)	
Yeast extract	45 g/l
Sodium phosphate (pH 7.2)	50 mM
Glycerol	40 mM
$NaNO_3$	10 mM
Ammonium iron(III) citrate	10 mM
L-Cysteine hydrochloride	1 mM

Ammonium iron(III) citrate as well as L-cysteine hydrochloride were added as iron and sulfur source for anaerobic expression of NreB.

3.2.2 Media for growth of *Escherichia coli*

LB (lysogeny broth)	**(Bertani, 1951)**
Tryptone/peptone from casein	10 g/l
Yeast extract	5 g/l
NaCl	5 g/l
Agar (addition for agar plates)	15 g/l

SOC (super optimal broth)	**(Sambrook and Russell, 2001; Hanahan, 1983)**
Tryptone/peptone from casein	20 g/l
Yeast extract	5 g/l
Glucose	20 mM
NaCl	10 mM
$MgCl_2$	10 mM
$MgSO_4$	10 mM
KCl	2.5 mM

3.2.3 Applied antibiotics

Antibiotic	**Stock solution**	**Concentration in medium**
Chloramphenicol (Cam)	20 mg/ml	10 µg/ml
Ampicillin (Amp)	50 mg/ml	100 µg/ml
Erythromycin (Ery)	2.5 mg/ml	2.5 µg/ml
Kanamycin (Kan)	50 mg/ml	50 µg/ml

3.2.4 Stock solutions of inductors for gene expression

IPTG (1 M): IPTG was resolved in $H_2O_{dest.}$ and was sterilized by filtration (ø 0.45 µm). Aliquots were stored at -20 °C. For induction the medium was supplemented with a concentration of 1 mM.

Xylose (3.3 M): Xylose induces the *xylA* promoter because it inactivates the repressor XylR. This promoter is used for protein expression in *S. carnosus*. Xylose

was resolved in $H_2O_{dest.}$ and was sterilized by filtration (ø 0.45 µm). The solution was stored at 4 °C. For induction the medium was supplemented with a concentration of 33 mM.

Anhydrotetracycline (2 mg/ml): In presence of anhydrotetracycline the *tet*-repressor is inactivated, leading to a derepression of the *tetA* promoter. Anhydrotetracycline was dissolved in dimethylformamid. It was used for induction at the concentration of 200 ng/ml which is not antibiotically effective.

3.2.5 Growth of *S. carnosus* m1 for testing *nreABC* complementation

For testing the complementation of *S. carnosus* m1 (Δ*nreABC*) by plasmid-encoded *nreABC* (pMW1040) anaerobic growth was monitored. The cells were grown in basic broth (BM) (Götz and Schumacher, 1987) with and without 10 mM sodium nitrate. The overnight cultures were grown in standing test tubes without agitation in an incubator at 37 °C. The main culture (40 ml BM) was inoculated to an OD_{578} of 0.1 and grown in rubber stoppered flasks (*Müller-Krempel,* Bülach, Switzerland) after replacing the gas phase with N_2 (99.99 %). To determine the optical density (OD) the blank value of BM was subtracted. For OD values above 0.5 the culture was diluted in BM.

3.2.6 Growth of *S. carnosus* for NreB-His_6 expression

For isolation of NreB-His_6 the strain *S. carnosus* m1 pCQE1nreB was used. *nreB* is encoded on the plasmid pCQE1nreB where the gene is cloned behind the inducible *xylA* promoter, receiving a C-terminal His_6-tag (Fedtke *et al*., 2002). This plasmid also encodes XylR which represses the xylA promoter in the absence of xylose. Both *xylR* and *xylA*-promoter originate from the *xyl* operon of *S. xylosus* (Wieland *et al*., 1995). For aerobic isolation this strain was grown in yeast extract production medium (YEP) on a rotary shaker at 160 rpm and 37 °C to an OD_{578} of 10. Then the cells were induced with 150 mM xylose for 6 h until reaching an OD_{578} of about 30-40. For anaerobic isolation of NreB-His_6, anaerobic growth of the strain was performed in yeast extract medium supplemented with 10 mM sodium nitrate, 10 mM ammonium iron(III) citrate and 1 mM L-cysteine hydrochloride. First the cells were grown and induced aerobically as described above to reach a high OD_{578} of 18. After growth to an OD_{578} of 35, the culture was transferred to anaerobic flasks (*Müller-Krempel,* Bülach, Switzerland). The flasks were filled to

the top leaving no air inside after sealing, and incubated by constant stirring (magnetic mixer) for 16 h at 4 °C (Müllner *et al*., 2008).

3.2.7 Growth of *S. carnosus* for *narG-lip* expression experiments

For the lipase kinetic analysis cells were grown in modified basic medium (BM) (Götz and Schumacher, 1987), without the addition of Na_2HPO_4 to avoid formation of precipitate during the lipase assay. The medium was supplemented with chloramphenicol (10 µg/ml). For expression studies the bacteria were grown aerobically or anaerobically with and without specific supplements as indicated. For aerobic growth an overnight culture was grown aerobically in a test tube on a rotary shaker. For the inoculation of the main culture, the bacteria were sedimented (5,000 ×*g*, 5 min, RT) and washed in modified BM. The main culture (40 ml modified BM) was inoculated to an OD_{578} of 0.1 and grown in baffled flasks (300 ml) on a rotary shaker to an OD_{578} of 0.5. Then the growth was stopped by centrifuging (12,000 ×*g*, 5 min, RT), and the supernatant was stored on ice until determination of lipase activity. Anaerobic growth was performed equally except for the following variations. The overnight culture was grown in standing test tubes, without agitation, in an incubator at 37 °C and the main culture was grown in rubber stoppered flasks (*Müller-Krempel,* Bülach, Switzerland) after replacing the gas phase with N_2 (99.99 %). To test the effect of nitrate on *narG* expression under aerobic or anaerobic conditions, the overnight cultures, as well as the main cultures were supplemented with 10 mM sodium nitrate. The effects of 5 mM sodium nitrite, 5 mM sodium sulfate, or 10 mM sodium chlorate (aerobic growth) and 0.5 mM sodium chlorate (anaerobic growth) were also tested.

3.2.8 Growth of *E. coli* for protein production

For the isolation of His_6-NreA and His_6-NreA(Y95A) the strains *E. coli* M15 pQE31nreA and *E. coli* M15 pQE31nreA(Y95A) were used. On these plasmids *nreA* stands under the control of the IPTG inducible T5 promoter. These strains were grown in LB to an OD_{578} of 0.5. Then the culture was induced by the addition of 1 mM IPTG for 5 h (Qiagen manual). For the isolation of His_6-NreA and His_6-NreA(Y95A) with bound nitrate (His_6-NreA·[NO_3^-] and His_6-NreA(Y95A)·[NO_3^-]) the medium was supplemented with 10 mM sodium nitrate at the beginning of growth and again 1 h and 4 h after induction. Growth of *E. coli* M15 was performed equal-

ly for isolation of His_6-NreA(W45A) (pMW1614), His_6-NreA(F28A) (pMW1613), His_6-NreA(L67N) (pMW1615), and His_6-NreA(E101Q) (pMW1801).

For the isolation of NreC-Strep and Strep-NreA the strains *E. coli* JM109 pMW1617 and *E. coli* JM109 pMW1243 were used. The plasmids carry a *tetA* promoter. The strains were grown in LB to an OD_{578} of 0.5. Then the cultures were induced by the addition of 200 ng/ml anhydrotetracycline for 5 h (IBA manual).

3.3 Biochemical methods

3.3.1 Qualitative detection of lipase activity

With BM agar plates, containing Tween-20, a qualitative detection of lipase activity was possible. Tween-20 (polyoxyethylene (20) sorbitan monolaurate) is a non-ionic surfactant. The lipase hydrolyzes Tween-20 which leads to the formation of lauric acid, a saturated fatty acid with 12 carbon atom chains. Its formation was detected by its white color which formed a clouding around lipase excreting colonies. These plates can be used for screening after transformation.

3.3.2 Lipase reporter gene assay

For the lipase reporter gene assay strains carrying plasmid-encoded *narG-lip* (plasmid pMW1001, pMW1040 and derivatives) were used. The lipase is excreted and is quantified in the supernatant without having to disrupt the cells. Lipase activity was assessed by hydrolysis of p-nitrophenyl caprylate (Fig. 4) in a 96-well plate assay. The lipase test buffer contained 5 mM p-nitrophenyl caprylate, 10 mM $CaCl_2$, 0.1 % Triton X-100, and 20 mM Tris/HCl pH 9.0 (Rosenstein *et al*., 1992). A volume of 225 µl of the buffer was added to each well together with 25 µl supernatant. The production of p-nitrophenolate was measured by absorbance at 415 nm using an extinction coefficient of $16.97 \times 10^3\ M^{-1}\ cm^{-1}$. The specific lipase activity (U/g dry weight) was determined by calculating p-nitrophenyl caprylate hydrolysis per min (1 U corresponds to the hydrolysis of 1 µmol p-nitrophenyl caprylate per min) and the cell density of the culture (1 ml culture with an OD_{578} of 1 corresponds to a dry weight of 0.245 mg).

The strains which were tested in this assay were *S. carnosus* m1 pMW1040 or *S. carnosus* TM300 pMW1001 ($NreA^+$, $NreB^+$, $NreC^+$), *S. carnosus* m1 pMW1001

(Δ*nreABC*), *S. carnosus* m1 pMW1532 (NreA$^+$, Δ*nreBC*), *S. carnosus* m1 pMW1393 or *S. carnosus* Δ*nreA* pMW1001 (Δ*nreA*, NreB$^+$, NreC$^+$), *S. carnosus* TM300 pMW1532 (NreA$^+$, NreB$^+$, NreC$^+$ and NreA from plasmid). Also tested was *S. carnosus* m1 pMW1298 (NreA(Y95A), NreB$^+$, NreC$^+$); *S. carnosus* m1 pMW1083 (NreA$^+$, NreB(C62S), NreC$^+$) and *S. carnosus* m1 pMW1897 (Δ*nreA*, NreB(C62S), NreC$^+$). The *narG-lip* expression was tested aerobically and anaerobically with or without nitrate, nitrite, sulfate, and chlorate.

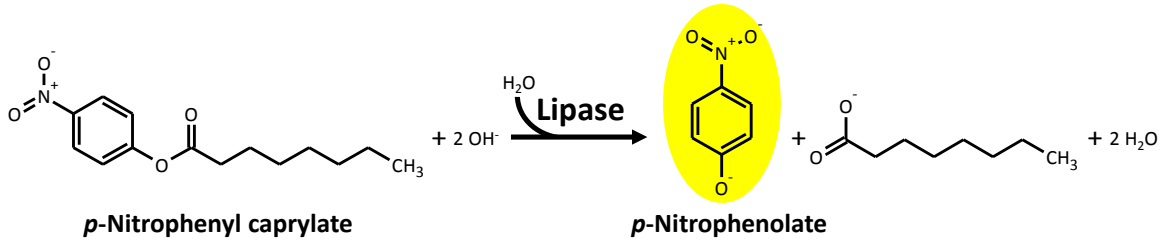

Figure 4: Colorimetric reaction for the determination of lipase activity. The chromogenic substrate p-nitrophenyl caprylate is hydrolyzed by the lipase in alkaline lipase test buffer. This leads to the production of p-nitrophenolate and caprylate. p-Nitrophenolate can be detected by photometric measurement at 415 nm.

3.3.3 Determination of protein concentration (Bradford, 1976)

The Bradford assay is a colorimetric protein assay. Under acidic conditions Coomassie Brilliant Blue G-250 forms complexes with cationic and nonpolar amino acids. This leads to a stabilization of the dye in its anionic sulfate form and a shift of its absorption maximum from 470 nm (red) to 595 nm (blue).

For measuring the protein concentration 200 µl Bradford reagent (5× Roti-Quant) were added to 800 µl protein sample (usually 780 µl $H_2O_{dest.}$ and 20 µl protein) and mixed by inverting. After incubation for 10 min at room temperature (RT) the extinction was measured at 595 nm. The calibration line was generated by using different concentrations (40-0.5 µg/ml) of BSA in the matching protein elution buffer. The blank was measured by using protein elution buffer.

3.3.4 SDS-PAGE

The sodium dodecyl sulfate polyacrylamide gel electrophoresis is based on the principal of separation of protein mixtures according to their molecular size in an

electric filed. The proteins are denatured by heat and the addition of the reducing agent DTT leads to a further denaturation by reducing disulfide linkages. SDS binds to the hydrophobic regions of the proteins and covers the charge of the proteins for a constant negative charge distribution. The linearized proteins are separated according to their molecular size in the gel. For SDS-PAGE the Mini-Protean Tetra Cell (BioRad) system was used.

For the discontinuous gel electrophoresis (Laemmli, 1970), a gel composed of a separation gel and a stacking gel was prepared. The switch between pH and pore size leads to a high resolution of the gel. Both gel solutions were prepared separately from each other. Ammonium persulfate (APS) was added to the acrylamide solutions as an initiator for polymerization. The separation gel was prepared first, by pipetting the acrylamide solution between two glass plates. It was covered by 50 µl n-butanol for straightening the layer. When the separation gel was fully polymerized then n-butanol was removed and the acrylamide solution for the stacking gel was prepared and pipetted on top of the separation gel. Then a comb was inserted into the gel to create sample wells. When the stacking gel was polymerized the comb could be removed and the gel was ready for use.

For gel electrophoresis the samples were prepared by mixing with SDS loading buffer (1×) and heating to 99 °C for 5 min. The gel was set up inside a container filled with running buffer (5.44 g/l Tris, 25.92 % glycine, 10 % SDS) and 5 µg of protein samples with known concentration were applied to the gel. An electric field of constant 120 V was applied for 50 min, causing the negatively charged proteins to migrate across the gel towards the positive electrode.

For visualizing the proteins in the gel the gel was dyed with Coomassie staining solution (0.5 g/l Coomassie Brilliant Blue R-250, 50 % methanol, 10 % glacial acid) for 30 min. The proteins were fixed by acetic acid and stained. The excess dye incorporated into the gel was removed by incubation in H_2O and heating in a microwave. When the gel was destained the protein bands could be detected as blue bands on a clear background. Then the gel was put on filter paper and dried in a gel drying device (Biotec-Fischer).

Acrylamide gel	Separation gel 12.5 %	Stacking gel 6.6 %
$H_2O_{dest.}$	5.7 ml	4.7 ml
Tris/HCl 0,5 M pH 6,8	4.5 ml	-
Tris/HCl 1,5 M pH 8,8	-	2.1 ml
SDS 10 %	180 µl	81 µl
TEMED	36 µl	22 µl
Acrylamide Rotiphorese Gel 30	7.5 ml	1.9 ml
APS 10 %	100 µl	46 µl

SDS loading buffer (2×) (Sambrook and Russell, 2001)	
Tris/HCl	100 mM pH 6,8
Dithiothreitol (DTT)	200 mM
SDS	4 % (w/v)
Bromophenol blue	0.2 % (w/v)
Glycerol	20 % (v/v)

3.3.5 Western blot and immunostaining

In Western blotting the proteins which were separated by SDS-PAGE are transferred from a polyacrylamide gel to a nitrocellulose membrane. Followed by an immunostaining with antibodies, the proteins can be visualized on the membrane.

The transfer of proteins from within the gel onto the membrane by applying an electric current is called electroblotting. Four filter papers and one nitrocellulose membrane were cut into the size of the gel and soaked in transfer buffer (25 mM Tris, 192 mM glycine, 20 % methanol). For equilibration the gel was incubated in transfer buffer for 5 min. Then two of the filter papers were laid on the anode of the Fast Semi-Dry Blotter (Thermo Scientific), followed by the nitrocellulose membrane. The gel was placed on top of the membrane and then the gel was covered with two filter papers. The cathode of the blotter was positioned on top. The electric current was determined by multiplying the size of the membrane by the factor 0.8 (x cm^2 × 0.8 = y mA). The proteins were blotted for 60 min.

After blotting, the membrane was blocked for 1 h at RT (or over night at 4 °C) with 5 % skim milk powder in PBS buffer (2.7 mM KCl, 10 mM Na_2HPO_4, 1.8 mM KH_2PO_4). This and following incubation steps were performed on a tumbling shaker for gentle agitation. Blocking was done to prevent unspecific binding of antibodies to the membrane. Afterwards, a dilute solution of primary antibody was applied to the membrane. In case of anti-NreA (polyclonal, from rabbit, first bleed, Eurogentec) a dilution of 1:4,000 and in case of anti-His (polyclonal, from mouse, Sig-

ma) a dilution 1:8,000 was prepared in antibody buffer (PBS, 1 % BSA, 0.1 % Tween-20) and the membrane was incubated with the first antibody (10 ml) for 1 h. This was followed by washing the membrane to remove unbound primary antibody with wash buffer (3× 10 min in 10 ml PBS and 0.1 % Tween-20). Then the secondary antibody was applied to the membrane (anti-IgG-rabbit 1:5,000, anti-IgG-mouse 1:10,000, diluted in antibody buffer, 10 ml) and incubated for 1 h. This was followed by washing the membrane again with wash buffer (3× 10 min in 10 ml wash buffer). The secondary antibody is linked to the reporter enzyme horseradish peroxidase (HRP). For the detection of the antibody, chemiluminescent HRP substrate (Millipore) was used. The HRP catalyzes oxidation of luminol, and the oxidized luminol emits light as it decays to its ground state. To create an image, a sensitive sheet of photographic film (Lucent Blue X-ray Film) was placed on the membrane and was exposed to the emitted light.

3.3.6 Isolation of proteins expressed in *Escherichia coli*

The preparation of His_6-NreA and His_6-NreA(Y95A) was performed as recommended (Qiagen) after aerobic growth and induction of *E. coli* M15 pQE31nreA and *E. coli* M15 pMW1733 respectively. Isolations of His_6-NreA(F28A) (pMW1613), His_6-NreA(W45A) (pMW1614), His_6-NreA(L67N) (pMW1615), and His_6-NreA(E101Q) (pMW1801) were performed equally. The disruption of *E. coli* cells was done aerobically with a French pressure cell press (3 passages, 13.8×10^7 kg s^{-2} m^{-1}). Cell debris was separated from solvent by centrifugation (20,000 ×*g*, 20 min, 4 °C). The proteins were isolated from the cleared supernatant by chromatography via His-tag on a Ni-NTA column. The column was washed with wash buffer (20 mM imidazole, 1 M NaCl, 50 mM sodium phosphate pH 7.2, 20 % glycerol) followed by eluting the protein from the column with elution buffer (150 mM imidazole, 300 mM NaCl, 50 mM sodium phosphate pH 7.2, 20 % glycerol).

For the isolation of His_6-NreA·[NO_3^-] and His_6-NreA(Y95A)·[NO_3^-] all steps were performed equally except that the cells were grown in $NaNO_3$ containing medium (as described above) and the lysis and wash buffers were supplemented with 100 mM $NaNO_3$ and the elution buffer with 20 mM $NaNO_3$.

Preparation of NreC-Strep was performed as recommended (IBA manual) after aerobic growth and induction of strain *E. coli* JM109 pMW1617. The cells were

pelleted (5,000 ×*g*, 20 min, 4 °C) and suspended in buffer W (100 mM Tris/HCl pH 8, 150 mM NaCl, 1 mM EDTA). Cells were disrupted in a French pressure cell press (3 passages, 13.8 × 10^7 kg s^{-2} m^{-1}) and cell debris was separated from solvent by centrifugation (20,000 ×*g*, 20 min and 4 °C). The proteins were isolated by chromatography via Strep-tag of the clear supernatant, on Step-Tactin Sepharose. The column was washed with buffer W followed by eluting the protein from the column with buffer E (buffer W and 2.5 mM desthiobiotin).

The preparation of NreA for the production of NreA antibodies from rabbit was performed equally as for NreC-Strep, on a Strep-Tactin column, but via N-terminal Strep-tag. Then isolated Strep-NreA was dialyzed in buffer W for removal of desthiobiotin and was again applied to a Strep-Tactin column for reaching a higher purity. For the removal of the Strep-tag the thrombin cleavage site between NreA and the Strep-tag was used. 10 U of thrombin were incubated with Strep-NreA for 16 h at 22 °C. During this incubation Strep-NreA was being dialyzed in buffer W for the removal of the tag from the protein solution. The purity and shift from 21.5 kDa to 19.2 kDa by cleavage of the Strep-tag was confirmed by SDS-PAGE. The purified NreA was then lyophilized for shipment to Eurogentec for the production of NreA antibodies in a rabbit.

3.3.7 Aerobic and anaerobic preparation of NreB

Preparation of aerobic NreB was performed after aerobic growth and induction of strain *S. carnosus* m1 pCQE1nreB. The procedure for preparation of anaerobic NreB from the anaerobic culture of *S. carnosus* m1 pCQE1nreB was performed equally, except that all steps were performed under anoxic conditions in an anaerobic chamber (Coy) using anoxic buffers. To handle the anaerobic bacteria or solutions outside the chamber, air tight sealed containers were used (Müllner *et al*., 2008).

The cells were pelleted by centrifugation at 5,000 ×*g* for 20 min and 4 °C. After suspending the cells in lysis buffer (10 mM imidazole, 300 mM NaCl, 50 mM sodium phosphate pH 7.2, 20 % glycerol, 10 mM ß-mercaptoethanol) the cells were disrupted with glass beads in a cell mill, by vigorous shaking. Cell debris was separated from solvent by centrifugation (20,000 ×*g*, 20 min, 4 °C). The proteins were isolated by chromatography of the clear supernatant on Ni-NTA agarose (as recommended by Qiagen).The column was washed with wash buffer (20 mM imidaz-

ole, 1 M NaCl, 50 mM sodium phosphate pH 7.2, 20 % glycerol, 10 mM ß-mercaptoethanol) to remove any unspecific binding proteins from the column. NreB-His_6 was then eluted with elution buffer (150 mM imidazole, 300 mM NaCl, 50 mM sodium phosphate pH 7.2, 20 % glycerol, 10 mM ß-mercaptoethanol) (Müllner *et al*., 2008; Kamps *et al*., 2004). NreB fractions of 1 ml were eluted with protein concentrations of up to 16 mg/ml. The isolated NreB fractions were tested for their iron and sulfur content by the colorimetric assays described below (chapter 3.3.8 and 3.3.9) and a spectrum was recorded to determine the A_{420}/A_{280} ratio.

3.3.8 Quantification of complexed iron (Fish, 1988)

The test is a sensitive colorimetric method based on the reduction of iron containing samples to Fe^{2+} by the addition of potassium permanganate. Fe^{2+} reacts with Ferrozine, a ferrous iron chromogen (Stookey, 1970), to form a colored, water soluble complex with an absorption maximum of 562 nm.

The Ferrozine reagent (6.5 mM Ferrozine, 13.1 mM Neocuproine, 2 M L-ascorbic acid, 5 M ammonium acetate) was prepared as described in Stookey, 1970. For the preparation of 10 ml Ferrozine reagent, ammonium acetate and ascorbic acid were dissolved in 3 ml $H_2O_{dest.}$ and then Neocuproine and Ferrozine were added. The total volume of 10 ml was reached by the addition of $H_2O_{dest.}$. Because of the sensitivity to light, it was stored in the dark. The Ferrozine reagent was stable for 3-6 weeks. A potassium permanganate solution was also prepared for this test by mixing the solution of KMnO4 (0.285 M, stored in dark) and HCl (1.2 M) in a volume ratio of 1:1. The solution was not stable and was prepared right before use. For quantification a calibration line was prepared. Samples (0.5-2.5 µg) of an iron standard (Titrisol, Merck) were used for the determination of iron concentrations of 0.4-2.2 mM.

20 µl of each protein fraction were submitted to this test and were filled up to 200 µl with $H_2O_{dest.}$. 500 µl of the potassium permanganate solution were added and mixed by inverting. The solution was incubated at 60 °C for 2 h in the thermomixer. Then 100 µl Ferrozine color reagent were added and the solution was incubated at RT for 30 min. Afterwards the absorption was measured at 562 nm.

3.3.9 Quantification of acid labile sulfide

Quantification of acid labile sulfide was performed as described by Siegel, 1965; Beinert, 1983; King and Morris, 1967. The protein was denatured with zinc hydroxide in alkaline medium, which leads to the formation of free sulfide. The sulfide precipitates as ZnS with $Zn(OH)_2$, which is reduced to H_2S by acid. H_2S and DMPD form methylene blue which has an absorption maximum at 670 nm.

All steps were performed in the anaerobic chamber (Coy; 95 % N_2, 5 % H_2), because sulfide is easily oxidized to H_2S. To create a calibration line a sulfide standard (2 mM) was prepared from $Na_2S{\cdot}9H_2O$ (M_r 240.18). A $Na_2S{\cdot}9H_2O$ crystal of 0.49 g was dissolved in 1 l NaOH (10 mM) inside the anaerobic chamber. 5-25 µl of standard were used for the determination of sulfide concentrations of 0.5-2.5 mM (Müllner, 2008).

20 µl of each protein fraction were submitted to this test and were filled up to 200 µl with $H_2O_{dest.}$. To prevent sulfide from being lost as H_2S gas, all steps were performed uninterruptedly. For each protein fraction 600 µl of zinc acetate (1 %) were added to the 200 µl of diluted protein. This was directly followed by the addition of 50 µl of NaOH (7 %) and the solution was mixed by inverting and incubated for 15 min at RT. The newly formed precipitation was centrifuged (11,000 ×*g*, 1 min, RT) and then 150 µl DMPD (0.1 % in 5 M HCl) were added by pipetting the solution carefully and slowly on the bottom of the centrifugation tube, inside the precipitate. This leads to the dissolving of the white precipitate ($Zn(OH)_2$ and ZnS). Then 150 µl $FeCl_3$ (10 mM in 1 M HCl) were added and the solution was vortexed for 30 s. The solution was incubated for 20 min at RT and the clouding of the solution was removed by centrifugation (11,000 ×*g*, 1 min, RT). The absorption was measured photometrically at 670 nm outside the anaerobic chamber.

3.3.10 Autophosphorylation assay of NreB

Autophosphorylation of NreB was assayed with isolated NreB. For anaerobically prepared NreB all steps were performed under anoxic conditions in an anaerobic chamber (Coy). For aerobically prepared NreB all steps were performed equally in presence of oxygen. NreB (15 µM) was diluted with reaction buffer consisting of 50 mM HEPES (pH 8), 50 mM KCl, 5 mM $MgCl_2$, 0.5 mM EDTA and 2 mM DTT (Kamps *et al*., 2004). The reaction mixture was adjusted to 45 µl by the addition of the protein elution buffer. To start the reaction 3 µl of [γ-^{33}P]-ATP (0.22 µM,

5.5 TBq/mmol) (Müllner *et al*., 2008) were added. After starting the reaction, 8 µl samples were taken from the reaction mixture at different time intervals (5-300 min) and mixed with 14 µl stop solution (SDS sample buffer). The samples were then subjected to SDS-PAGE on 12.5 % polyacrylamide gels. Subsequently the gels were folded in saran wrap, and the phosphor imaging plate was exposed to the gels (FUJIFILM BAS 2040 imaging plate) for 18 h at 4 °C. The ß-irradiation was then detected by evaluating the plate in the phosphoimager. The relative contents of radioactivity were determined with Gel-Pro Analyzer 6.0 after subtracting the background of the imaging plate (Müllner *et al*., 2008).

For testing the effects of NreA, NreA·[NO_3^-], NreA(Y95A), and NreA(Y95A)·[NO_3^-] the proteins were added at concentrations of 600 µM, or as indicated, to the reaction mixture before or after the addition of [γ-^{33}P]-ATP. For an experimental control, the same volume of protein elution buffer was added.

To monitor the phosphotransfer from NreB to NreC, NreB (30 µM) was autophosphorylated as described in the autophosphorylation assay, but the reaction volume was increased to 120 µl. The reaction was started by the addition of 20 µl of [γ-^{33}P]-ATP (0.22 µM, 5.5 TBq/mmol). 150-240 min after the addition of [γ-^{33}P]-ATP, NreC (30 µM) was added. After the addition of NreC the volume of withdrawn samples was increased as indicated. To monitor the effect of NreA on NreC phosphorylation and phosphotransfer, NreA was added either at the beginning of NreB phosphorylation or at the same time together with NreC.

3.3.11 Gel filtration chromatography

To separate phosphorylated NreB from residual ATP, gel filtration (GF) was performed using the porous matrix Sephadex G50 Superfine. The smaller ATP has greater access and the larger NreB is excluded from the matrix and was eluted in an earlier fraction than ATP. First, 1 ml of anaerobically prepared NreB (27 µM) was phosphorylated with 127 µl [γ-33P]-ATP (0.22 µM, 5.5 TBq/mmol) in reaction buffer (see chapter 3.3.10) in an anaerobic chamber. A column (1 cm^2 × 10 cm) filled with Sephadex G50 was equilibrated with anaerobic buffer (50 mM sodium phosphate buffer pH 7.2, 300 mM NaCl, 20 % glycerol). After phosphorylation for 200 min, NreB in 1 ml elution buffer was applied to the matrix and eluted by rinsing with anaerobic buffer. Fractions of 1 ml were collected from the column and the fraction with the highest NreB concentration was used for testing the effect of

NreA, NreA·[NO_3^-], NreA(Y95A), and NreA(Y95A)·[NO_3^-] on the phosphorylation state of NreB. The proteins were added at a concentration of 400 µM to the isolated NreB-P (10 µM). The state of phosphorylation of NreB was determined after SDS-PAGE and phosphoimaging as described above.

3.3.12 Hexokinase assay: Removal of ATP during autophosphorylation assay

The hexokinase from *Saccharomyces cerevisiae* (Sigma) was used to remove residual ATP from a reaction mixture during an autophosphorylation assay to test the effect of NreA on phosphorylated NreB in absence of ATP. The hexokinase is an enzyme that phosphorylates hexoses with ATP, forming hexose phosphate and ADP. Anaerobically isolated NreB (15 µM) was phosphorylated with [γ-^{33}P]-ATP in presence of D-glucose (0.4 µM). After 49 min 40 U/l were added to the reaction mixture for ATP depletion. After 85 min NreA (400 µM) was added. This assay was performed in reaction buffer, as described for the autophosphorylation assay (see chapter 3.3.10). The state of phosphorylation of NreB was determined after SDS-PAGE and phosphoimaging as described above

3.3.13 ADP-Glo Kinase assay: Determination of ADP production

To monitor the ADP production the ADP-Glo Kinase Assay (Promega) was used. It is a method for measuring the kinase activity by quantifying the amount of ADP produced during a kinase reaction. The assay was performed in two steps as described in the protocol. First, the ADP-Glo Reagent was added to terminate the kinase reaction and deplete the remaining ATP. Then the Kinase Detection Reagent was added to convert ADP to ATP, and the newly synthesized ATP was used in a luciferase/luciferin reaction. The generated luminescence was measured using a luminometer (Omega) in solid white 384-well plates.

Anaerobically isolated NreB (10 µM) was phosphorylated with ATP (150 µM). After different time intervals (5-120 min) samples were taken to detect the ADP production. The ADP-Glo Reagent was added directly when samples were taken. For better comparability the Kinase Detection Reagent was added to all samples at the same time, to eliminate the chance of a decreased signal of luminescence between early and late taken samples. The ADP production was also detected in presence of NreA (400 µM) and the effects of NreA and protein elution buffer on ADP production were also tested in absence of NreB as an experimental control.

3.3.14 Co-immunoprecipitation

To determine NreA-NreB interaction a co-immunoprecipitation experiment was performed. NreA was overproduced in strain *S. carnosus* m1 pMW1951 and NreB-His_6 was overproduced in strain *S. carnosus* m1 pCQE1nreB. The strains were grown in 500 ml yeast extract medium in 2 l baffled flasks. When reaching an OD_{578} of 10 induction of protein expression was induced by the addition of 0.33 mM xylose. When reaching an OD_{578} of 30 the cells were pelleted by centrifugation (11,000 ×*g*, 20 min, 4 °C) and were resuspended in 10 ml lysis buffer (50 mM Tris pH 8, 150 mM NaCl). To open the cells glass beads were added and the cell wall was ruptured by intense shaking in a homogenizer (FastPrep-24 MP) (4× 30 s, 5.5 m/s). Then the cell debris was removed by centrifugation (20,000 ×*g*, 20 min, 4 °C). 0.5 ml of cleared supernatant containing NreA and 0.5 ml of cleared supernatant containing NreB-His_6 were incubated for 1 h. The co-immunoprecipitation was performed using the magnetic µMACS Anti-His MicroBeads (Miltenyi Biotec), as described in the manual. 25 µl of the magnetic Anti-His MicroBeads were added to the protein solutions for labeling and incubated for 30 min. Then the protein solution was applied to a µColumn which was placed in the magnetic field of the µMACS separator. The column was washed 3 times with 200 µl lysis buffer and once with 100 µl wash buffer (20 mM Tris/HCl pH 7.5). Then elution buffer (50 mM Tris/HCl pH 6.8, 50 mM DTT, 1 % SDS, 1 mM EDTA, 0.005 % bromophenol blue, 10 % glycerol) was preheated to 95 °C and applied to the column. The eluate was collected and was applied to SDS-PAGE and after Western blot the nitrocellulose membrane was cut lengthwise, separating proteins bigger than 30 kDa from proteins smaller than 30 kDa. By immunostaining the presence of NreA or NreB-His_6 on the membrane was detected. The upper half of the membrane was incubated with polyclonal anti-His as primary antibody and with polyclonal anti-IgG-mouse as secondary antibody which was linked to HRP. The lower half of the membrane was incubated with the highly specific, polyclonal anti-NreA as primary antibody. As secondary antibody polyclonal anti-IgG-rabbit, which was also linked to HRP, was used. The proteins were made visible by chemiluminescent HRP substrate (Millipore). The photographic film was exposed to the upper half of the membrane for 3 min and the lower half for 1 h. As an experimental control 0.5 ml of protein solutions containing overproduced NreA were incubated with 0.5 ml lysis buffer and were tested as described above.

3.4 Molecular genetic methods

3.4.1 Isolation of genomic DNA from *Staphylococcus carnosus*

The isolation of genomic DNA from *S. carnosus* was performed by the phenol/chloroform-extraction (Chomczynski and Sacchi, 1987).

Cells of a preculture were centrifuged (3,000 ×*g*, 5 min, 4 °C) and the supernatant was discarded. The pellet was resuspended in 250 µl resuspension buffer P1 (Qiagen PlasmidPrep Kit) and the cells were opened by the addition of glass beads and intense shaking in a homogenizer (FastPrep-24 MP) (25 s, 5 m/s). The glass beads were removed by centrifugation (11,000 ×*g*, 3 min, RT) and the supernatant was incubated for 1 h at 37 °C with 20 µl protein kinase K (20 mg/ml in 10 mM Tris/HCl pH 7.4), 25 µl SDS (10 %) and 50 µl RNase A/T1-mix (2mg/ml, Thermo Scientific). To extract the DNA, 500 µl phenol/chloroform/isoamyl alcohol (25:24:1) were added and the mixture was inverted for 1 min. By centrifugation (30 min at 13,000 ×*g*) two phases formed and the upper hydrous phase was taken off and the extraction was repeated. This was followed by a chloroform/isoamyl alcohol extraction. 500 µl of chloroform/isoamyl alcohol (24:1) were added and the solution was mixed by inverting for 1 min. The upper hydrous phase was again taken off and treated with 50 µl acetate (3 M, pH 5.2) and was carefully inverted. Then the DNA was precipitated by the addition of 1 ml ethanol (100 %, -20 °C). The DNA was pelleted by centrifugation (11,000 ×*g*, 10 min) and washed with ethanol (75 %, 4 °C). After centrifugation (11,000 ×*g*, 3 min) the supernatant was removed and the pellet was dried at RT. The pellet was resuspended in 30 µl $H_2O_{dest.}$.

3.4.2 Plasmid isolation from *E. coli* and *S. carnosus*

The plasmid isolation from *E. coli* was performed with the QIAprep Spin Miniprep Kit as described in the manual (QIAprep Miniprep Handbook, Second Edition). The plasmid isolation from *S. carnosus* was also performed with the same kit as for *E. coli* but with an additional procedure. The opening of the cell wall of *S. carnosus* could not be achieved with the lysis buffer supplied in the kit. Therefore, the cells were opened mechanically with glass beads after suspending the cells in buffer P1 (of the Kit). 0.5 g of glass beads were added and rupture of the cell wall was performed in the homogenizer (FastPrep-24 MP), for 25 s, at 5 m/s. The glass beads were removed by centrifugation. All further steps for plasmid preparation were per-

formed as described in the manual. The DNA concentration was detected photometrically with an UV/Vis biophotometer.

3.4.3 Gel electrophoresis of nucleic acids

An agarose gel was used for the separation of DNA fragments. 2 g agarose (2 %) were resolved in 200 ml TAE buffer (40 mM Tris, 20 mM acetic acid, 1 mM EDTA) by heating in a microwave and then 5 µl ethidium bromide (10 mg/ml) were added. Before applying the DNA samples to the gel, they were mixed with sample loading die (40 % saccharose, 0.25 % xylene cyanol, 0.25 % Orange G). As a DNA marker the 1 kb Ladder (Thermo) was applied to the gel. The electrophoresis was run in a constant electric field of 90 V in TAE buffer for 30-40 min. To visualize the DNA bands on the gel, it was irradiated with UV light.

3.4.4 Polymerase chain reaction (PCR)

DNA molecules were amplified by PCR in the thermal cycler MyCycler (Biorad). For the PCR of genomic DNA the Phusion Polymerase (Finnzymes) was used. For the site directed mutagenesis the PfuUltra2 (Agilent Technologies) was used. Primers were designed by using the program Clonemanager, which were then ordered at Eurofins MWG Operon. The melting temperature (T_M) of the primers was determined by using the program OligoCalculator 3.26 (Northwestern University). The composition of the reaction mixture and the annealing temperature and elongation time were determined by the manual of the used polymerase.

3.4.5 Cleavage of DNA-molecules

For the cleavage of DNA molecules restriction enzymes were used as described in the manual (Thermo Scientific). For analytic purposes, between 300 ng and 1 µg of DNA were digested and applied to an agarose gel (2 %) for electrophoresis. For preparatory purposes, 5-10 µg DNA were digested and afterwards purified by using the PCR purification kit (Qiagen). This removes enzymes and buffer for further use. To avoid religation of vector DNA, after cleavage, with restriction enzymes, the DNA was dephosphorylated. For this purpose the shrimp alkine phosphatase (SAP, Thermo Scientific) was used as described in the manual.

3.4.6 Ligation of DNA molecules

Cloning of restriction enzyme-generated fragments was performed by using the T4 DNA ligase (Thermo Scientific). For the ligation, vector DNA and fragment DNA were incubated in a molecule ratio of 1:5 for 1 h, at 22 °C. The reaction mixture was prepared as described in the manual.

After the ligation the DNA was purified to remove protein and salt which decreases transformation efficiency. For purification the ligated DNA was precipitated by the addition of 500 µl n-butanol. The solution was vortexed for 10 s and the DNA was pelleted at 11,000 ×*g,* for 10 min. The supernatant was carefully removed and 500 µl ethanol (75 %) were put on the DNA pellet, without stirring the DNA. The DNA was centrifuged again (3 min, 11,000 ×*g*), the supernatant was taken away and the pellet was dried at RT. The dried pellet was resuspended in 20 µl $H_2O_{dest.}$and 10 µl were used for one transformation.

3.4.7 Electrotransformation of *Staphylococcus carnosus*

The production of electrocompetent cells of either *S. carnosus* TM300 or *S. carnosus* m1 and their transformation by electroporation were performed by the method described by Löfblom *et al.*, 2006.

For the production of electrocompetent cells, 500 ml of BM were inoculated with a preculture. The culture was incubated on a rotary shaker (160 rpm, 37 °C) in a 2 l baffled flask, grown to an OD_{578} of 0.6. Growth was stopped by incubating the culture for 15 min at 4 °C. All following steps were performed on ice. The cells were pelleted in 30 ml centrifugation tubes (12,000 ×*g*, 15 min, 4 °C), and washed 3 times with 30 ml, 4 °C cold, sterile $H_2O_{bidest.}$. Then the cells were washed with 30 ml, 4 °C cold, sterile glycerol (10 %) pelleted again and resuspended in 1 ml, 4 °C cold, sterile electroporation buffer (10 % glycerol, 0.5 M saccharose). Aliquots of 60 µl were stored at least for 24 h at -80 °C before use.

For the electrotransformation the electrocompetent cells were thawed at RT and the DNA (4 µg) was added. The cells were transferred to an electroporation cuvette which was put into an electroporator. The cells were electroporated by applying a pulsed electric field of 2.5 kV making the cell wall permeable for DNA. Immediately after poration the cells were transferred into 1 ml of BM and incubated for 2 h on a rotary shaker (200 rpm, 37 °C). Then the cells were pelleted (12,000 ×*g*,

1 min, 4 °C), resuspended in 200 µl BM, and put on BM agar plates supplemented with chloramphenicol (10 µg/ml). The plates were incubated for 48 h at 37 °C.

3.4.8 Electrotransformation of *Escherichia coli*

The production of electrocompetent cells of either *E. coli* JM109 or *E. coli* M15 was performed with the method of Farinha *et al*., 1990. The transformation via electroporation was performed with the method of Dower *et al*., 1988.

For the production of electrocompetent cells, 20 ml of LB were inoculated with a preculture. The culture was grown on a rotary shaker (200 rpm, 37 °C) to an OD_{578} of 0.5 and then the cells were pelleted by centrifugation (3,000 ×*g*, 10 min, 4 °C). All following steps were performed on ice. The cells were washed with 10 ml and with 1 ml 4 °C cold buffer (1 mM MOPS, 15 %glycerol). The cells were resuspended in 200 µl 4 °C cold MOPS buffer and aliquots of 40 µl were stored at -80 °C until use.

For the electrotransformation the electrocompetent cells were thawed on ice. For transformation of intact plasmid, 5 ng DNA were added to the cells. The cells were transferred to cooled electroporation cuvettes and the cells were electroporated by applying a pulsed electric field of 2.5 kV. Immediately after electroporation the cells were suspended in 1 ml SOC medium and incubated for 1 h on a rotary shaker (200 rpm, 37 °C). The cells were then pelleted (12,000 ×*g*, 10 s, 4 °C) and resuspended in 200 µl SOC medium and put on selective LB agar plates. The plates were incubated for 24 h, at 37 °C.

3.4.9 Heat pulse transformation of *Escherichia coli*

The transformation of heat competent cells of *E. coli* XL1-Blue (Stratagene) was performed as described by the manual of the QuickChange Site-Directed Mutagenesis Kit.

For the production of competent XL1-Blue cells, 30 ml of LB were inoculated with a preculture. The culture was incubated on a rotary shaker (200 rpm, 37 °C) in a 300 ml baffled flask and grown to an OD_{578} of 0.5-0.6. Growth was stopped by incubating the culture for 10 min at 4 °C. The cells were pelleted by centrifugation (3,000 ×*g*, 15 min, 4 °C) and washed in 10 ml TSB (100 g/l PEG 6000, 10 mM $MgSO_4$, 10 mM $MgCl_2$, 20 g/l LB) This was repeated two times and the cells were suspended in 300 µl TSB and aliquots of 50 µl were stored at -80 °C until use.

For the heat pulse transformation, 50 µl of competent cells were incubated with plasmid DNA (1.5 µl of DpnI digested plasmid) for 30 min on ice. Then the cells were heated to 42 °C for 45 s, which was directly followed by 2 min incubation on ice. After the addition of 1 ml SOC medium, the cells were incubated on a rotary shaker (200 rpm, 37 °C) for 1 h. The bacteria were then pelleted (12,000 ×*g*, 10 s, 4 °C) and suspended in 200 µl SOC medium and put on selective LB agar plates. The plates were incubated for 24 h at 37 °C.

3.4.10 Construction of plasmids for *narG-lip* expression study

The staphylococcal promoter probe vector pPS44 (Peschel *et al*., 1993) was used to construct the plasmid pMW1001, carrying the reporter gene fusion *narG-lip*. The used primers are shown in Table 1. The promoter of *narG* was amplified from genomic DNA of *S. carnosus* TM300 by PCR using primers pnarG-BamH1-F and pnarG-BamH1-R and inserting BamHI restriction sites. The amplified *narG* promoter sequence comprises region -389 to +185, including two NreC recognition sites. The sequence is shown in Figure 5. The promoter was inserted into the single BamHI restriction site of pPS44. The plasmid pMW1001 (Fig. 6) was then transferred into *S. carnosus* TM300 and *S. carnosus* m1 by electroporation.

For construction of plasmid pMW1040 (Fig. 6) the reporter gene fusion *narG-lip* from pMW1001 was amplified by PCR using primers narGlip-SbfI-F and narGlip-NheI-R to insert SbfI and NheI restriction sites. The fragment was inserted into the vector pRB473nreABC at the SbfI and NheI restriction sites, creating pMW1040. pRB473nreABC is a derivative of the *E. coli*/*S. carnosus* shuttle vector pRB473 (Brückner, 1992) carrying the *nreABC*-operon with its native promoter (Müllner *et al*., 2008). pMW1040 was amplified in *E. coli*, isolated and transformed into *S. carnosus* m1 by electroporation.

The plasmid pMW1393 (Fig. 6) is a pMW1040 derivative with an *nreA* deletion. This deletion was performed by amplification of the plasmid pMW1040 without nreA with primers Del-nreA-F and Del-nreA-R, inserting a BglII restriction site. The fragment was then religated at the BglII restriction sites, resulting in a deletion of *nreA* except for the first twelve base pairs of *nreA* and a deletion of the first six base pairs of *nreB*. *nreB* is put in frame with the beginning of *nreA*, being positioned under control of the native promoter. This plasmid was transformed into *S. carnosus* m1.

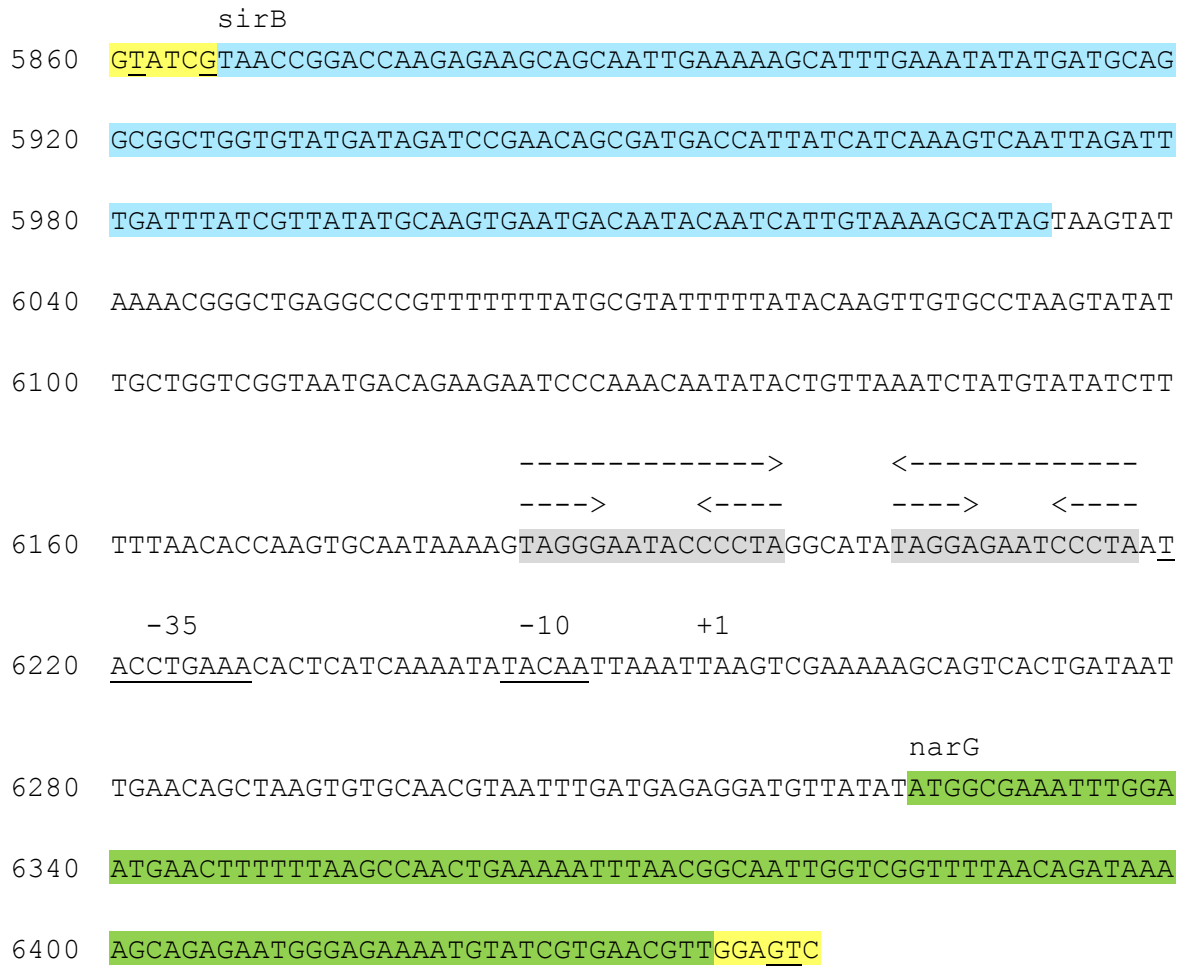

Figure 5: *narG* promoter sequence integrated into BamHI restriction site of pPS44. The sequence has a length of 580 bps (base pairs). It contains 173 bps of the preceding gene *sirB* (blue) and 115 bps of the gene *narG* (green). The underlined bps at the ends of the sequence were mutated for the generation of BamHI restriction sites. The start of transcription is indicated at position +1 and the predicted -10 and -35 regions are underlined. The arrows point out the palindromic sequences and the grey labeled nucleotides present the recognition sites for NreC (Fedtke *et al*., 2002). The numbers indicate the position of the nucleotide sequence in the GenBank (NCBI) that is retrievable under the accession number AF029224.

To create the plasmid pMW1083 encoding NreB(C62S) the residue cysteine-62 of NreB was mutated to alanine on plasmid pMW1040 by site-directed mutagenesis (Stratagene) with the primers F-C62S(TCG)-NreB and R-C62S(TCG)-NreB. This plasmid was amplified in *E. coli* and transformed into *S. carnosus* m1.

To create the plasmid pMW1897 encoding NreB(C62S) and an *nreA* deletion the residue cysteine-62 of NreB was mutated to alanine on plasmid pMW1393 by site-directed mutagenesis (Stratagene) with the primers F-C62S(TCG)-NreB and R-

C62S(TCG)-NreB. This plasmid was amplified in *E. coli* and transformed into *S. carnosus* m1. The correctness of the constructed plasmids was verified by sequencing.

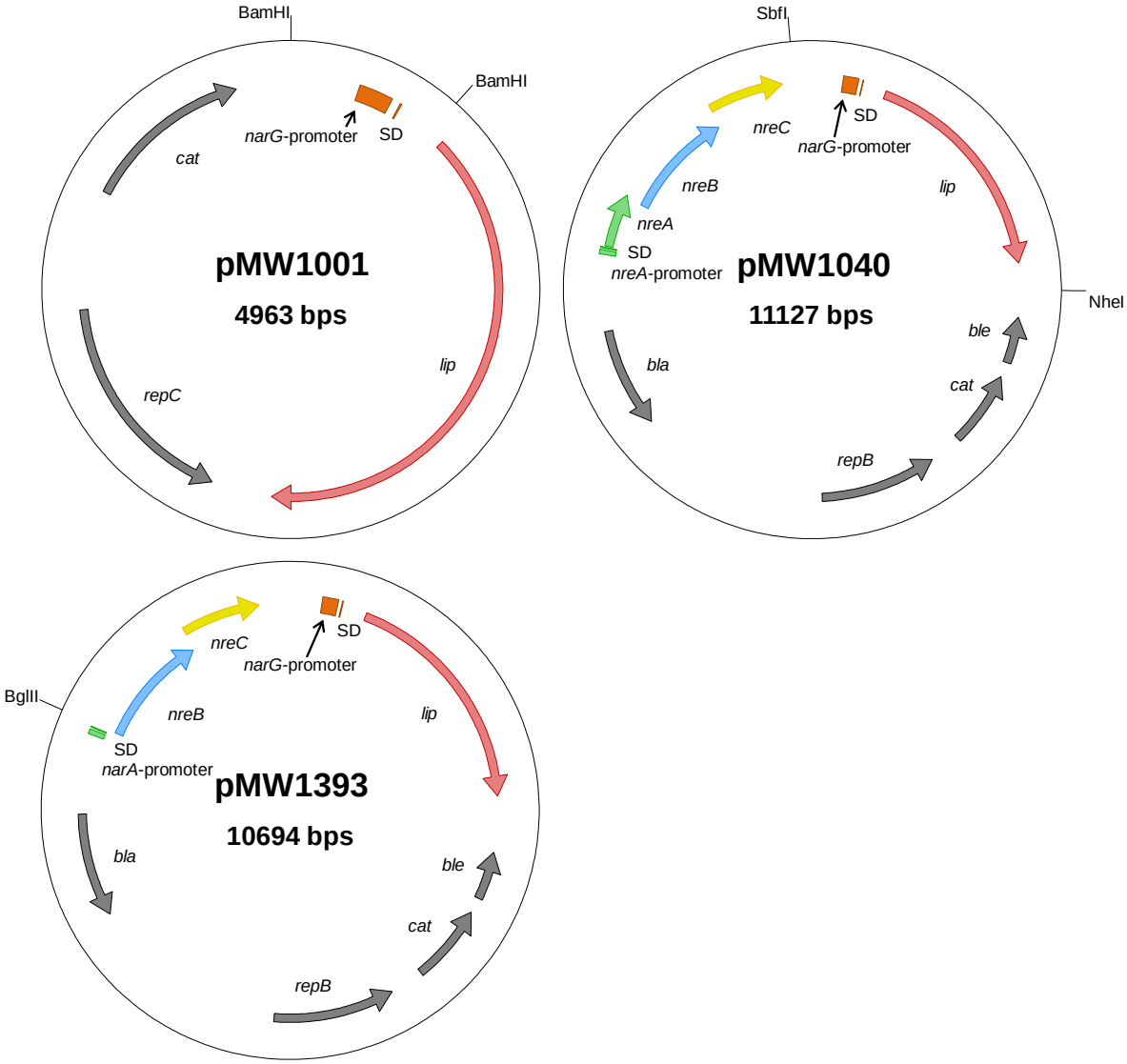

Figure 6: Staphylococcal plasmids with *narG-lip* reporter gene fusion for quantification of *narG* expression. pMW1001 is a staphylococcal plasmid derived from the promoter probe vector pPS44. It carries the promoterless lipase gene lip which was put under the control of the *narG* promoter by insertion into a BamHI restriction site, resulting in formation of the reporter gene fusion *narG-lip*. The sequence inserted before *lip* also includes the SD (Shine Dalgarno sequence) of *narG*. The plasmid carries the gene *cat* for chloramphenicol resistance and *repC* for replication.
pMW1040 is a derivative of pRB473, a shuttle vector for *S. carnosus* and *E. coli*. It carries the reporter gene fusion *narG-lip* and the *nreABC*-operon with its native promoter and terminator. Additionally, it carries a chloramphenicol resistance (*cat*) which is expressed in *S. carnosus* and an ampicillin resistance (*bla*) which is expressed in *E. coli*. It also carries a resistance for bleomycin (*ble*) and the replication gene *repB*. The plasmid pMW1393 is a pMW1040 derivative with an *nreA* deletion. *nreB* is put in frame with the start codon of *nreA* receiving the *nreA* promoter and SD.

Table 1: Primer sequences for construction of plasmids pMW1001, pMW1040, pMW1393, pMW1083, and pMW1897.

Primer	**Sequence 5' → 3'**	**T_M [°C]**
pnarG-BamH1-F	GGTAAAGAATGGATCCTAACCGGAC	65.8
pnarG-BamH1-R	CGACTTTATCGTGGATCCAACGTTC	65.8
narGlip-SbfI-F	GTCACTACCTGCAGGAAGAACG	64.2
narGlip-NheI-R	GAGTATTTAGCTAGCGAACTTTATGAC	63.7
Del-nreA-F	GTTTTACAGATGAGATCTATAAGCAACCG	66.2
Del-nreA-R	CAAAGTAATCTGAAGATCTTACACTATTCAAC	66
F-C62S(TCG)-NreB	GACGAATGCAGTTTGTCGCAGATCGGAAGGATATT	74.3
R-C62S(TCG)-NreB	AATATCCTTCCGATCTGCGACAAACTGCATTCGTC	74.3

3.4.11 Construction of plasmids for overexpression of NreA, NreA-mutants, and NreC

For the production of anti-NreA antibodies the plasmid pMW1243 (Fig. 7) coding for *nreA* with an n-terminal Strep-tag was constructed. *nreA* was amplified with primers NreA(XhoI)-F and NreA(EcoRV)-R (Table 2) and inserted into the MCS of pASK-IBA13plus. The additional thrombin cleavage site of this vector allowed the removal of the Strep-tag.

For overproduction of His_6-NreA(Y95A) the plasmid pMW1733, a pQE31nreA (Schlag, 2008) derivative, was created. By site directed mutagenesis the residue tyrosine-95 was mutated to alanine with the primers nreA-Y95A-F and nreA-Y95A-R. This plasmid was transferred into *E. coli* M15. Mutagenesis of *nreA* for production of further mutants was performed equally, using the plasmid pQE31nreA for mutagenesis. For production of His_6-NreA(F28A) plasmid pMW1613 was created with primers nreA-F28A-F/R. For production of His_6-NreA(W45A) plasmid pMW1614 was created using primers nreA-W45A-F/-R. For production of His_6-NreA(L67N) plasmid pMW1615 was created using primers nreA-L67N-F/-R and for production of His_6-NreA(E101Q) plasmid pMW1801 was created with primers nreA-E101Q-F/-R. The plasmids were transferred into *E. coli* M15.

For overproduction of NreC the pASK-IBA3plus expression vector was used and *nreC* was inserted by amplification with primers NreC-BsaI-F and NreC-BsaI-R into the BsaI site. This way the plasmid pMW1617 (Fig. 7) with *nreC* carrying a C-terminal Strep-tag was created and transformed into *E. coli* JM109. The correctness of the constructed plasmids was verified by sequencing.

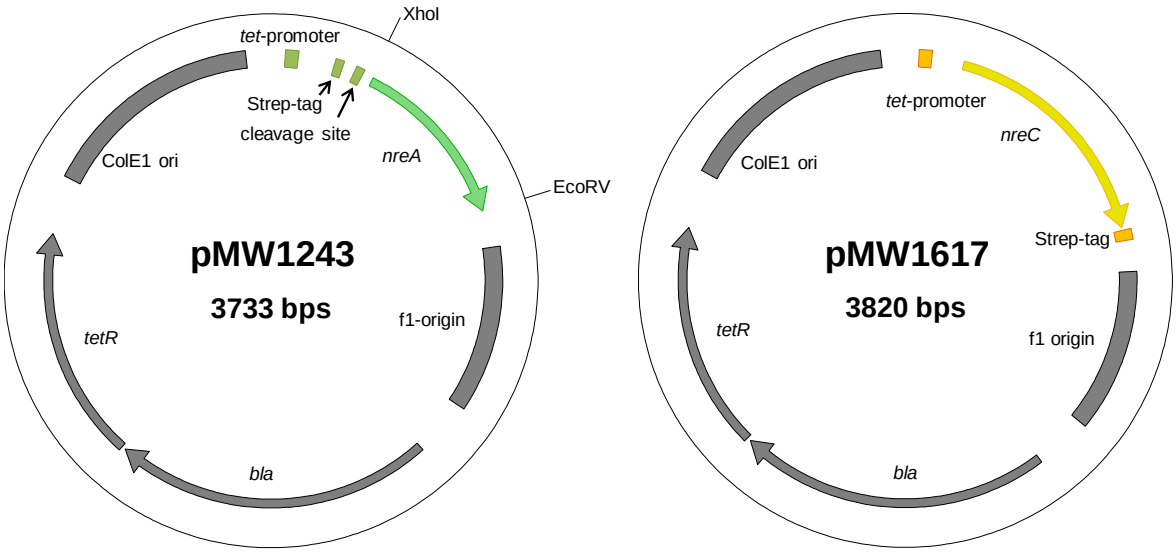

Figure 7: Plasmids for production of Step-NreA and NreC-Strep in *E. coli*. pMW1243, a pASK-IBA13plus derivative carries *nreA* put under the control of the *tet* promoter. By insertion of nreA into XhoI and EcoRV restriction sites it receives an N-terminal Strep-tag with a downstream thrombin cleavage site for removal of the tag. pMW1617, a pASK-IBA3plus derivative, carries *nreC* put under the control of the *tet* promoter with a C-terminal Strep-tag, by insertion into BstI restriction site. Both plasmids contain the ampicillin resistance gene *bla*, the f1-origin, ColE1 ori, and the repressor of the *tet* promoter *tetR*.

Table 2: Primer sequences for construction of plasmids pMW1243, pMW1733, pMW1613, pMW1614, pMW1615, pMW1801, and pMW1617.

Primer	**Sequence 5' → 3'**	**T_M [°C]**
NreA(XhoI)-F	GTGAGGGCTCGAGATGTTGAATAG	65.2
NreA(EcoRV)-R	GTTAATAAATCTTGATATCTATCACGGTTGC	65.6
nreA-Y95A-F	GACAAATTAGGTGCTCCGATTGTTTTGAG	67.4
nreA-Y95A-R	CTCAAAACAATCGGAGCACCTAATTTGTC	67.4
nreA-F28A-F	CAGAGAAATTTGATGCTGCAGCGATTGC	68.5
nreA-F28A-R	GCAATCGCTGCAGCATCAAATTTCTCTG	68.5
nreA-W45A-F	CGGTCATTAAAGCGAAATATGCTTCCGG	68.5
nreA-W45A-R	CCGGAAGCATATTTCGCTTTAATGACCG	68.5
nreA-L67N-F	GACCAGGAAAAGGTAATGCTGGTCTG	67.9
nreA-L67N-R	CAGACCAGCATTACCTTTTCCTGGTC	67.9
nreA-E101Q-F	GTTTTGAGTCAAGCACTAACAGCAATGG	67.2
nreA-E101Q-R	CCATTGCTGTTAGTGCTTGACTCAAAAC	67.2
NreC-BsaI-F	TAGGAGGGTCTCAAATGAAGTAGTGATTGCAGA	71.6
NreC-BsaI-R	GATTCCGGTCTCTGCGCTAAAATCAAGTAACTTTTTCT	73.3

3.4.12 Construction of NreA production plasmid for co-immunoprecipitation

For co-immunoprecipitation the plasmid pMW1951 (Fig. 8) was constructed for overproduction of NreA in *S. carnosus*. The primers for construction are listed in Table 3. For the purpose of NreA overproduction the inducible promoter *xylA* from *S. xylosus* was positioned in front of *nreA*. The plasmid pMW418 was amplified with primers pMW418-HpaI-F and pMW418-BamHI-R leading to the production of the linearized plasmid missing the native promoter of *nreABC*. The linearized plasmid features a BamHI restriction site at the C-terminus and an HpaI restriction site at the N-terminus, right in front of *nreA*. The repressor gene *xylR* and the promoter of *xylA* were amplified from pCQE1 by using the primers xylA-F and xylA-R. The fragment was inserted into the linearized vector putting the promoter of *xylA* right in front of *nreA*. For deletion of *nreBC* the primers Del-nreBC-F and Del-nreBC-R were used for amplifying the plasmid without *nreBC* and by inserting BglII restriction sites. The fragment was then religated resulting in an *nreBC* deletion and *nreA* receiving the terminator sequence of the operon. The correctness of the constructed plasmid was verified by sequencing.

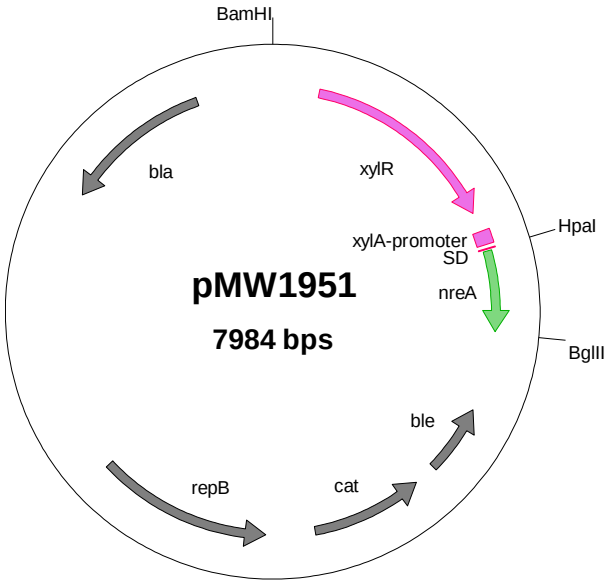

Figure 8: Plasmid for *nreA* expression in *S. carnosus* for the co-immuniprecipitation experiment. pMW1951, a pMW1040 derivative, carries the *nreA* gene which is put under the control of the *xylA* promoter (*Staphylococcus xylosus*) and SD (Shine Dalgarno sequence). The promoter stands under the control of the repressor XylR. The expression is induced by the addition of xylose and repressed by the addition of glucose. The fragment containing *xylR* and *xylA* promoter was inserted into the BamHI and HpaI restriction sites. The genes *nreBC* are deleted by insertion of BglII restriction sites at the beginning of *nreB* and at the end of *nreC*, cleavage and relegation of the plasmid without *nreBC*.

Table 3: Primer sequences for construction of plasmid pMW1951.

Primer	Sequence 5' → 3'	T_M [°C]
pMW418-HpaI-F	GTGAGGGGTTAACATGTTGAATAGTG	64.6
pMW418-BamHI-R	TGTAGAATAGGATCCCCGGGTAC	64.6
xylA-F	TATGAGAAATCGGATCCTAATTATTG	60.1
xylA-R	TTTCATCTGGTTAACCTCCTTAATG	60.9
Del-nreBC-F	GAAAAAGTTACTAGATCTTTGATGAATTTTTGG	65.1
Del-nreBC-R	CTGCGTTAATAGATCTTGTAATTTATCACG	65.1

3.5 Websites used in this study

Information	Website
Blast	http://blast.ncbi.nlm.nih.gov/Blast.cgi
Clustal Omega	http://www.ebi.ac.uk/Tools/msa/clustalo/
DNA-sequencing	http://www.starseq.com
Gen and Genome	http://www.genome.jp/kegg/
NCBI-PubMed	http://www.ncbi.nlm.nih.gov/
Molecular weight calculator	http://web.expasy.org/compute_pi/
Oligonucl. TM Calculator	http://www.basic.northwestern.edu/biotools/oligocalc.html
Sequence alignments	http://www.ebi.ac.uk/Tools/emboss/align/index.html

3.6 Equipment

Equipment	Type	Producer
Anaerobic chamber	Type A chamber	Coy
Biophotometer	UV/Vis photometer	Eppendorf
Blotter	Pierce Fast Semi-Dry	Thermo Scientific
Cell mill	Vi4	Vibrogen
Centrifuge (small)	Biofuge Primo R	Thermo Scientific
Centrifuge (big)	Avanti JE	Beckman Coulter
Centrifuge (Table)	mini Spin plus	Eppendorf
Electroporator	Easyject Prima	EQUIBIO
Film processor	SRX-101A	Konica Minolta
French Pressure Cell Press	FA078E 1	Aminco
Gel drying device	PH-t 20	Biotec Fischer
High vacuum pump	TVE 20	Alcatel
Incubator	BD115 ATP-LIN	WTB Binder
Luminometer Microplate	LUMIstar Omega	BMG LABTECH
Magnetic mixer	MR3001	Heidolph
Oxygen/hydrogen sensor	Model 10	Coy
pH-meter	Digital-pH-Meter	Knick
Phosphoimager	FLA-7000	Fuji Film
Phosphor imaging plate	BAS 2040	Fuji Film
Photometer	Ultrospec 2100 pro	Amersham Biosciences

Equipment	Type	Producer
Photometer	Ultrospec 2100 pro	Amersham Biosciences
Photometer (96-well)	EL 808	Biotec
Rotary shaker	Excella E24 Incubator	New Brunswick Scientific
SDS-PAGE equipment	Mini-Protean Tetra Cell	BioRad
Thermocycler (PCR)	My Cycler thermal cycler	BioRad
Thermomixer	Thermomixer compact	Eppendorf
Tumbling shaker	Duomax 1030	Heidolph
UV-transilluminator	312 nm	Bachofer
Vacuum pump	IP44 KNF	Neuberger Laborport
Vortex	Vortex-Gene 2	Scientific Industries Inc.

3.7 Material and chemicals

Substance	Supplier
Acetic acid >99 %	Carl Roth GmbH
Acrylamide Rotiphorese Gel 30	Carl Roth GmbH
ADP-Glo Kinase Assay	Promega
Agar-Agar, Kobe 1	Carl Roth GmbH
Agarose NEEO Ultra-Qualität	Carl Roth GmbH
Anhydrotetracycline	IBA
Ammonium acetate ($NH_4C_2H_3O_2$)	RPR
Ammonium iron(III) citrate	Carl Roth GmbH
Ammonium persulfate (APS)	Fluka
Ampicillin	Carl Roth GmbH
ATP, 2 Na × 3 H_2O	Roth
ATP [γ-^{33}P] SRF-301	Hartmann Analytics
L-Ascorbic acid	Carl Roth GmbH
Albumin Fraction V (BSA, Bovine Serum Albumin)	Carl Roth GmbH
Bromophenol blue	AppliChem
n-Butanol	Carl Roth GmbH
Calcium chloride ($CaCl_2$)	Carl Roth GmbH
Chloramphenicol	Fluka
Chloroform	Prolabo
Co-immunoprecipitation Test Kit	Miltenyi Biotec
Coomassie Brilliant Blue R-250	Merck
L-cysteine hydrochloride	Merck
Desthiobiotin	Sigma
Dimethyl-4-phenylenediamine (DMPD)	Fluka
Dimethyl sulfoxide DMSO	Fluka
Disodium hydrogen phosphate (Na_2HPO_4)	Carl Roth GmbH
Dithiothreitol (DTT)	Fluka
Ethylenediaminetetraacetic acid (EDTA)	Carl Roth GmbH
Erythromycin	Fluka
Ethanol	Merck

Substance	Supplier
Ethidium bromide	Fluka
Ferrozine	Serva
Glass beads (Ø = 0,1 mm)	Carl Roth GmbH
Glucose	Carl Roth GmbH
Glycerol (86 %)	Carl Roth GmbH
Glycin	AppliChem
Hexokinase from *S. cerevisiae* (1KU)	Sigma
HEPES	Sigma
HRP substrate (chemiluminescent)	Millipore
Hydrochloric acid (HCl)	Fluka
Imidazole	Carl Roth GmbH
Iron chloride ($FeCl_3$)	Fluka
Iron standard Titrisol 1.09972	Merck
Isoamyl alcohol	Fluka
Isopropyl β-D-1-thiogalactopyranoside (IPTG)	Thermo Fischer
Kanamycin	AppliChem
Lysozyme	Carl Roth GmbH
Methanol	Carl Roth GmbH
β-Mercaptoethanol	Carl Roth GmbH
Milk Powder, Skim	Fluka
Magnesium chloride ($MgCl_2$)	Fluka
Magnesium sulfate ($MgSO_4$)	Fluka
MOPS buffer	Carl Roth GmbH
Neocuproine	Sigma
Ni-NTA	Qiagen
Nitrocellulose membrane Whatman	GE Healthcare
p-Nitrophenyl caprylate	Sigma
Orange G	Fluka
Pfu Ultra II Fusion HS DNA Polymerase	Agilent Technologies
Phenol	Amresko
Lucent Blue X-ray Film	Advansta
Phusion Polymerase	Finnzymes
Polyethylene glycol 6000 (PEG 6000)	Carl Roth GmbH
Potassium chloride (KCl)	Carl Roth GmbH
Potassium dihydrogen phosphate (KH_2PO_4)	Carl Roth GmbH
Potassium permanganate ($KMnO_4$)	Janssen Chimica
Proteinkinase K	Merck
RNase A/T1-Mix	Thermo Scientific
Roti-Quant	Carl Roth GmbH
D-Saccharose	Carl Roth GmbH
Sephadex G50 Superfine	GE
Shrimp Alkine Phosphatase	Thermo Scientific
Sodium acetate ($C_2H_3NAO_2$)	Merck
Sodium dihydrogen phosphate (NaH_2PO_4)	Carl Roth GmbH
Sodium dodecyl sulfate (SDS)	Carl Roth GmbH
Sodium chloride NaCl	Carl Roth GmbH

Substance	Supplier
Sodium hydroxide (NaOH)	Fluka
Sodium nitrite ($NaNO_2$)	Fluka
Sodium nitrate ($NaNO_3$)	Fluka
Sodium sulfide (Na_2S $9H_2O$)	Sigma
Tryptone/peptone from casein (8952.3)	Carl Roth GmbH
Tween-20	Serva
Xylene cyanol	Serva
D-(+)-Xylose	Sigma
Yeast extract (servabacter, 24540)	Serva
Zinc acetate dehydrate $C_4H_{10}O_6Zn$	Fluka

4. Results

4.1 *nreA, nreB,* and *nreC* are required for control of *narG-lip* expression

To determine the effect of the NreABC system of *S. carnosus* on nitrate reductase (*narG*) expression *in vivo*, a stable reporter gene system was established. The gene *lip* from *Staphylococcus hyicus* was used which encodes a lipase that is secreted by the cells and is not sensitive to adverse parameters like oxygen or nitrate. For *narG* expression studies the promoter of *narG* was fused to the reporter gene *lip* resulting in the reporter gene *narG-lip*. The *narG* promoter possesses two GC-rich palindromic sequences representing the NreC recognition sites (Fedtke *et al*., 2002). Therefore, the *narG-lip* expression stands under the transcriptional control of NreC and the lipase activity can be correlated to the *narG* expression. The produced lipase was quantified by determining the lipase activity in the supernatant with a colorimetric assay (Rosenstein *et al*., 1992) which is based on the hydrolysis of the chromogenic substrate p-nitrophenyl caprylate. The effect of NreABC was tested with the expression plasmid pMW1040. It carries the *nreABC*-operon with its native promoter and the reporter gene *narG-lip* and was expressed in a strain with the chromosomal deletion of *nreABC*. The role of NreB-NreC or NreA (and variants and deletions thereof) was studied in transcriptional regulation of *narG-lip* in response to oxygen and nitrate availability.

First it was tested if the plasmid-encoded *nreABC*-operon (with native promoter) complements the *nreABC* deletion in *S. carnosus* m1. This was tested by anaerobic growth of *S. carnosus* m1 pMW1040 and the growth was compared to that of the wild type *S. carnosus* TM300 and of *S. carnosus* m1 (Fig. 9). The strain *S. carnosus* m1 pMW1040 showed low growth in absence of nitrate and the growth rate was increased 3-fold in the presence of nitrate. In the absence of nitrate the wild type showed a low growth rate which was also increased (4-fold) in the presence of nitrate. In the *nreABC* deficient strain *S. carnosus* m1, an increase of growth rate was not achieved by the addition of nitrate. This shows that the plasmid-encoded *nreABC*-operon is capable of complementation, because growth is increased by nitrate like in the wild type. Therefore, the plasmid pMW1040 was suitable for testing the effect of NreABC on *narG-lip* expression.

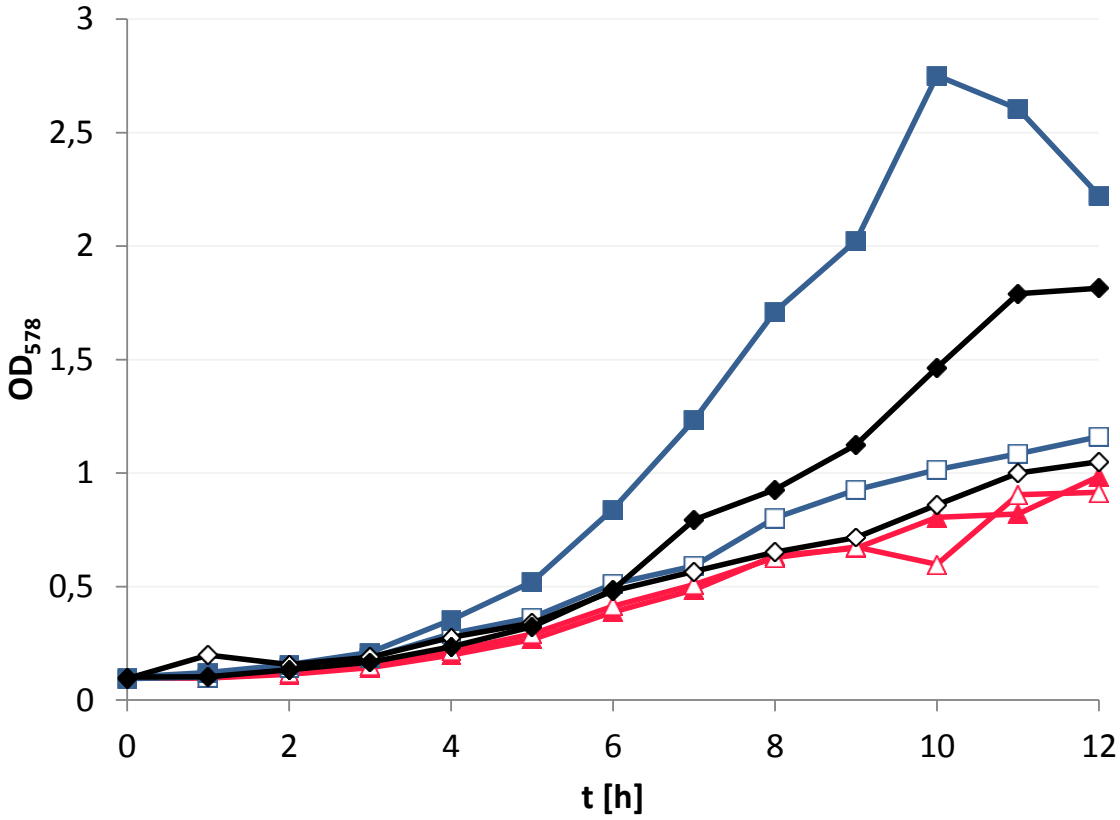

Figure 9: Anaerobic growth for determination of complementation by plasmid-encoded *nreABC* in *S. carnosus* m1. The cells were grown anaerobically in BM medium supplemented with 10 mM nitrate (closed symbols) or without nitrate (open symbols) starting at an OD_{578} of 0.1. Growth was tested of *S. carnosus* m1 (*ermB*::*nreABC*) with plasmid pMW1040 (*nreABC*) (black, diamonds). For comparison growth curves of the wild type *S. carnosus* TM300 (dark blue, squares) and of *S. carnosus* m1 (red, triangles) were recorded.

Figure 10 shows lipase activity measured during aerobic and anaerobic mid-exponential growth of *S. carnosus*. The lipase activity was determined to quantify *narG-lip* expression. The white bars show lipase activity of *S. carnosus* m1 pMW1040. Under the $NreA^+$ $NreB^+$ $NreC^+$ condition, the low lipase activity was slightly increased by nitrate during aerobic growth, but by a factor of 13.3 in the absence of oxygen. By the addition of nitrate the anaerobic expression was further increased 2.3-fold. A strain deficient of the *nreABC*-operon (*S. carnosus* m1 pMW1001, red bars) showed only very low lipase activity under all conditions. Similar low activities were obtained with the strain deficient of the *nreBC* two-component system (*S. carnosus* m1 pMW1532, yellow bars).

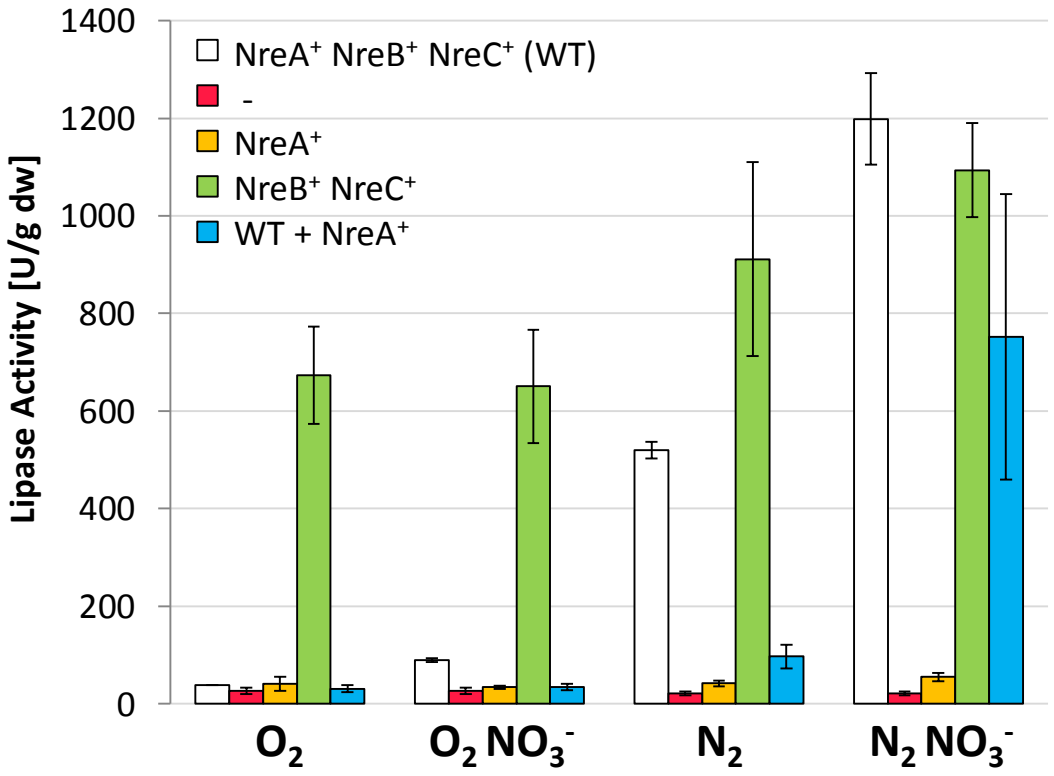

Figure 10: Quantification of *narG-lip* expression *in vivo*. The effect of O_2 and NO_3^- on the *narG* expression was tested in the presence of *nreABC* (*S. carnosus* m1 pMW1040, white bars) and in an *nreABC* deletion mutant (*S. carnosus* m1 pMW1001, red bars). Additional tests were performed with an *nreBC* deletion mutant (*S. carnosus* m1 pMW1532, yellow bars), with an *nreA* deletion mutant (*S. carnosus* m1 pMW1393, green bars) and with a strain which carries chromosomal *nreABC* and also plasmid-encoded *nreA* (*S. carnosus* TM300 pMW1532, blue bars).
The *narG* expression was quantified by measuring the lipase activity photometrically at 415 nm. Supernatant of a culture grown to an OD_{578} of 0.5 was used. The culture was grown in modified BM medium which was supplemented with 10 mM $NaNO_3$ when indicated. The graphs show averages of three independent experiments, where each independent experiment was repeated three times; error bars indicate the standard deviation.

A strain lacking *nreA* (*S. carnosus* m1 pMW1393) but was positive for $NreB^+$ and $NreC^+$ was tested to identify the importance of NreA for control of *narG-lip* expression (green bars). The deletion of *nreA* caused high lipase activity during aerobic growth, which was further increased (1.4-fold) under anaerobic conditions. However, there was no significant nitrate effect visible, neither in presence nor in absence of oxygen. Furthermore, a strain (*S. carnosus* TM300 pMW1532) was tested which carries plasmid-encoded *nreA* in addition to the chromosomal *nreABC* (*S. carnosus* TM300 pMW1532) to produce conditions of NreA overproduction

(blue bars). In presence of oxygen very low lipase activities were measured and nitrate caused no significant induction. By absence of oxygen only a weak induction in contrast to the wild type was caused. Interestingly, addition of nitrate raised *narG-lip* expression to high levels, which was, however, still below the corresponding expression of the wild type. In the absence of oxygen the higher concentration of *nreA* (and presumably NreA) in the cell led to an increase in nitrate effect: That is, the difference between the enzyme activities measured with nitrate and those measured without nitrate was strongly increased (8-fold). To verify the effect of *nreABC* and Δ*nreA* on *narG-lip* expression the lipase activity was measured in two additional strains, one with chromosomal *nreABC* and one with a chromosomal *nreA* deletion (Fig. 11).

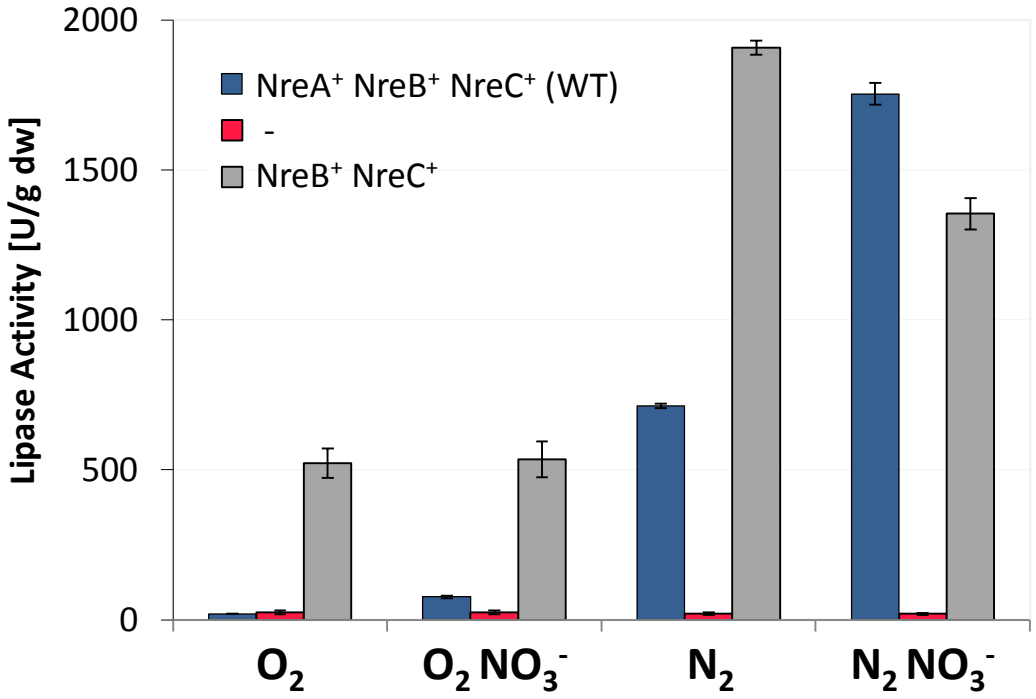

Figure 11: Quantification of *narG-lip* expression in *S. carnosus* with chromosomal *nreABC*, Δ*nreABC*, and Δ*nreA*. The effect of O_2 and NO_3^- on the *narG* expression was tested in the presence of chromosomal *nreABC* (*S. carnosus* TM300 pMW1001, dark blue bars) and in an *nreABC* deletion mutant (*S. carnosus* m1 pMW1001, red bars). The modified BM medium was supplemented with 10 mM $NaNO_3$ when indicated. Additional tests were performed with a chromosomal *nreA* deletion mutant (*S. carnosus* Δ*nreA* pMW1001, grey bars). The *narG* expression was quantified by measuring the lipase activity photometrically at 415 nm. Supernatant of a culture grown to an OD_{578} of 0.5 was used. The culture was grown in modified BM medium which was supplemented with or without 10 mM $NaNO_3$. The graphs show averages of one experiment which was repeated three times; error bars indicate the standard deviation.

The strain *S. carnosus* TM300 pMW1001 also presents the situation of $NreA^+$ $NreB^+$ $NreC^+$ (dark blue bars) but here the *nreABC*-operon is chromosomally encoded and the plasmid only carries the *narG-lip* reporter gene. The low lipase activity was 4-fold increased by nitrate during aerobic growth and by a factor of 37 in the absence of oxygen. The anaerobic expression was further increased 2.5-fold by nitrate. The lipase activity measured after anaerobic growth was here about 1.4-fold higher that in the strain *S. carnosus* m1 pMW1040. The difference can be a result of chromosomal expression but the proportions are similar. However, the results verified the *narG-lip* expression with plasmid-encoded *nreABC*.

The strain *S. carnosus nreA* pMW1001 presents the situation of $NreB^+$ $NreC^+$ (grey bars) but here *nreB* and *nreC* are chromosomally encoded and *nreA* is removed from the chromosome by an in-frame deletion, with *nreB* positioned behind the *nreA*-promoter (Schlag, 2008). The strain showed high lipase activity during aerobic growth, which was further increased (3.6-fold) under anaerobic conditions. In presence of nitrate lipase activity slightly decreased. Under aerobic and anaerobic conditions there was no nitrate effect visible. Similar results were obtained with the strain with plasmid-encoded *nreBC* in the Δ*nreABC* strain *S. carnosus* m1 which confirms the effect of *nreA* deletion.

Additionally, the effects of nitrite and sulfate on *narG-lip* expression were tested, which is shown in Figure 12A. The addition of 5 mM nitrite led to a 2-fold reduced lipase activity. 5 mM sulfate did not show an effect on lipase activity. Nitrate interfered with *narG-lip* expression, whereas sulfate did not influence *narG-lip* expression. It was also tested whether chlorate, an analog for nitrate, showed an effect on *narG-lip* expression (Fig. 12B). Under aerobic conditions *narG-lip* expression and growth was not influenced. However, under anaerobic conditions *narG-lip* expression was reduced 1.8-fold in comparison to the wild type and growth was strongly impaired. This shows that chlorate did not functionally act as an analog for nitrate in *S. carnosus*.

Altogether, an interpretation that the O_2-sensitive transcriptional activating system NreB-NreC is modulated by NreA is compatible with the quantitative data obtained with the *narG-lip* reporter. The data show that NreA regulates *narG-lip* expression in a negative manner in the absence, and in a positive manner in the presence of nitrate.

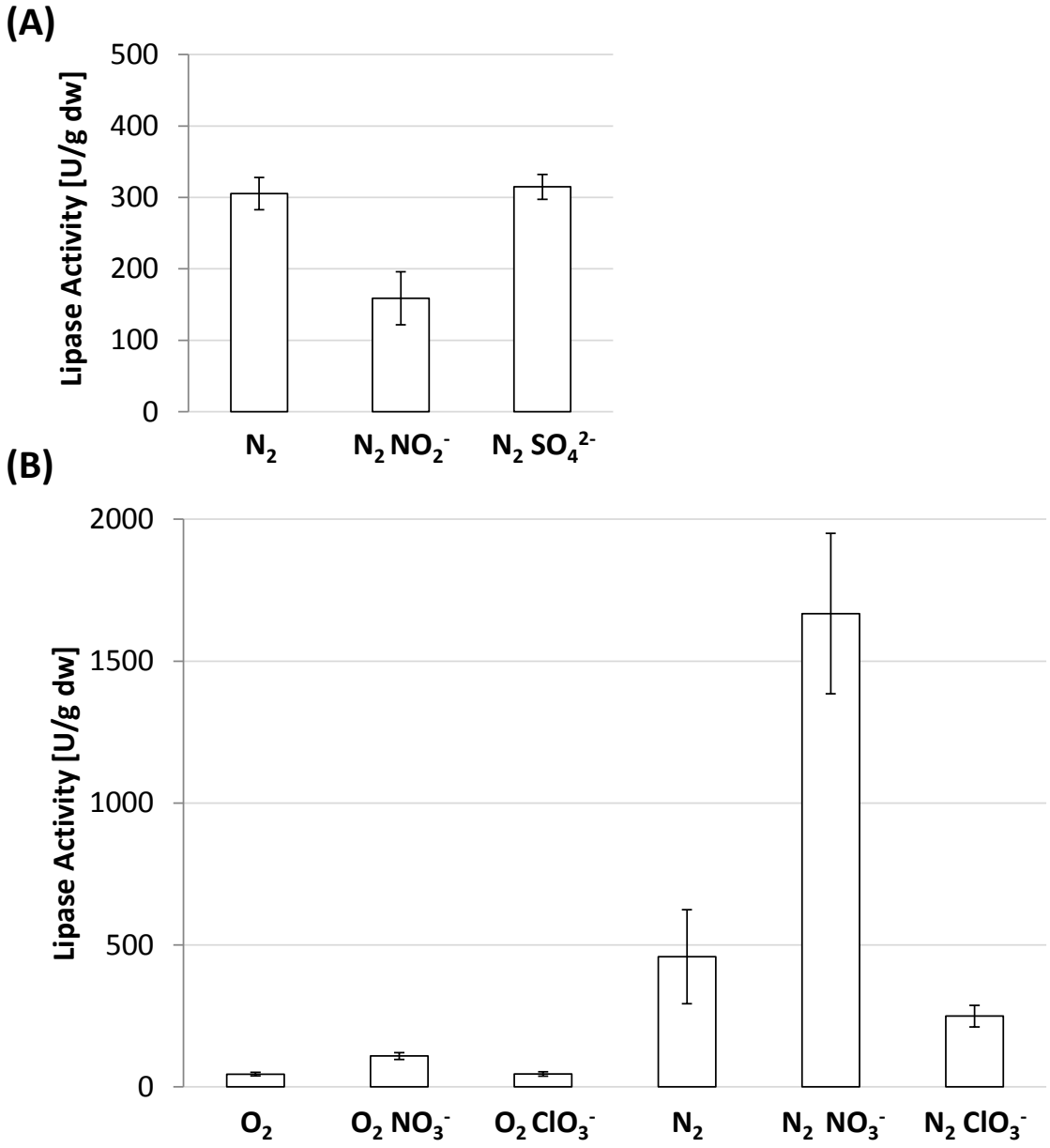

Figure 12: Effect of nitrite and sulfate (A) and chlorate (B) on *narG* expression.
(A) The effect of NO_3^- and SO_4^{2-} on the *narG* expression under anaerobic conditions was tested in the presence of NreABC (*S. carnosus* m1 pMW1040). The medium was supplemented with 5 mM $NaNO_2$ or 5 mM $NaSO_4$. The graphs show averages of three independent experiments, where each experiment was repeated three times.
(B) The effect of ClO_3^- on the *narG* expression under aerobic and anaerobic conditions was tested in the presence of NreABC (*S. carnosus* m1 pMW1040). The medium was supplemented with 10 mM $NaNO_3$ or with 10 mM $NaClO_3$ under aerobic conditions and 0.5 mM $NaClO_3$ under anaerobic conditions. The graphs show averages of three independent experiments, where each independent experiment was repeated three times. The *narG* expression was quantified by measuring the lipase activity photometrically at 415 nm. Supernatant of a culture grown to an OD_{578} of 0.5 was used. The error bars indicate the standard deviation.

4.2 NreB phosphorylation is modulated by NreA in response to nitrate availability

For identifying the effect of NreA on NreB autophosphorylation activity, the proteins were overproduced and purified. NreB-His_6 was produced in *S. carnosus* under anaerobic conditions and purified anaerobically as described by Müllner *et al*., 2008. To verify the isolation of fully active, anaerobic NreB, containing the diamagnetic $[4Fe\text{-}4S]^{2+}$ cluster (Müllner *et al*., 2008), the iron and sulfide contents of NreB were determined. The colorimetric assays revealed an iron content of 1.95 mol and a sulfide content of 1.85 mol per mol NreB. From the Fe and S contents, it can be estimated that at the most 0.46 mol of $[4Fe\text{-}4S]^{2+}$ cluster were incorporated per mol of NreB. This NreB preparation was brown in color and the absorption spectrum showed a shoulder at 420 nm which is characteristic for [4Fe-4S] cluster containing proteins (Green *et al*., 1996; Khoroshilova *et al*., 1997).

His_6-NreA was overproduced in *E. coli* M15 pQE31nreA and purified. Overproduction was performed aerobically to reach high protein concentrations of up to 34 mg/ml. To test the effect of nitrate on NreA function it was necessary to overproduce and isolate NreA in the presence of nitrate. Merely the addition of nitrate during the phosphorylation assay or pre-incubation of nitrate with already isolated NreA did not have an effect on NreA function. Therefore, the growth medium was supplemented with nitrate. The isolation buffers were supplemented with nitrate as well to prevent nitrate from being washed away during isolation. After isolation with nitrate, concentrations of 55 mg/ml were obtained. To test the effect of NreA on anaerobic NreB, the air was evacuated from the protein samples to prevent iron-sulfur cluster degradation by oxygen.

In the autophosphorylation assay the effect of NreA on phosphorylation of anaerobically isolated NreB was tested *in vitro*. Phosphorylation of NreB was tested by radiolabeling with [^{33}P]-phosphate derived from [γ-^{33}P]-ATP. The amount of NreB-[^{33}P] was detected by quantitative autoradiography after SDS-PAGE to remove phosphate from the protein which was not covalently bound. Anaerobically isolated NreB was phosphorylated after addition of [γ-^{33}P]-ATP (Fig. 13). Addition of NreC caused instant dephosphorylation of NreB and NreC was instantly phosphorylated. This was shown by the shift in [^{33}P]-content from 40 kDa to 25 kDa on the autoradiogram in Figure 13B. NreC was dephosphorylated rapidly down to background

levels. This indicates that the NreB and NreC phosphorylation and phosphoryl-transfer cascade are intact in the isolated system.

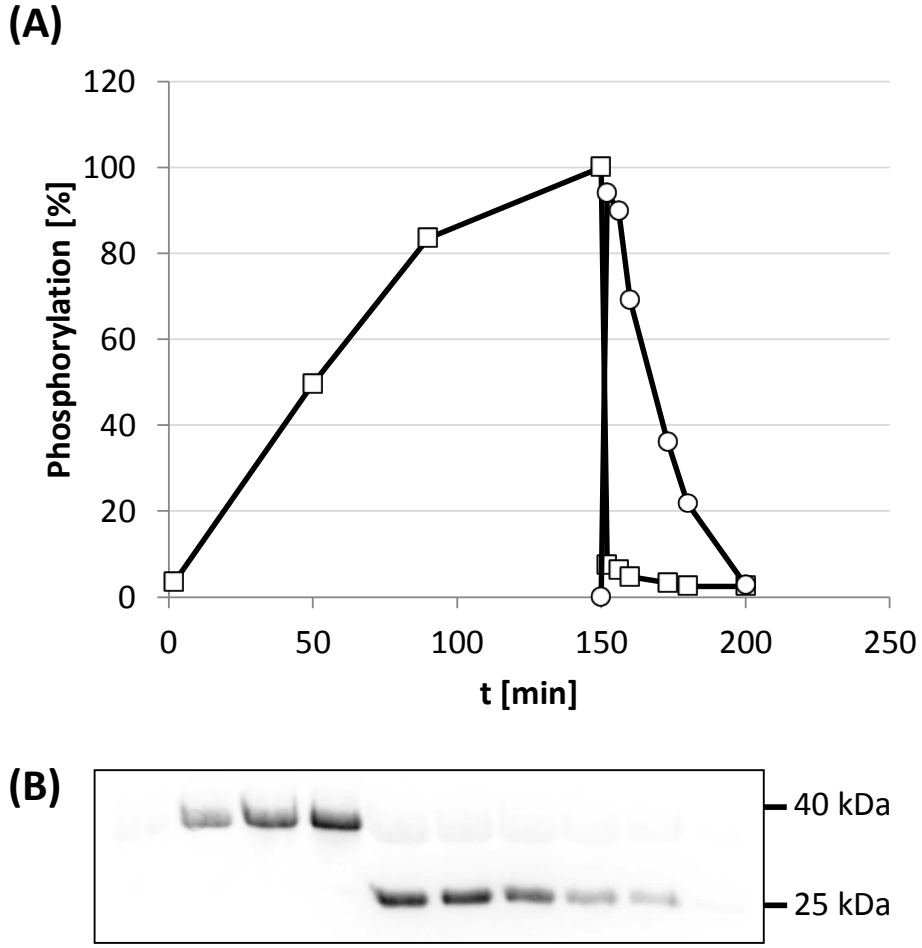

Figure 13: Phosphotransfer from NreB to NreC shown in a kinetic (A) and in the corresponding autoradiogram (B). (A) Anaerobically isolated NreB-His_6 (30 µM) (white square) was phosphorylated by the addition of [γ-^{33}P]-ATP (20 µl of 0.22 µM, 5.5 TBq/mmol) *in vitro*. Samples of 0.15 nmol NreB were applied to SDS-PAGE and [^{33}P] was detected by phosphoimaging. The autoradiogram (B) was used for quantifying [^{33}P] by using the Gel-Pro Analyzer 6.0. After 150 min NreC (white circle) was added to the reaction mixture with a concentration of 30 µM. Samples were taken at different time intervals. NreC was added to the reaction mixture at a concentration of 30 µM. After the addition of NreC-Strep, samples were subjected to the phosphorylation assay containing 0.47 nmol NreC and 0.42 nmol NreB.

It was tested if NreA has an effect on phosphoryl transfer. Therefore, NreA was incubated with NreC and both proteins were added to phosphorylated NreB (Fig. 14). When no NreA and only NreC was added NreC phosphorylation reached 38 %. When NreA and NreC were added together then NreC phosphorylation

reached 35 %. In both cases NreC is fully dephosphorylated after 55 min. This indicates that NreA does not have an effect on the phosphoryl transfer from NreB to NreC.

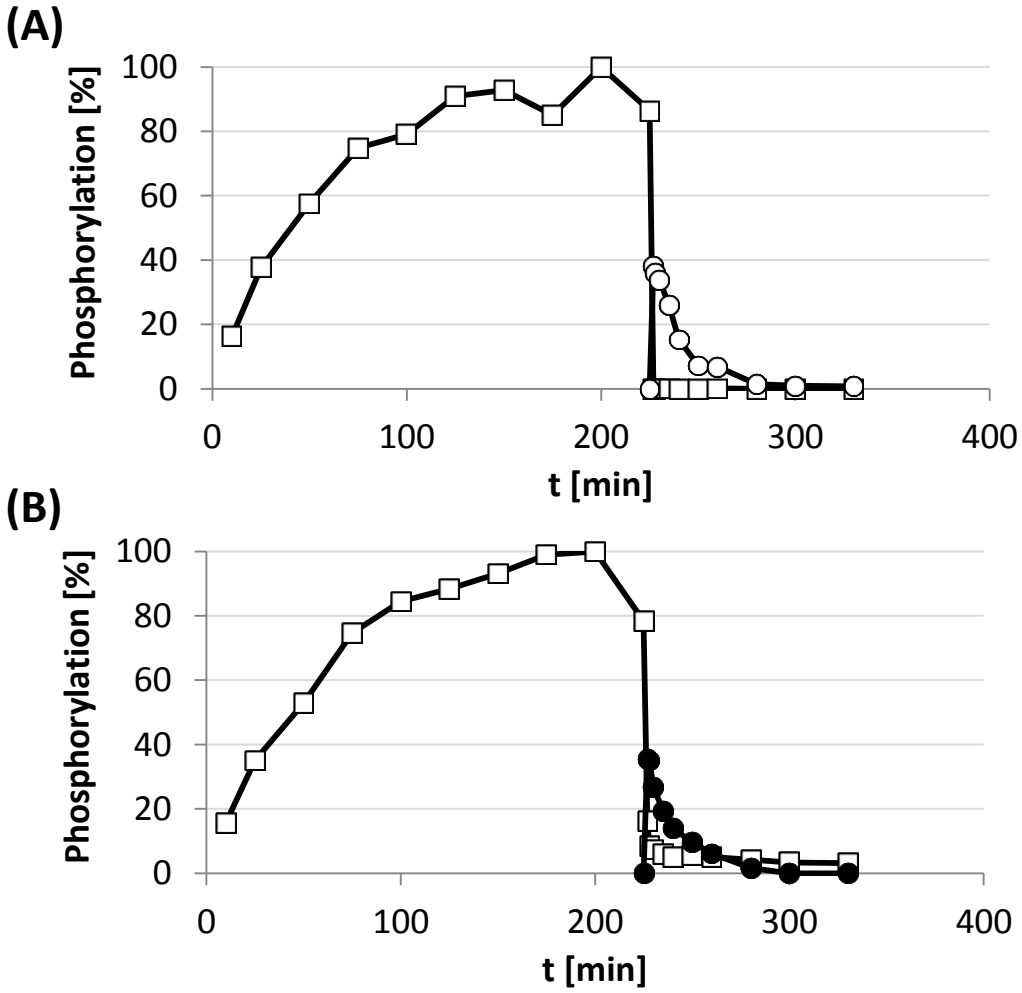

Figure 14: Phosphotransfer from NreB to NreC in absence (A) and in presence (B) of NreA. Anaerobically isolated NreB-His_6 (30 µM) (white square) was phosphorylated by the addition of [γ-^{33}P]-ATP (20 µl of 0.22 µM, 5.5 TBq/mmol) *in vitro*. In (A) and (B) NreB phosphorylation at 200 min is set to 100 %. Samples of 0.14 nmol NreB were applied to SDS-PAGE and [^{33}P] was detected by phosphoimaging. After 225 min NreC (circle) was added to the reaction mixture without NreA (A) and with NreA (B). NreC and NreA were incubated together for 2 h prior to addition and were added at a concentration of 30 µM and 400 µM, respectively. After the addition of NreC-Strep and His_6-NreA, samples were subjected to the phosphorylation assay containing 0.62 nmol NreC and 0.32 nmol NreB.

For testing whether NreA has a direct effect on NreB phosphorylation, labeling of NreB with [^{33}P] was performed in presence and absence of NreA (Fig. 15). NreA

significantly decreased the rate and level of NreB phosphorylation and the autoradiogram also showed that NreA was not phosphorylated.

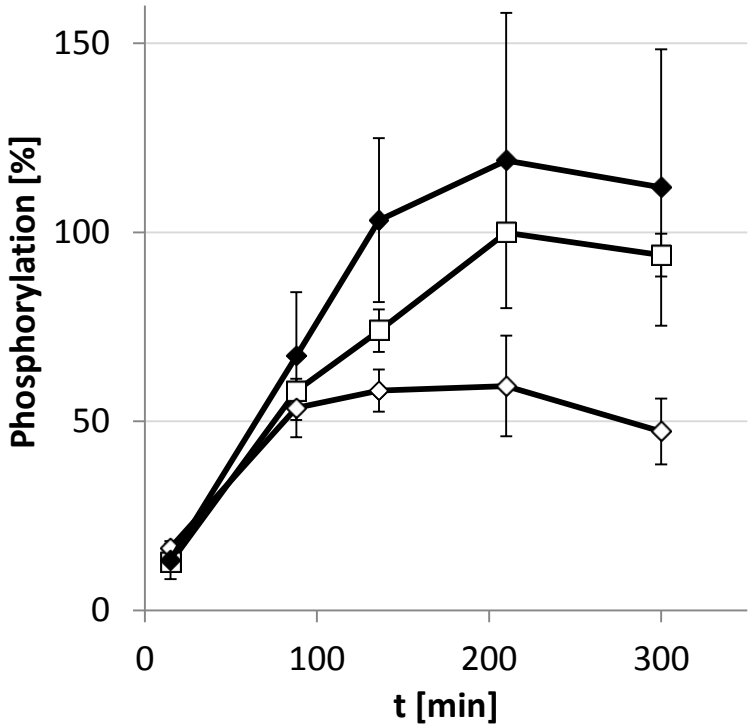

Figure 15: The effect of NreA and NreA·[NO_3^-] on NreB autophosphorylation activity. NreA was added to the reaction mixture before starting the phosphorylation of anaerobically isolated NreB (15 µM) by the addition of [γ-^{33}P]-ATP. NreA and NreA·[NO_3^-] were added at a concentration of 600 µM. The graphs show NreB phosphorylation (white square) in the presence of NreA (white diamond) and NreA·[NO_3^-] (black diamond), with averages of three independent experiments for each measurement. The error bars indicate the standard deviation.

After 200 min the highest level (100 %) of NreB phosphorylation in absence of NreA was reached, while phosphorylation in presence of NreA only reached 60 %. NreA with bound nitrate (NreA·[NO_3^-]), on the other hand, stimulated the amount of NreB phosphorylation by an additional 19 %. This effect of nitrate was only observed with NreA that was overproduced and isolated in the presence of nitrate. Addition of nitrate to isolated NreA (and also long incubation of NreA with nitrate, before addition to NreB) did not have an effect on NreA function. Furthermore, mere addition of nitrate to the reaction mixture had no effect on NreB phosphorylation. This demonstrates that NreA is required for the nitrate effect (Fig. 16).

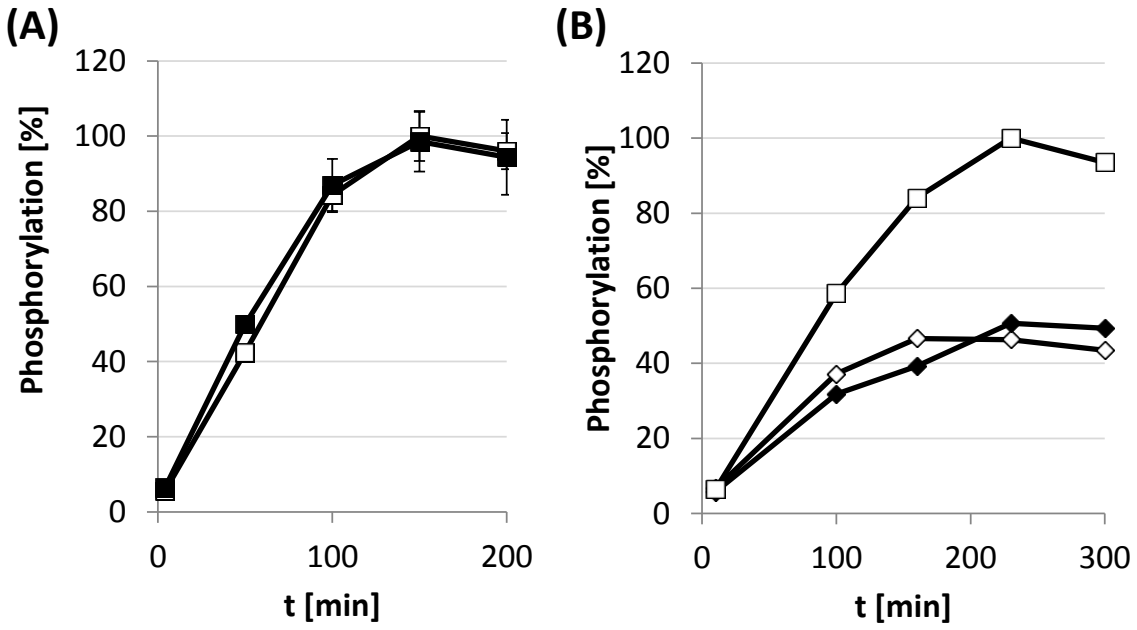

Figure 16: The effect of nitrate on NreB autophosphorylation (A) and on NreA which was isolated without nitrate (B). (A) Anaerobically isolated NreB (15 µM) was phosphorylated by the addition of [γ-^{33}P]-ATP in presence of 5 mM $NaNO_3$ (black square) and without nitrate (white square). Nitrate was added to the reaction mixture before starting the phosphorylation. The graphs show averages of two independent experiments. The error bars indicate the standard deviation. (B) NreB (15 µM) phosphorylation was also monitored in presence of NreA (300 µM) with the addition of $NaNO_3$ (90 mM) (black diamond). NreA was incubated with nitrate beforehand for 1 h. In addition, the NreB phosphorylation was tested in presence of NreA (300 µM) (white diamond) and without addition of NreA (white square).

To show the effect of NreA on NreB and NreC phosphorylation, NreB phosphorylation and phosphotransfer were performed in the presence of NreA (Fig.17). In the presence of NreA, NreB phosphorylation is reduced from 100 % (Fig. 17A) to 60 % (Fig. 17B). In the consequence of low NreB phosphorylation, NreC phosphorylation reaches only 30 % in comparison to high NreC phosphorylation in absence of NreA with 108 %. This shows that NreA decreases NreB phosphorylation which consequently leads to a decreased phosphorylation of the response regulator NreC.

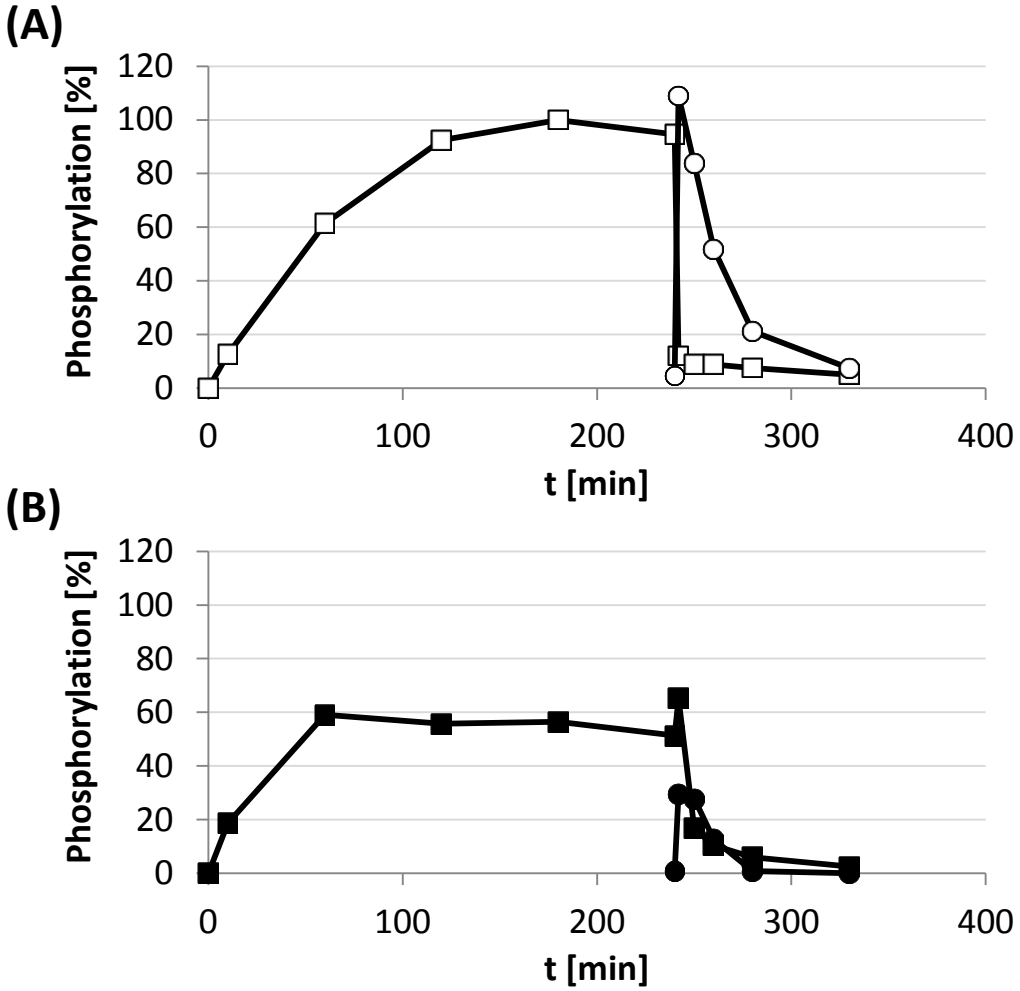

Figure 17: Phosphorylation of NreB and phosphotransfer to NreC in absence (A) and presence (B) of NreA. Anaerobically isolated NreB-His_6 (26 µM) (white square) was phosphorylated by the addition of [γ-^{33}P]-ATP (20 µl of 0.22 µM, 5.5 TBq/mmol) in the absence of NreA (A) and in the presence of 470 µM NreA (B). Samples of 0.13 nmol NreB were applied to SDS-PAGE and [^{33}P] was detected by phosphoimaging. After 240 min NreC (circle) was added to the reaction mixture at a concentration of 25 µM. After the addition of NreC-Strep, samples were subjected to the phosphorylation assay containing 0.5 nmol NreC and 0.44 nmol NreB.

4.3 Mutation Y95A in NreA increases effect of NreA on NreB phosphorylation

Previous studies have shown that mutation of tyrosin-95 to alanine (Y95A) in NreA has a far-reaching effect on induction of nitrate reductase expression by NreA (Niemann *et al*., 2013). The residue Y95 of NreA was initially mutated to alanine by M. Koch-Singenstreu and tested in *narG* expression experiments. The measurement was repeated in this study (and showed the same expression pattern as in Niemann *et al*., 2013) for comparison to NreB phosphorylation experiments with

the purified NreA(Y95A) mutant. In Figure 18 the effect of the variant NreA(Y95A) on *narG-lip* expression and on NreB autophosphorylation are presented for comparison.

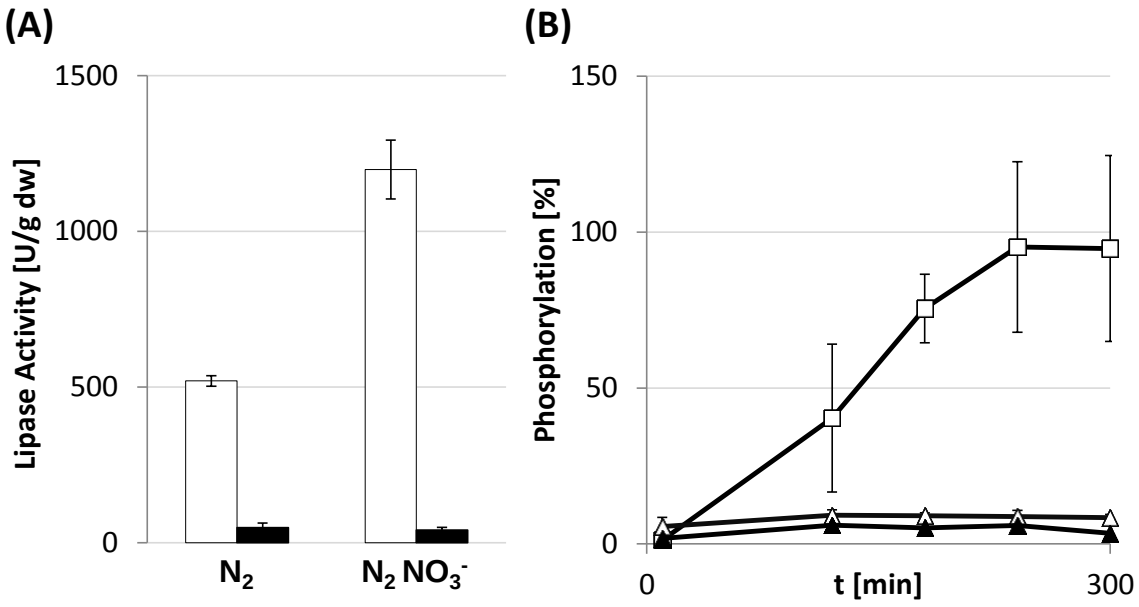

Figure 18: Effect of NreA(Y95A) on *narG-lip* expression (A) and NreB autophosphorylation (B) with and without nitrate. (A) The effect of the mutation Y95A in *nreA* on *narG* expression was tested with the strain *S. carnosus* m1 pMW1298 (black bars) in comparison to wild type *nreA* (*S. carnosus* m1 pMW1040, white bars) under anaerobic conditions. The *narG* expression was quantified as describes above. The graphs show averages of three independent experiments, where each independent experiment was repeated three times; error bars indicate the standard deviation. (B) NreA(Y95A) as well as NreA(Y95A) isolated with nitrate were added to the reaction mixture before starting the phosphorylation of anaerobically isolated NreB (15 µM) by the addition of [γ-^{33}P]-ATP. NreA(Y95A) with and without nitrate were added at a concentration of 600 µM. The graphs show NreB phosphorylation alone (white square) and in presence of NreA(Y95A) (white triangle) and NreA(Y95A)·[NO_3^-] (black triangle), with averages of three independent experiments. The error bars indicate the standard deviation.

Figure 18A shows the effect of NreA(Y95A) on *narG-lip* expression which was tested in *S. carnosus* m1 pMW1298. This strain produces, in addition to $NreB^+$ and $NreC^+$, NreA(Y95A) from plasmid. The measured lipase activities were comparable to those obtained with the *nreABC* deletion strain *S. carnosus* m1 pMW1001 (black bars). Under all tested conditions (aerobic, anaerobic, with and without nitrate) there were only low lipase activities measured. This shows that NreA(Y95A)

has a strong negative effect on *narG-lip* expression, even in the presence of nitrate.

For testing the effect of NreA(Y95A) on NreB phosphorylation *in vitro*, NreA(Y95A) was overproduced and isolated in the absence and the presence of nitrate. By overproduction, protein fractions with concentrations of 52 mg/ml were obtained when isolated with nitrate. When NreA(Y95A) was overproduced and isolated without nitrate, protein concentrations were too low (17 mg/ml) for the NreB phosphorylation assay. The concentration was increased with concentrator columns (vivaspin) to 34 mg/ml. Figure 18B shows the effect of purified NreA(Y95A) on NreB phosphorylation. The NreA(Y95A) protein decreased NreB autophosphorylation to background levels; only 6 % of the NreB phosphorylation was reached. The same inhibition of NreB phosphorylation was observed with NreA(Y95A) which was prepared in the presence of nitrate.

To clearly demonstrate the differences of NreA, NreA·[NO_3^-], and NreA(Y95A) on NreB phosphorylation, the initial rates of NreB phosphorylation were determined as a function of the concentration of the NreA variants. The rate of NreB phosphorylation was set at 100 % in absence of NreA (Fig. 19). The phosphorylation rate of NreB gradually decreased with increasing concentration of wild type NreA. In the presence of 550 µM NreA the phosphorylation rate was decreased to 40 %. NreA(Y95A) was a more efficient inhibitor. In the presence of 550 µM NreA(Y95A) the phosphorylation decreased to 7 % of the original activity. A comparably small effect was shown with NreA·[NO_3^-]. In the presence of 300 µM NreA·[NO_3^-], the NreB phosphorylation rate was stimulated by approx. 20 %, and this level of stimulation remained constant for levels up to 2700 µM NreA·[NO_3^-]. NreA and in particular NreA(Y95A) have an inhibitory effect on NreB phosphorylation. This inhibitory effect is lost in the nitrate conformation of wild type NreA.

Altogether, the data of this study show that NreA has an effect on NreB phosphorylation. The effect is made more clear and explicit by NreA(Y95A) which leads to a full inhibition of phosphorylation of NreB. The strong inhibition by this mutant makes it distinct that NreA in fact has an effect on NreB phosphorylation.

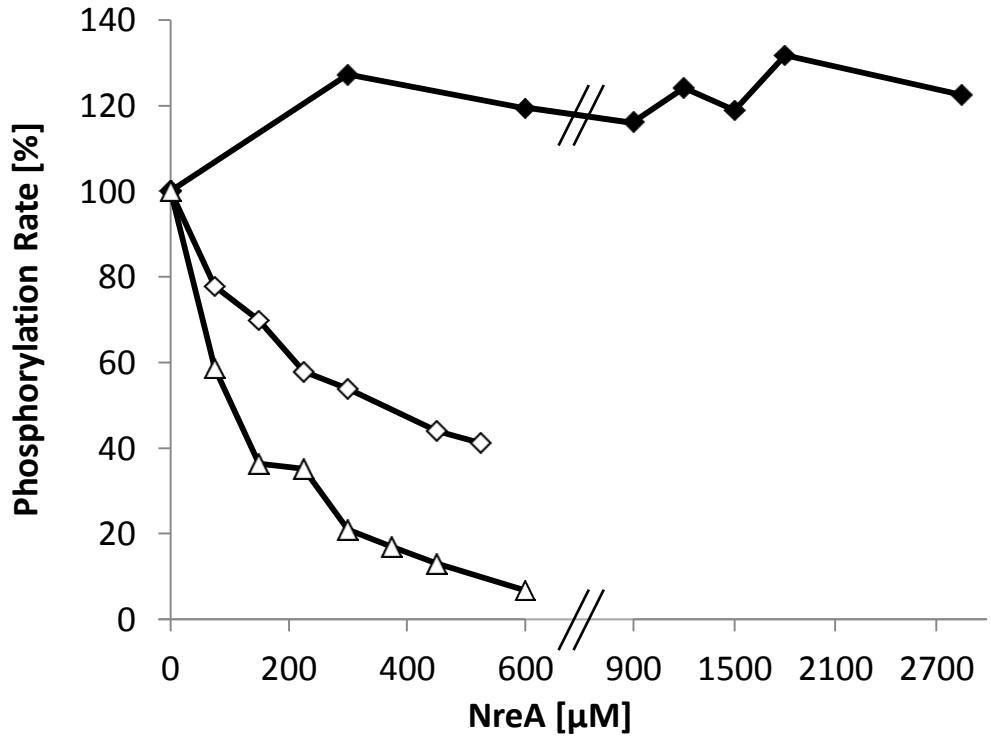

Figure 19: Phosphorylation rate of NreB with rising NreA, NreA·[NO_3^-], and NreA(Y95A) concentrations. The initial rate or amount of NreB phosphorylation after 100 min was determined in the presence of different NreA concentrations, to measure the NreB phosphorylation rate. The phosphorylation rate of NreB, in absence of NreA, was set to 100 %. The graphs show the NreB phosphorylation rate with rising concentrations of NreA (white diamond), NreA·[NO_3^-] (back diamond), and NreA(Y95A) (white triangle).

It was also attempted to isolate other NreA mutants to test their effects on NreB autophosphorylation. Tryptophan-45 was mutated to alanine (W45A) and leucine-67 to asparagine (L67N). Both residues are part of the nitrate binding pocket and are involved in nitrate binding. When NreA(W45A) was isolated a concentration of only 1.6 mg/ml was obtained. SDS-PAGE showed only protein bands of different sizes than NreA(W45A) which shows that isolation was not successful. Isolation of NreA(L67N) resulted in protein concentrations of 0.8 mg/ml when isolated without nitrate and 1.5 mg/ml when isolated with nitrate. An SDS-PAGE showed a high impurity of the protein fractions, but a faint protein band of the expected size of 18 kDa was visible. Two additional residues of NreA were mutated which are not involved in nitrate binding. Phenylalanine-28 was mutated to alanine (F28A). This resulted in a protein concentration of only 5 mg/ml and an SDS-PAGE showed only protein bands of different sizes than NreA(F28A). A mutation of glutamic acid-

101 to glutamine (E101Q) resulted in a protein concentration of 0.9 mg/ml. An SDS-PAGE showed a band of the expected size of NreA(E101Q) but the gel also showed an impurity of the protein solution. Because of the unsuccessful isolation, or low purity and low concentration these mutants could not be tested in the phosphorylation assay.

4.4 NreA and NreA·[NO_3^-] do not effect dephosphorylation of NreB-P

The negative effect of NreA on NreB phosphorylation could be due to inhibition of NreB phosphorylation, but there is also the possibility that NreA stimulates cleavage of the phosphoryl group from NreB-P. Phosphorylation experiments with addition of NreA to already phosphorylated NreB (Fig. 20) showed that NreB phosphorylation was inhibited. However, the experiment could not show a clear result on the question whether NreA is an inhibitor of the kinase or a phosphatase of NreB, because a competition by NreA dephosphorylation and NreB autophosphorylation with residual ATP was possible. This would result in a constant phosphorylation level.

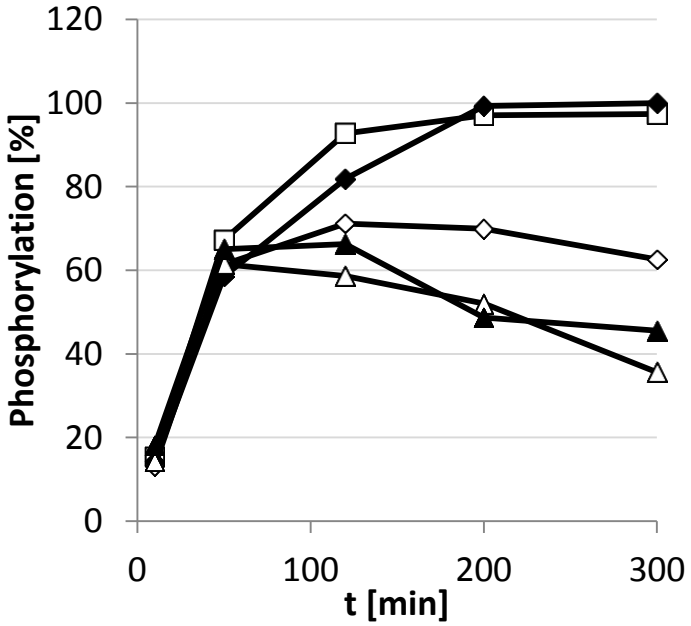

Figure 20: NreB autophosphorylation with late addition of NreA and NreA(Y95A) with and without nitrate. NreB was phosphorylated in the presence of NreA (white diamond) and NreA·[NO_3^-] (black diamond) as well as NreA(Y95A) (white triangle) and NreA(Y95A)·[NO_3^-] (black triangle). The NreA variants were added to the reaction mixture at a concentration of 600 µM, 40 min after starting the phosphorylation of anaerobically isolated NreB (15 µM) by the addition of [γ-^{33}P]-ATP. NreB phosphorylation without additional protein (white square) was monitored for comparison.

To be able to test NreA function, ATP had to be removed from the reaction mixture after NreB-P was produced. To adjust conditions where no further phosphorylation by ATP is possible, residual ATP was removed by anaerobic gel-filtration chromatography. The column had a size exclusion of 50 kDa and NreB which presents a permanent dimer (84 kDa) (Müllner *et al*., 2008) was excluded from the matrix and eluted in early fractions. The smaller ATP had a greater access and was eluted in later fractions. This is shown in Figure 21A. In fraction 5 80 % of applied NreB protein was eluted and it contained 15.4 % of [^{33}P]. Most of [^{33}P] was detected in fractions 9 to 13, which shows that separation of NreB from [γ-^{33}P]-ATP was successful and that [^{33}P] which is present in fraction 5 is bound to NreB. NreB from fraction 5 was used to test the effect of NreA. Figure 21B shows phosphorylation of NreB before application to the gel filtration column and also shows how NreA, NreA·[NO_3^-], NreA(Y95A), and NreA(Y95A)·[NO_3^-] affect NreB-P after removal of residual ATP. The autoradiogram showed a very slow decrease of NreB phosphorylation. This is compatible with the observation that histidyl phosphate is spontaneously dephosphorylated due to intrinsic lability (Krell *et al*., 2010). However, there was no NreB-P dephosphorylation when NreA or NreA(Y95A) were added, either with or without nitrate. Therefore, NreA did not stimulate NreB-P dephosphorylation.

In a similar experiment, residual ATP was removed after phosphorylation of NreB-P by using the hexokinase of *Saccharomyces cerevisiae*. The addition of hexokinase and glucose results in a fast and complete consumption of ATP by the exergonic hexokinase reaction. After phosphorylation of NreB and removal of ATP, NreA was added to the reaction mixture. Again there was no stimulation of NreB-P dephosphorylation which is shown in Figure 22. Therefore, both experiments are in clear contrast to the presence of significant phosphatase activity supplied or stimulated by NreA.

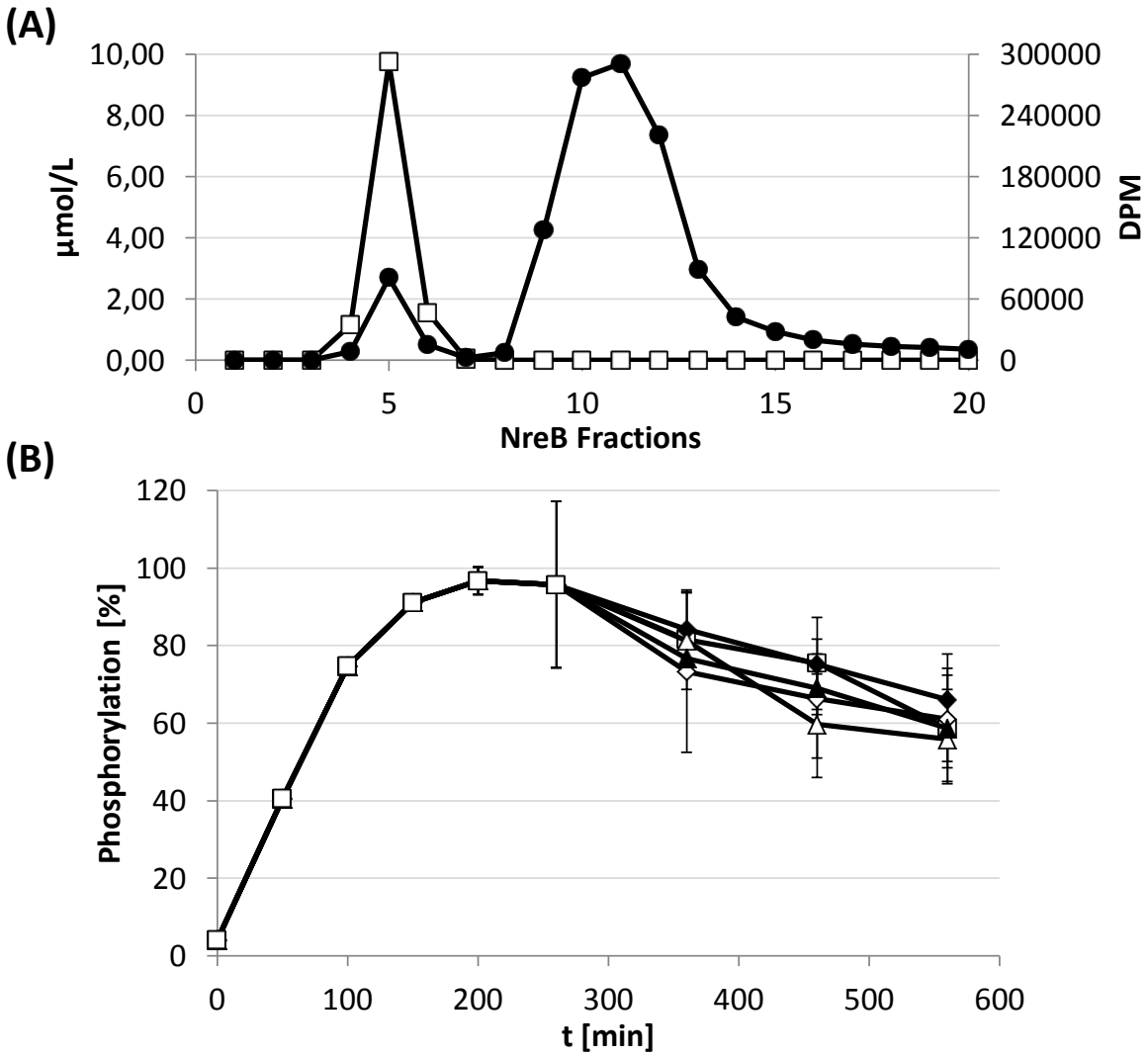

Figure 21: The separation of NreB and ATP (A) and effect of NreA and NreA(Y95A) on phosphorylated NreB (B). Anaerobically isolated NreB (27 µM) was phosphorylated for 200 min by [γ-^{33}P]-ATP and then applied to the gel filtration matrix Sephadex G50 Superfine to remove residual [γ-^{33}P]-ATP. (A) 20 fractions were collected from the column and the protein concentration was detected by Bradford assay (white square). Additionally, the decay per minute (DPM) of [^{33}P] from 10 µl of each fraction was detected by liquid scintillation counting (black circle). Fraction 5 was used for the experiment to monitor the effect of NreA, NreA·[NO_3^-], NreA(Y95A) and NreA(Y95A)·[NO_3^-].
(B) The purified NreB-[^{33}P] (10 µM) from fraction 5 was incubated with NreA (white diamond), NreA·[NO_3^-] (black diamond), NreA(Y95A) (white triangle) and with NreA(Y95A)·[NO_3^-] (black triangle). The proteins were added at a concentration of 400 µM after collecting NreB from the column. For comparison, NreB phosphorylation was monitored without the addition of protein (white square). The diagram shows NreB phosphorylation before application to the column (0 min, 50 min, 100 min, 150 min, 200 min), after collecting fraction 5 from the column (260 min) and after addition of NreA, NreA·[NO_3^-], NreA(Y95A), and NreA(Y95A)·[NO_3^-] (360 min, 460 min, 560 min). The NreA proteins were added to NreB-P directly after 260 min. The phosphorylation state was detected by SDS-PAGE followed by phosphoimaging. The graphs show averages of two independent experiments. The error bars indicate the standard deviation.

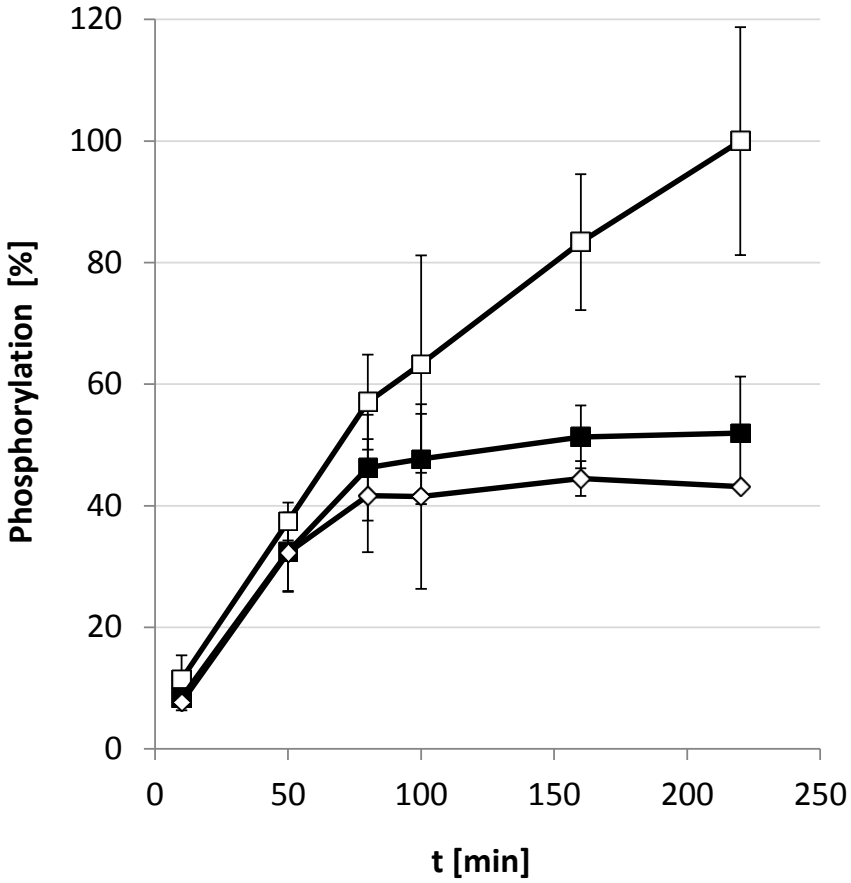

Figure 22: The effect of NreA on phosphorylated NreB after removal of ATP via hexokinase. Anaerobically isolated NreB (15 µM) was phosphorylated with [γ-^{33}P]-ATP in presence of glucose (0.4 µM). After 49 min 40 U/L were added to the reaction mixture for ATP dephosphorylation. After 85 min NreA (400 µM) was added. The graphs show the NreB phosphorylation without hexokinase and without NreA (white square), with hexokinase (black square) and with hexokinase and NreA (white diamond). Averages of three independent experiments were measured; error bars indicate the standard deviation.

A different approach for testing the effect of NreA on NreB autophosphorylation was the detection of ADP production by NreB. This was performed with the ADP-Glo Kinase Assay (Promega) where the kinase activity is detected by quantifying the amount of produced ADP. This assay was also intended for testing whether NreA stimulated dephosphorylation or inhibition of NreB kinase. If NreA stimulated NreB dephosphorylation this would lead to an increase in ADP production.

ATP was subjected to the assay with an abundant concentration. If NreB would be dephosphorylated then the ADP concentration would exceed the NreB concentration. On the other hand, if NreA inhibited NreB phosphorylation this would lead to a reduced NreB phosphorylation. The kinase assay showed that ADP production by

NreB alone did not exceed the NreB concentration. In the presence of NreA and (Y95A)·[NO_3^-] ADP production is highly stimulated. However, the ADP-Glo Kinase Assay showed that ADP production was already stimulated in the presence of NreA alone (Fig. 23A). It was therefore tested if the protein elution buffer shows an effect on ADP production. Figure 23B shows that ADP production is strongly stimulated by the protein elution buffer. This makes it impossible to draw a conclusion from these results on ADP production by NreB in presence of NreA under these circumstances.

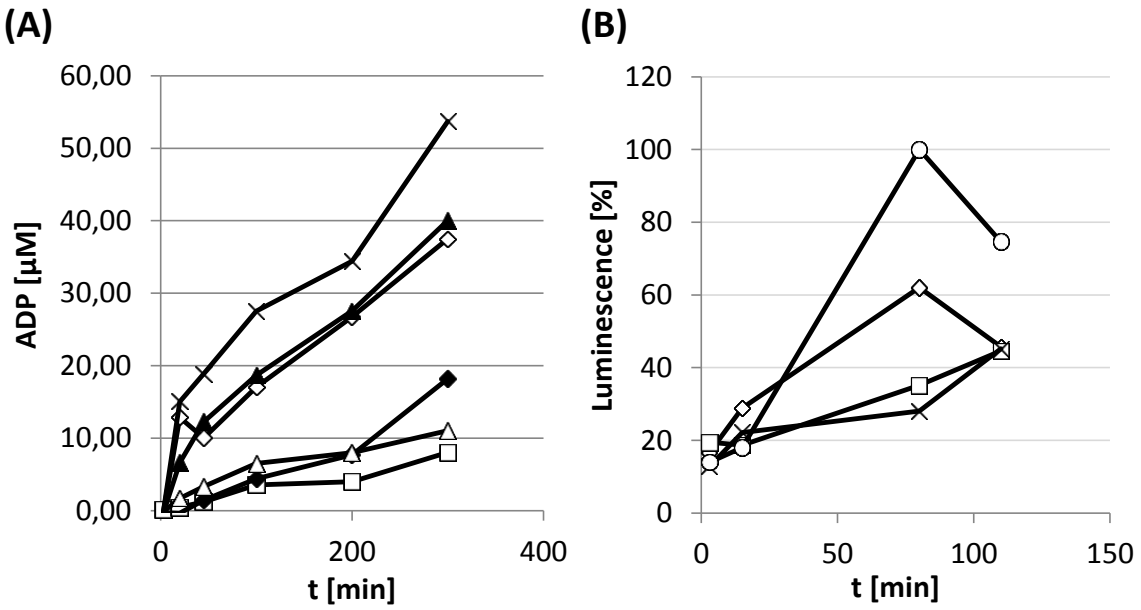

Figure 23: The effect of NreA and NreA(Y95A) (A) and protein elution buffer (B) on ADP production by NreB using the ADP-Glo Kinase Assay. (A) ADP production by anaerobically isolated NreB (10 µM) was monitored in the presence of NreA (white diamond), NreA·[NO_3^-] (black diamond), NreA(Y95A) (white triangle), and with NreA(Y95A)·[NO_3^-] (black triangle). NreA and variants were added at a concentration of 400 µM and ATP at a concentration of 150 µM. As an experimental control, ADP production was monitored in the presence of NreB alone (white square) and NreA alone (black cross). The concentration of ADP production was quantified via calibration line.
(B) ADP production by anaerobically isolated NreB (10 µM) was monitored in the presence 150 µM ATP and 400 µM NreA (white diamond) and protein buffer C (white square). As an experimental control, ADP production was monitored in the presence of only NreA (black cross) and only protein elution buffer C (white circle). The concentrations of ADP production were not quantified via calibration line.

4.5 NreA interacts specifically with NreB

The experimental data suggest that NreA interacts with NreB to control phosphorylation. It was tested by co-immunoprecipitation whether NreA and NreB interact in *S. carnosus*, as only one of the proteins carries a His_6-tag for binding to the magnetic anti-His MicroBeads (Miltenyi Biotec) on a µColumn in a magnetic field. The supernatant of the cell homogenate was tested for co-immunoprecipitation of the non-tagged NreA. If NreA interacts with NreB it should be eluted from the column together with NreB (Fig. 24).

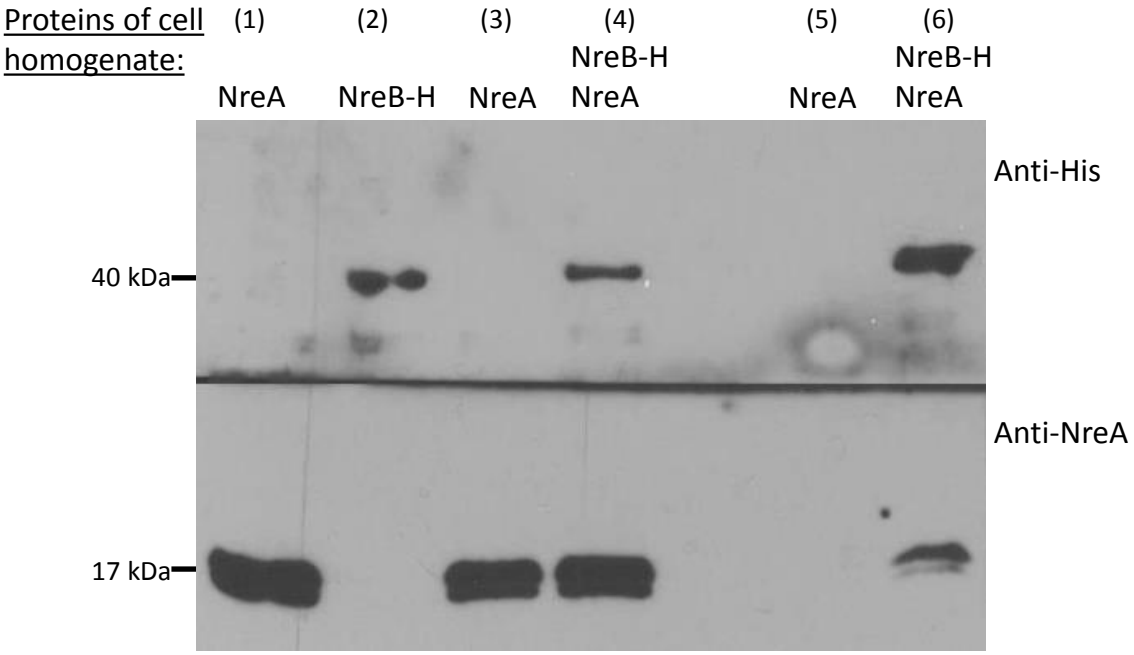

Figure 24: Co-immunoprecipitation of NreA with NreB-His_6. To determine the NreA-NreB interaction NreA (pMW1951) and NreB-His_6 (NreB-H) (pCQE1nreB) were expressed in *S. carnosus* m1. The cleared cell homogenate and eluate were subject to SDS-PAGE, Western blot and immunostaining. For immunostaining the membrane was cut lengthwise (black line) and the upper half was tested with anti-His antibodies and the lower half was tested with anti-NreA antibodies. The cleared cell homogenates from NreA overexpression (1) and from NreB-H overexpression (2) were tested. The mixture from NreA cell homogenate and NreB cell homogenate was incubated with Anti-His MicroBeads and tested before application to the µColumn (4) and also after elution from the µColumn (6) for presence of NreB-His and NreA with anti-His and anti-NreA antibodies. As an experimental control only NreA cell homogenate was incubated with Anti-His MicroBeads and tested before application to the µColumn (3) and also after elution from the µColumn (5) for presence of NreA with anti-NreA antibodies.

For this experiment NreA and NreB-His_6 were overproduced separately and the cleared cell homogenates of both overproductions were tested by Western blotting with anti-His and anti-NreA antibodies for their overproduction. The Western blot of Figure 24 shows that expression of NreB-His_6 and NreA was successful. The cell homogenates containing NreA and NreB-His_6 were mixed 1:1 and were incubated with Anti-His MicroBeads. The mixture was tested with anti-His and anti-NreA before application to the µColumn which shows that both NreA and NreB-His_6 are present. Then the solution was applied to a µColumn where the magnetic MicroBeads are bound, due to the application of a magnetic field. After washing the µColumn the proteins were eluted from the column and were tested by SDS-PAGE and immunoblotting for the presence of NreA and NreB-His_6. The eluate contained NreB-His_6 and in addition also NreA. This indicates that NreA interacted with NreB-His_6 and was not washed from the column and co-immunoprecipitated together with NreB-His_6. As an experimental control, only cell homogenate containing NreA was incubated with Anti-His MicroBeads and was applied to the µColumn. The experimental control shows that no NreA was present in the eluate which eliminates the possibility of unspecific interaction of NreA with the Anti-His MicroBead and the µColumn. The experiment therefore demonstrates that NreA and NreB interact which allows NreA to co-immunoprecipitate with NreB via His_6-tag and Anti-His MicroBeads.

4.6 Effect of NreA on aerobic NreB phosphorylation

The phosphorylation of aerobic NreB was tested. For this purpose NreB was isolated in the presence of oxygen. Aerobically isolated NreB contained 0.00 mol iron and 0.07 mol sulfide per mol NreB which shows that no iron-sulfur cluster is incorporated. Also the spectrum showed no shoulder at 420 nm. In Figure 25A the phosphorylation of aerobic NreB is presented next to the phosphorylation of anaerobically isolated NreB. In comparison to anaerobic NreB, aerobic NreB phosphorylation is decreased to 69 %. This shows that NreB still shows activity and is not fully inactivated by the absence of an Fe-S cluster.

Figure 25B shows the effect of NreA and NreA(Y95A) on aerobic NreB. NreA and NreA·[NO_3^-], as well as NreA(Y95A) and NreA(Y95A)·[NO_3^-] showed a similar effect as on anaerobic NreB: The presence of NreA decreased phosphorylation to 30 %. NreA with bound nitrate NreA·[NO_3^-], on the other hand, stimulated the

phosphorylation of NreB by 11 %. The NreA(Y95A) protein decreased NreB autophosphorylation to background levels; only 8 % of the NreB phosphorylation was reached. NreA(Y95A)·[NO_3^-], also decreased phosphorylation to 10 % after 300 min.

This experiment indicates that NreA does not directly influence the Fe-S cluster of the sensor domain of NreB because NreA has the same effect on aerobic and anaerobic NreB. Aerobic NreB, which is in its less active form, still shows autophosphorylation activity which is affected by NreA in the same way as anaerobic NreB is affected.

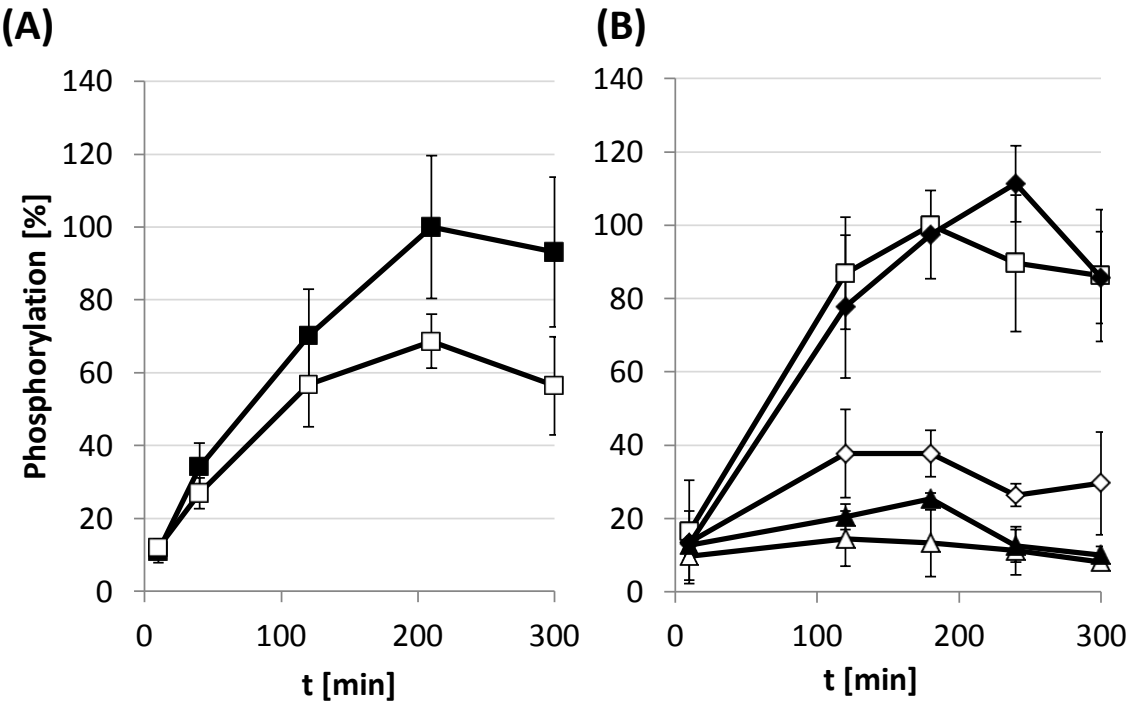

Figure 25: Autophosphorylation of aerobic NreB (A) and the effect of NreA and NreA(Y95A) on aerobic NreB (B). (A) The phosphorylation of aerobic NreB (15 µM, white square) was measured next to anaerobic NreB (15 µM, black square). The phosphorylation was started by the addition of [γ-^{33}P]-ATP. The graphs show averages of four independent experiments. The error bars indicate the standard deviation.
(B) The effect of NreA and NreA(Y95A) on aerobically isolated NreB was detected. NreA was added to the reaction mixture before starting the phosphorylation of anaerobically isolated NreB (15 µM) by the addition of [γ-^{33}P]-ATP. NreA and NreA·[NO_3^-] as well as NreA(Y95A) and NreA(Y95A)·[NO_3^-] were added at a concentration of 600 µM. The graphs show NreB phosphorylation (white square) in the presence of NreA (white diamond), NreA·[NO_3^-] (black diamond), NreA(Y95A) (white triangle) and NreA(Y95A)·[NO_3^-] (black triangle) with averages of three independent experiments for each measurement. The error bars indicate the standard deviation.

4.7 The effect of the mutation C62S on NreB

The cysteine residue C62 is one of the four conserved cysteine residues of NreB. Mutation of this residue should lead to an inactivation of NreB, causing it to permanently transform into its aerobic Fe-S-less conformation (Kamps *et al*., 2004). The effect of the C62S mutation was tested indirectly by determining the expression of the reporter gene *narG-lip* and is presented in Figure 26.

The test plasmid pMW1040 which carries the reporter gene *narG-lip* and the *nreABC*-operon with its native promoter was mutated to *nreAB*(C62S)*C* and the *narG-lip* expression was studied in *S. carnosus* m1 in response to nitrate and oxygen availability (purple bars). Under aerobic conditions the expression was low for all strains and there was no nitrate effect. Under anaerobic conditions the expression in the C62S mutant was slightly elevated to 21 % of anaerobic, wild type expression. There was again no nitrate effect visible.

In a different approach the effect of mutation C62S on *narG-lip* expression was determined in the *nreA* deficient strain *S. carnosus* m1 pMW1393 that was positive for NreB and NreC (orange bars). The combination of the mutation C62S in NreB and a deletion of *nreA* led to low *narG-lip* expression. The lipase activity was comparably low under aerobic and anaerobic conditions as in the strain lacking the *nreABC*-operon and there was no nitrate effect.

These results indicate that mutation C62S has a different effect on NreB than a permanent transfer into its aerobic Fe-S-less conformation. The autophosphorylation assay with aerobically isolated NreB and [γ-^{33}P]-ATP still showed phosphorylation activity which was reduced by NreA but not by NreA·[NO_3^-] (Fig. 25). This nitrate effect, under aerobic conditions, was also monitored in the *narG-lip* expression assay for 'aerobic' NreB. This was, however, not monitored in presence of *nreAB*(C62S)*C*.

A deletion of *nreA* in *S. carnosus* (Fig. 10) led to high *narG-lip* expression during aerobic growth. However, a combination of *nreA* deletion and of mutant NreB(C62S) in NreB caused strongly reduced lipase activity. *narG-lip* expression was not increased which also implies that NreB is not transferred into a permanent 'aerobic' state by mutation C62S.

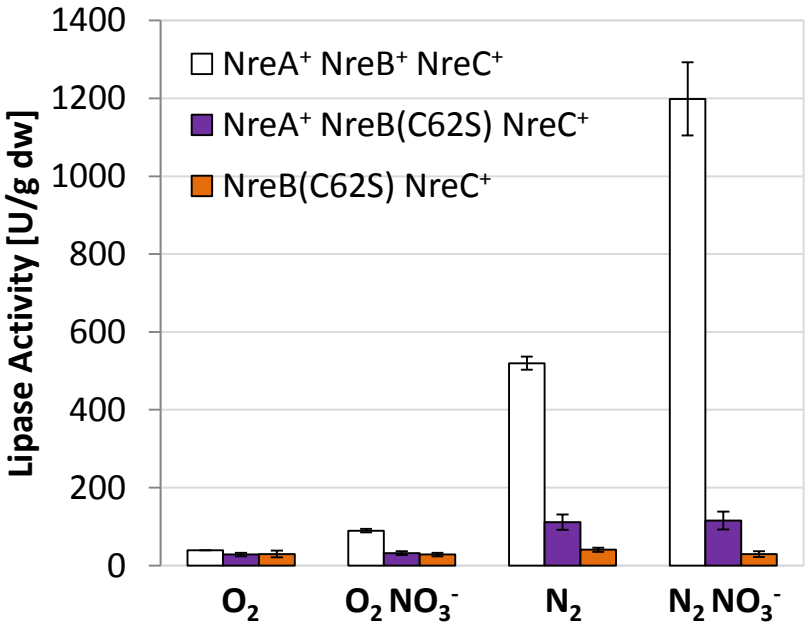

Figure 26: The effect of mutation C62S in NreB on *narG* expression *in vivo*. The effect of O_2 and NO_3^- on the *narG* expression was tested in in an *nreAB*(C62S)*C* mutant (*S. carnosus* m1 pMW1083, purple bars) and in the *nreA* deletion mutant with *nreB*(C62S)*C* (*S. carnosus* m1 pMW1897, orange bars). The expression in presence of WT NreABC (*S. carnosus* m1 pMW1040) is presented for comparison (white bars). The *narG* expression was quantified by measuring the lipase activity photometrically at 415 nm. Supernatant of a culture grown to an OD_{578} of 0.5 was used. The graphs show averages of three independent experiments, where each independent experiment was repeated three times; error bars indicate the standard deviation.

5 Discussion

5.1 NreA presents a nitrate receptor and is part of the NreABC system

In *Staphylococcus carnosus* the Nre (Nitrate regulation) system consisting of NreA, NreB, and NreC regulates the expression of genes for the dissimilatory nitrate reduction under anaerobic conditions. Oxygen sensing is effected by the sensor histidine kinase NreB that is activated under anaerobic conditions by liganding a $[4Fe\text{-}4S]^{2+}$ cluster at four conserved cysteine residues. Active NreB shows high autophosphorylation activity (Kamps *et al*., 2004; Müllner *et al*., 2008). The phosphoryl group at the kinase domain of NreB is transferred to the response regulator NreC and NreC-P binds to the promoters of genes of the nitrate reductase *narGHJI*, the nitrite reductase *nirRBDsirAB*, and nitrate transporter *narT* (Fedtke *et al*., 2002). The third protein of the system is NreA. It is found in all bacteria containing NreBC of the Staphylococcus type with NreB featuring four conserved cysteine residues (Unden *et al.*, 2013). The *nreA* gene is co-localized with the *nreBC* genes in the *nreABC*-operon (Schlag *et al.*, 2008).

The crystal structure of NreA has recently been solved by Niemann *et al*., 2013 and it was shown that NreA folds into a single GAF domain. NreA features a recessed pocket for nitrate binding and the residues involved in nitrate binding are highly conserved among homologs in other staphylococci (Niemann *et al*., 2013). The aim of this study was to physiologically and biochemically confirm NreA as the nitrate regulator of the NreABC system, and to analyze how nitrate regulation is achieved by NreA. *In vivo* and *in vitro* experiments were performed that show that nitrate sensing is performed via NreA and that *narG* expression is controlled by NreA in a nitrate dependent manner. The study gives an insight on NreA function in presence and absence of nitrate and also on the joint regulation by nitrate and oxygen via NreABC system.

5.2 Regulation of *narG* expression by NreABC is dependent on nitrate and oxygen availability

To study the *narG* expression in response to the regulation of the NreABC system a reporter gene system has been established for *Staphylococcus carnosus*. It con-

sists of the lipase gene *lip* (van Oort *et al*., 1989) as the reporter of the system which was fused to the promoter of the nitrate reductase. The promoter region of *narG* comprises two GC-rich palindromic sequences for NreC binding. Therefore, the reporter *lip* stands under the control of NreABC and is expressed in the same pattern as the nitrate reductase. The reporter gene fusion is encoded on a plasmid that also contains the *nreABC*-operon. The plasmid features the properties of a shuttle vector which allowed replication in *E. coli* and *S. carnosus*. The plasmid was used in *E. coli* for well-established genetic procedures (like mutations or deletions of NreA, NreB or NreC) and the effect of NreA, NreB, NreC, and variants or deletions thereof were studied in *S. carnosus* m1, a strain with a chromosomal *nreABC* deletion. Since the reporter gene is not chromosomally integrated it was present in an increased copy number in the cell. The *nreABC*-operon was also present in an increased copy number which leads to a non-wild type expression. However, the plasmid-encoded *nreABC*-operon was suitable for research on the regulation of *narG*, since the Δ*nreABC* mutant *S. carnosus* m1 was successfully complemented by the plasmid-encoded *nreABC*-operon (Müllner *et al*., 2008; this study).

Previous studies on the nitrate reductase expression were based on measurements of nitrate reductase activity. Since the nitrate reductase expression is sensitive to oxygen it could not be distinguished between changes in gene expression or post translational effects, like putative oxygen inactivation. Direct measurements of nitrate reductase activity were performed with benzyl viologen as electron donor. This test system is also sensitive to oxygen. Therefore, an insensitive test system was established that allows a direct measurement of nitrate reductase expression.

The lipase is well suited as a reporter since it is not sensitive to adverse parameters like oxygen, nitrate or nitrite. The lipase is excreted by *Staphylococcus carnosus* and can be detected in the cell medium. Although *S. carnosus* lacks the metalloprotease SphII (which is necessary for cleaving the pro-lipase to form the lipase) the pro-lipase with 50 % activity is capable of achieving well-measurable enzyme activities in the cell medium. The enzyme activity can be correlated with the *narG-lip* expression and coincidentally with *narG* expression.

The *narG-lip* expression study shows that in *S. carnosus* with wild type *nreABC*, expression of *narG* is induced by anaerobiosis and further stimulated by the pres-

ence of nitrate (nitrate effect). This experiment shows that *narG* expression is regulated by these two stimuli. This is plausible because nitrate respiration is performed in the absence of oxygen and in the presence of the alternative electron acceptor nitrate.

The missing *narG-lip* expression in the Δ*nreABC*-mutant under both aerobic and anaerobic conditions in the presence and absence of nitrate confirms that expression of the nitrate reductase operon is dependent on the presence of *nreABC*. A deletion of *nreBC* leads to a comparably low expression under these conditions. Thus, NreA alone is not capable of activating *narG* expression.

A deletion of only *nreA* shows a loss of nitrate effect. The anaerobic *narG* expression in absence of nitrate is not lower than *narG* expression in the presence of nitrate. Therefore, nitrate regulation is dependent on the presence of NreA, and NreA is involved in inhibition of *narG* expression in the absence of nitrate. Interestingly, the *narG* expression is already strongly induced under aerobic conditions. This indicates that the NreBC two-component system is active in the presence of oxygen. This will further be discussed in chapter 5.7. A different approach for identifying the effect of *nreA* on *narG* expression was to generate a situation of NreA overproduction in the cell. A higher copy number of NreA protein in proportion to NreBC leads to lower *narG* expression under anaerobic conditions in the absence of nitrate. The addition of nitrate led to a strong increase of expression although it was still slightly lower than *narG* expression in the wild type. This shows that a higher copy number of NreA leads to a stronger inhibition of *narG* expression in the absence of nitrate. In the presence of nitrate this repression is almost fully annihilated. This increase in nitrate effect by NreA overproduction supports the assumption that NreA is a negative regulator of *narG* expression and responsive to nitrate.

It was also tested whether structurally related electron acceptors like nitrite or sulfate have an effect on *narG* expression. It was shown that sulfate has no effect and nitrite has a negative effect on *narG* expression. This is coherent with the finding that nitrite destructs iron-sulfur clusters by the formation of iron-nitric oxide complexes (Reddy *et al*., 1983). Nitrite could affect the iron-sulfur cluster of NreB and interfere with its functionality, which would lead to a decreased *narG* expression. Additionally, it was tested whether an analog for nitrate shows an effect of up-regulation of *narG* expression. ClO_3^- is used as an analog for NO_3^- in microor-

ganisms and plants (Kucera, 2006; Deane-Drummond and Glass, 1982). However, it did not lead to an increase of *narG* expression in *S. carnosus*. *narG* expression was negatively affected by chlorate. This indicates that chlorate is not a functional substitute for nitrate in the NreA protein. Also growth of cells was strongly affected by chlorate under anaerobic conditions but not in the presence of oxygen, which indicates that it interferes with anaerobic metabolism.

Recently, it was shown in an *nreA* expression study with *nreA-lip* that expression of *nreA* is slightly enhanced in the presence of nitrate under anaerobic conditions (Handel, 2013). This small increase of *nreA* and supposedly also *nreBC* expression could contribute to a higher *narG* expression in the wild type under anaerobic conditions, in the presence of nitrate. This upregulation could be affected by the redox and oxygen sensory two-component system AirSR. It has been shown by Yan *et al*., 2011 that AirSR from *S. aureus* is activated under anaerobic conditions and binds to the promoter of the *nreABC*-operon. Also *airSR* expression is increased in the presence of nitrate under anaerobic conditions. Additionally, it was described that AirR binds to the promoter of *narG* and expression of *narG* in *S. aureus* is dependent on the presence of AirSR (Yan *et al*., 2011). It seems likely that regulation of *narG* expression in *S. carnosus* is similarly affected by AirSR, because a homolog system is present in *S. carnosus*. However, the regulation by AirSR in *S. carnosus* still has to be tested by further research.

Overall, the *in vivo* experiments of this study show that expression of *narG* responds to O_2 and nitrate and regulation is performed by NreABC. The response to O_2 is effected by the NreB-NreC two-component system (Kamps *et al.*, 2004; Müllner *et al.*, 2008), whereas NreA is responsible for nitrate regulation together with the NreB-NreC proteins (Schlag *et al.*, 2008).

5.3 NreA controls kinase activity of NreB in a nitrate dependent manner

Under anaerobic conditions NreB binds a $[4Fe\text{-}4S]^{2+}$ cluster and is transferred to its active conformation. Active NreB shows high autophosphorylation activity at the kinase domain where the conserved histidine residue H159 is phosphorylated (Kamps *et al*., 2004; Müllner *et al*., 2008). To study the function of NreA it was tested *in vitro* if it affects NreB phosphorylation. NreB was isolated anaerobically and the phosphorylation was monitored (by radiolabelling) in presence and absence of NreA. This experiment showed on the one hand that NreA obviously in-

hibited autokinase activity of anaerobic (active) NreB. On the other hand NreA·[NO_3^-] did not inhibit NreB phosphorylation. When NreA is purified in the presence of nitrate, it is bound in the nitrate binding pocket, as was shown by the crystal structure (Niemann *et al*., 2013). Then NreA switches to a non-active conformation. Nitrate alone did not show an effect on NreB autophosphorylation.

This experiment is coherent with the *in vivo narG-lip* expression experiments where *narG* expression is repressed by NreA and this repression is relieved in the presence of nitrate. Also a deletion of *nreA* leads to a loss of inhibition *in vivo*. The results of the autophosphorylation assay allow a closer characterization of this inhibitory effect of NreA. NreA is the nitrate receptor of the system that transmits the nitrate state via NreB to the transcription factor NreC. It was shown that NreA does not bind to the promoter of *narG* (Reinhart, 2010), interact with NreC (Nilkens *et al*., 2013), or directly affect NreBC phosphotransfer. Overall, it can be stated that the nitrate receptor NreA inhibits NreB phosphorylation, and this inhibition is relieved by nitrate. Thus, nitrate regulation in *S. carnosus* is closely intertwined with O_2 sensing by NreB and the nitrate receptor NreA modulates the NreB kinase. The close link between both systems is reflected on the genetic level by organizing *nreA* with *nreBC* in the same operon.

5.4 The mutant NreA(Y95A) illustrates the effect of NreA on NreB autophosphorylation

The crystal structure (Niemann *et al*., 2013) defined the nitrate binding pocket of NreA. When nitrate binds in the pocket it is shielded from solvent by hydrophobic residues and nitrate is coordinated by hydrogen bonds with the four amino acids L67, A68, I97, and W45. In addition the side chain of Y95 acts as a lid which seals the nitrate binding pocket (Niemann *et al*., 2013). The importance of this residue became obvious by mutation. The mutation Y95A in NreA strongly affected the *narG-lip* expression in *S. carnosus*. The mutation diminishes efficient expression of *narG* under aerobic and anaerobic conditions either with or without nitrate, suggesting that the variant is permanently in the inhibitory form and represents a more efficient inhibitor than wild type NreA. The mutation also showed a strong effect on NreB autophosphorylation. NreA(Y95A) led to a total repression of NreB phosphorylation under aerobic and anaerobic conditions. This repression was not relieved in the presence of nitrate. Thus, the *in vivo* and *in vitro* data correspond to

each other. The reason for the strong effect of this mutation can be explained on a structural basis. The structurally stable NreA(Y95A) mutation exhibits a leaky nitrate binding pocket (Niemann *et al.*, 2013) making it impossible for NreA to bind nitrate and to switch to its inactive conformation. This makes NreA(Y95A) a permanent inhibitor of NreB.

It was also intended to test other NreA mutants in the *in vitro* phosphorylation assay. Mutants which showed interesting phenotypes as shown in Niemann *et al*., 2013 were chosen for mutagenesis like W45A and L67N. The residues are part of the binding pocket of NreA and contribute to nitrate binding. Mutations like F28A and E101Q which are more distant from the binding pocket and also showed interesting phenotypes (Koch-Singenstreu, 2013) were chosen for mutagenesis as well. Isolation of these variants was, however, not possible or the concentration and purity was too low. Melting points of different NreA variants have shown reduced protein stability like NreA(W45F) (Niemann *et al*., 2013) which complicates isolation of the protein. The melting temperature for NreA(Y95A) was only slightly reduced from 50 to 49.2 °C (Niemann *et al*., 2013) which shows that the mutation Y95A did not significantly affect protein stability and allow isolation of NreA(Y95A).

5.5 NreA is an inhibitor of NreB autophosphorylation

According to the phosphorylation experiments NreA has a negative effect on NreB autophosphorylation. In the beginning, it was not clear, whether the decreased phosphorylation was due to an inhibition of the kinase activity, or due to a competition between NreA dephosphorylation and NreB autophosphorylation with residual ATP. For differentiation of both possibilities residual ATP was removed to prevent NreB rephosphorylation after the supposed dephosphorylation. The removal of residual ATP was performed by reaction with glucose and hexokinase or by removal via gel filtration chromatography. By both approaches, a constant phosphorylation state of NreB-P was achieved when NreB-P was incubated with NreA and NreA (Y95A) either with or without nitrate.

For NreA(Y95A) a strong phosphatase activity would be required to explain the complete inhibition of NreB phosphorylation. The results of the experiments show that the function of NreA cannot be explained by NreA being a phosphatase. Therefore, the effect of NreA on NreB has to be due to an inhibition of the kinase. The strong NreA and NreB interaction is also compatible with the proposed func-

tion of NreA as an inhibitor of the kinase. Proteins with PAS domains often use co-sensors or co-activators to enable signal integration and merging (Razeto *et al.*, 2004; Partch and Gardner, 2010; Witan *et al.*, 2012). NreB and NreA possibly represent a further example for a PAS/GAF domain interaction.

5.6 NreA and NreB physically interact

The *in vivo* and *in vitro* experiments coincidently show that NreA interacts physically and functionally with NreB in a nitrate dependent manner. The physical interaction became evident from the co-immunoprecipitation analysis where NreA binds to His_6-NreB and co-precipitates. A cross linker, which is used for the detection of weak or transient interactions was not necessary. This indicates a strong and significant NreA-NreB interaction that is stronger than anticipated. The components of the Nre system interacted also *in vivo* when the BACTH bacterial two hybrid system (Karimova *et al*., 1998; 2005) was used. NreA, NreB, and NreC were fused to the T25 and T18 domains of the adenylate cyclase, and interaction of the proteins was tested pairwise by their ability to reconstitute active adenylate cyclase from the fusion proteins in *E. coli*. The response of the NreA and NreB pair suggested NreA/NreB interaction that was decreased, to a large extent in the presence of nitrate (Koch-Singenstreu, 2013; Nilkens *et al*., 2013). This is consistent with the *in vivo* regulation experiment with *narG-lip*, where in the presence of nitrate maximal expression is observed.

The BACTH analysis also showed a strong nitrate independent interaction with NreB and NreC which is coherent with a phosphotransfer from sensor histidine kinase to the response regulator. On the other hand, there was no interaction between NreA and NreC, indicating that NreA transmits the nitrate state exclusively to NreB.

5.7 Aerobic NreB shows phosphorylation activity that is affected by NreA

The sensor histidine kinase NreB is inactivated under aerobic conditions. The presence of oxygen leads to a degradation of the $[4Fe\text{-}4S]^{2+}$ cluster to a $[2Fe\text{-}2S]^{2+}$ cluster which leads to an inactivation of NreB. Further oxygen exposure leads to a full degradation of the cluster and the formation of apo-NreB (Müllner *et al*., 2008).

Surprisingly, 'aerobic' NreB, that is NreB which is prepared in the presence of oxygen, showed an autophosphorylation activity which is lower than the activity of an-

aerobic $[4Fe\text{-}4S]^{2+}$·NreB but still significant. It turns out that NreA shows the same inhibitory effect on aerobic NreB as on anaerobic NreB, leading to a reduced kinase activity. This inhibition is relieved by nitrate (NreA·$[NO_3^-]$) whereas the variant NreA(Y95A) showed a strong nitrate independent inhibition. Since 'aerobic' NreB does not bind an iron-sulfur cluster, it can be excluded that the inhibitory effect of NreA on NreB autophosphorylation is a consequence of the state or presence of an iron-sulfur cluster. Therefore, NreA controls the kinase activity in a different way.

Analysis of *narG-lip* expression in the *S. carnosus* containing wild type *nreABC* under aerobic conditions always showed a small but significant nitrate effect, which is lost by deletion of *nreABC*. This indicates that a low expression of *nreABC*-operon is still performed under aerobic conditions. The *nreABC*-operon is presumably constitutively expressed since the promoter of *S. aureus* resembles a σ^A-promoter (Schlag *et al*., 2008) and an *nreA-lip* expression study has shown *nreA* expression in *S. carnosus* under aerobic conditions (Handel, 2013). Therefore, it is likely that regulation by NreABC is to a small extend also performed under aerobic conditions, also because aerobic NreB shows phosphorylation activity. Surprisingly, a deletion of *nreA* showed that there is not only a loss of nitrate effect but also a high *narG* expression in the presence of oxygen.

The low *narG* expression under aerobic conditions in the presence of NreA could be a consequence of a low nitrate concentration in the cell. *narT* expression is reduced under aerobic conditions (Kretzschmar, 2013). It has been shown for different bacterial organisms that nitrate transport is inactivated by oxygen (Denis *et al*., 1990; Hernandez *et al*., 1991; Sohaskey 2005). An inactivation of nitrate transport by NarT could lead to a situation of no nitrate in the cell. Then NreA would permanently inhibit NreB. When NreA is deleted a repression by NreA is no longer possible which could be the reason for this high *narG* expression in presence of oxygen.

Another explanation for the strong difference in aerobic *narG* expression between the wild type and the Δ*nreA*-mutant could be due to a loss of putative regulatory elements of NreB by the deletion of *nreA*. With the deletion of *nreA*, *nreB* is put under the control of the *nreA* promoter. It has not been confirmed to date if expression of *nreB* is solely dependent on the *nreA* promoter or if there are additional regulatory sequences. It is possible for cis-regulatory elements to reside within

the translated region of the preceding gene (Pérez-Roger *et al*., 1991; Mitra *et al*., 2005). This *nreA* deletion could lead to a higher expression of *nreB* and *nreC* which would lead to a stronger *narG* expression.

A different approach for analyzing aerobic NreB was performed by mutagenesis. It was supposed that mutagenesis of one of the four conserves cysteine residues of NreB leads to transfer of NreB to its aerobic state since the binding of an Fe-S cluster is no longer possible (Kamps *et al*., 2004). The expression of *narG* was strongly reduced under aerobic and anaerobic conditions. The loss of nitrate effect is inconsistent with *narG-lip* expression in the presence of wild type *nreABC* and oxygen. This indicates that the mutation C62S in NreB might have a different effect than transferring NreB into the aerobic state. An additional deletion of *nreA* did not increase *narG-lip* expression like in wild type *S. carnosus* in the presence of oxygen. This also indicates that an insertion of the mutation C62S in NreB does not transfer NreB into the aerobic state. This mutation might destabilize the protein which leads to a loss of functionality.

5.8 Phosphotransfer from NreB to NreC

NreB and NreC form a two-component system and phosphorylation of both proteins was demonstrated (Fedtke *et al*., 2002). NreB slowly autophosphorylates at the conserved histidine residue H159 and the phosphoryl group is transferred to the aspartate residue D53 of NreC. The phosphotransfer is fast and NreB is instantly dephosphorylated leading to an immediate increase in NreC phosphorylation. NreA has no direct effect on phosphotransfer. It only affects NreC phosphorylation by inhibition of NreB. When NreB phosphorylation is decreased by NreA, then subsequently NreC phosphorylation is decreased accordingly. NreC-P is not stable and is rapidly dephosphorylated. Thus, either NreB or NreC has to contain phosphatase activity as well. Both situations have been identified in two-component systems (Stock *et al*., 1989). However, the former situation with NreB presenting a phosphatase is more likely.

NreB presents a histidine kinase of the HisKA_3 subfamily of sensors from two-component systems. The same type of histidine kinase is also found in the nitrate sensor NarX of *E. coli* which is part of the NarXL two-component system. Here a conserved DxxxQ motif was identified inside the dimerization and histidine phosphotransfer (DHp) domain. The motif is positioned adjacent to the phosphor-

accepting histidine residue H399 (Huynh *et al*., 2010). It was shown that glutamine Q404 is necessary for phosphatase activity, but not for autokinase or phosphotransfer activities. Aspartate D400 is important for the autokinase activity of NarX and for phosphatase activity (Huynh *et al*., 2010). Phosphatase functions of most two-component systems are only poorly characterized. In addition, it is often difficult to assign the phosphatase function to conserved protein sequences. For the chemotaxis protein CheZ and for Ras-like GTPases the mechanism for phosphoryl group hydrolysis is documented: The glutamine residue of the active site orients a nucleophilic water molecule for a hydrolysis of the phosphoryl group (Zhao *et al*., 2002; Li *et al*., 2004).

The sequence alignment in Figure 27 of the kinase domains of NarX, NreB homologs from different organisms, and AirS from *S. aureus* (Sun *et al*., 2012) shows high sequence conservation of the DxxxQ motif. This motif is present in NreB from *S. carnosus*, adjacent to the conserved histidine residue H159. It is also found in the kinase domains of the NreB homolog from *Bacillus subtilis*, in the NreB homolog from *Lactobacillus plantarum*, and in AirS from *S. aureus*. The kinases of these proteins are also of the HisKA_3 type.

The presence of the DxxxQ motif in NreB from *S. carnosus* indicates that NreB is not only a kinase but accommodates also the phosphatase function. A phosphatase activity of NreB could explain the rapid NreC dephosphorylation. In two-component systems a phosphatase activity of the sensor histidine kinase leads to a decrease in the number of phosphorylated response regulators which results in a loss of signal. Phosphatase activity can also limit cross-talk from non-related kinases. Cells can set the level of phosphorylated response regulators by regulating the phosphatase and kinase activity of the histidine kinases (Willett and Kirby, 2012). Further tests will show whether the supposed phosphatase activity of NreB is also subject to regulation. Frequently, however, only one of the reactions (ON or OFF) is regulated, whereas the other is constant.

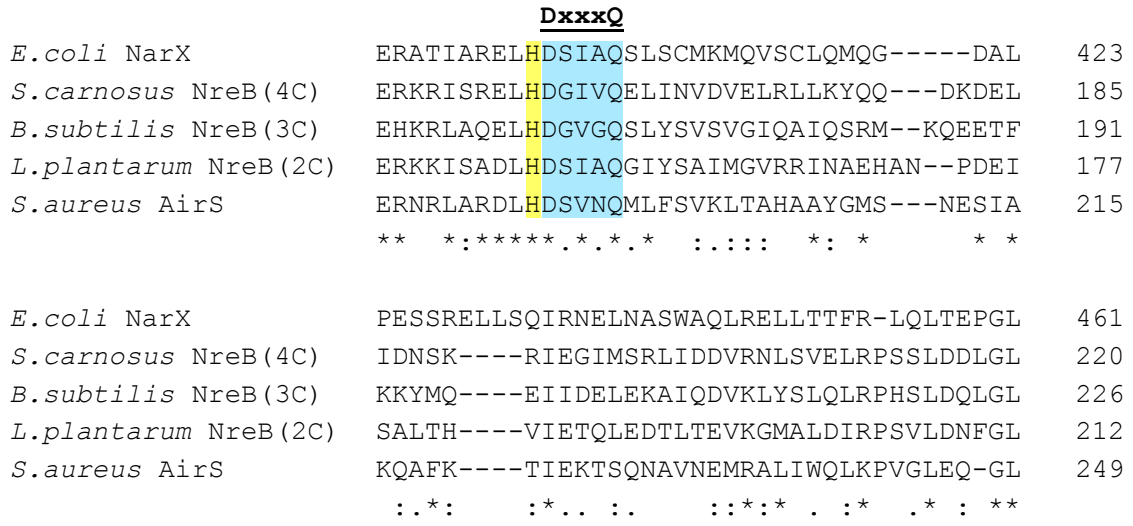

Figure 27: Sequence alignment of the histidine kinase domains of NreB, NarX and AirS shows a DxxxQ motif. The histidine kinase domains of $NreB_{Sca}$ (AA 150-219) and $NarX_{Eco}$ (AA 390-453) are both of the HisKA_3 type. The domains were predicted by a domain database search with InterPro Scan (expasy.org). An alignment of full NreB and NarX amino acid sequences was performed with Clustal Omega. The figure shows the alignment of the histidine kinase domains of NreB and NarX. It shows a high sequence identity of 22/74 (29.7 %), a sequence similarity of 37/74 (50 %), and gaps of 7/74 (9.5 %). The asterisk indicates fully conserved residues, the colon strong and the period weak similar properties. The symbols are only referred to $NarX_{Eco}$ and $NreB_{Sca}$ sequences.
The alignment additionally shows the conserved histidine kinases of NreB of *Bacillus subtilis* and *Lactobacillus plantarum,* and AirS of *Staphylococcus aureus*. $NreB_{Sca}$ features four (4C), $NreB_{Bsu}$ three (3C), and $NreB_{Lpl}$ two (2C) conserved cysteine residues at the sensor domain. The domains show conserved histidine residues (yellow) which in $NreB_{Sca}$ and $NarX_{Eco}$ presents the residue for binding of a phosphoryl group during autophosphorylation. The histidine residue lies adjacent to a conserved DxxxQ motif (blue). It was shown by Huynh *et al*., 2010 that this motif is necessary for phosphatase function of NarX in *E. coli*.

5.9 A model for an NreA/NreB sensor complex that controls *narG* in response to O_2 and NO_3^-

NreA presents a nitrate receptor that binds one molecule of nitrate (Niemann *et al*., 2013) and is necessary for nitrate sensing. NreA interacts with NreB and modulates the kinase activity of anaerobic, active NreB (Müllner *et al.*, 2008; Kamps *et al.*, 2004), by inhibiting the kinase activity of NreB in the absence of nitrate. The following model, depicted in Figure 28, for the function of NreA in nitrate sensing arises.

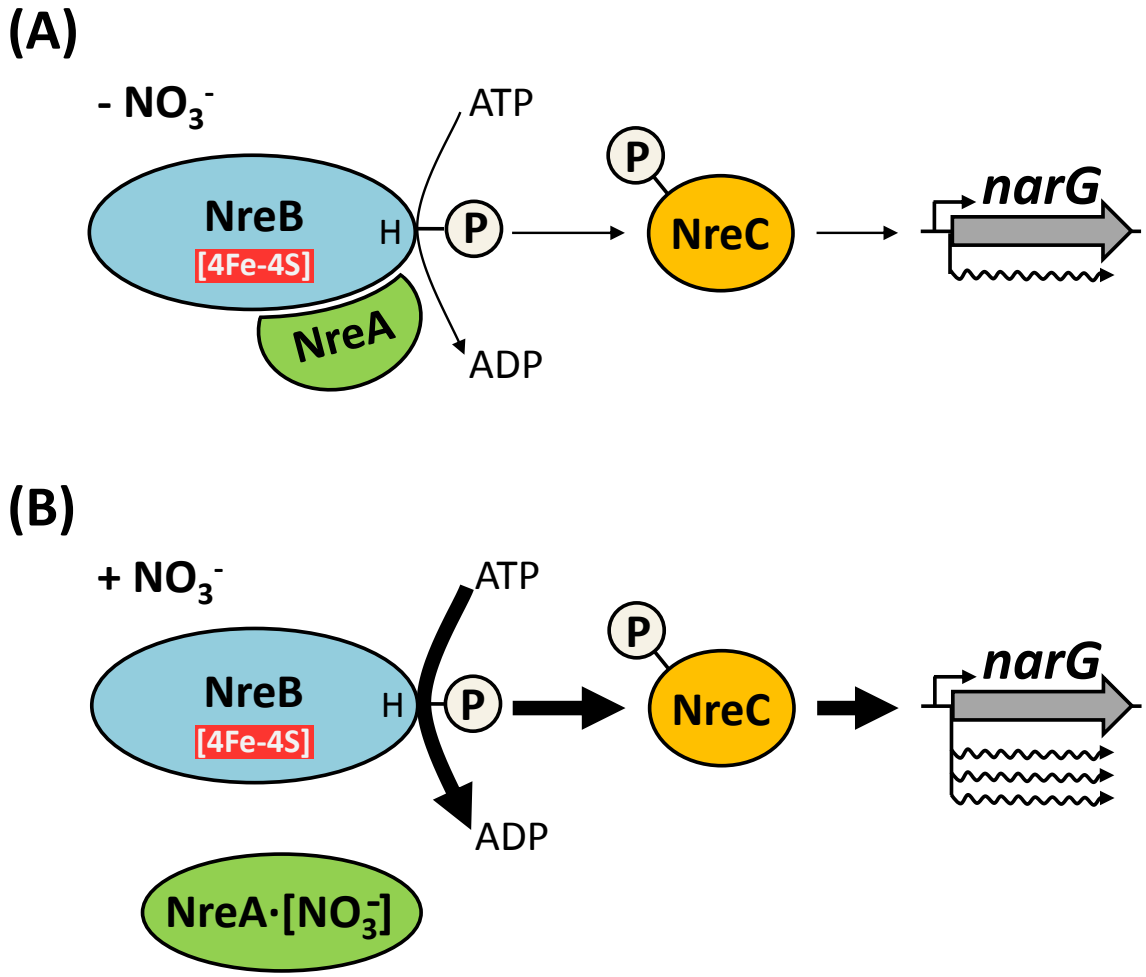

Figure 28: Model for the function of NreA and NreA·[NO_3^-] in regulation of *narG* expression under anaerobic conditions. When no nitrate is present, NreA binds to NreB and inhibits NreB autophosphorylation. This leads to a decreased phosphorylation of the response regulator NreC and, consequently, to a decreased *narG* expression. When nitrate is present NreA binds nitrate in the binding pocket of the GAF domain and NreA·[NO_3^-] is formed. The binding of nitrate decreases interaction of NreA with NreB and the inhibitory effect of NreA is lost. Consequently, NreB shows full autophosphorylation activity which leads to a strong *narG* expression. NreA and NreB form a sensor complex for response to O_2 and NO_3^-.

Under anaerobic conditions NreB is fully activated by binding of a [4Fe-4S] $^{2+}$ cluster. This leads to autophosphorylation activity at the kinase domain where H159 is phosphorylated. The phosphate residue is transferred to aspartate D53 of the response regulator NreC. In the absence of nitrate (Fig. 28A) NreA binds to NreB and inhibits NreB kinase activity, although NreB is in the active ([4Fe4S]$^{2+}$ containing) conformation. In this study this situation is characterized experimentally by NreA/NreB co-immunoprecipitation, *in vivo narG* expression measurements and

by the inhibition of NreB autophosphorylation *in vitro*. This suggests the formation of an NreA/NreB sensor complex.

In the presence of nitrate the NreA·[NO_3^-] complex is formed (Niemann *et al.*, 2013) (Fig. 28B). NreA·[NO_3^-] no longer inhibits NreB kinase activity and shows decreased interaction with NreB. *In vivo* in absence of oxygen and presence of nitrate maximal expression of the *narG-lip* reporter is observed. When *nreA* is deleted similar results are obtained: By deletion of *nreA* the inhibiting effect of NreA is missing and increased expression of *narG-lip* is observed. *narG-lip* is then expressed even under aerobic conditions where NreB is mostly inactive (Müllner *et al.,* 2008). The phosphorylation of 'aerobic' NreB is decreased by NreA in a similar way as anaerobic NreB which was shown experimentally *in vitro*. This indicates that NreA does not influence the iron-sulfur cluster integration of NreB, but controls the kinase activity in different mode.

5.10 NreABC from *S. carnosus* compared to NarXL and FNR from *E. coli*

Regulation by nitrate and oxygen in *S. carnosus* differs fundamentally from NarXL and FNR containing bacteria like *E. coli*. *S. aureus* and *S. carnosus* encode neither homologs of the nitrate sensor NarX known from *E. coli* (Williams and Stewart, 1997), nor of the periplasmic nitrate binding protein NrtA from *Synechocystis sp.* (Koropatkin *et al.*, 2006), or of the nitrate responsive RNA binding NasR, functioning as a translational regulator (Boudes *et al.*, 2012).

In *E. coli narG* expression is performed by two independent systems. The NarXL two-component system responds to nitrate availability and the one-component system FNR responds to the presence of oxygen. The promoter of $narG_{Eco}$ features binding sites for the regulators NarL and FNR and both systems detect and transmit the signals independently to the target gene. On the other hand NreABC presents a system that combines nitrate and oxygen sensing. It contains the oxygen sensor NreB, and the nitrate receptor NreA that modulates the function of NreB in response to nitrate. NreA is not able to regulate *narG* expression or NreC phosphorylation directly. Co-sensing by NreA/NreB of nitrate and oxygen integrates the presence of two biochemically different stimuli. A coordinated regulation of expression often results in an efficient, hierarchical control of aerobic and anaerobic respiration or fermentation (Gunsalus, 1992; Unden *et al*., 1997). In *S. carnosus* this coordinated regulation by NreABC results in an efficient regulation of

nitrate respiratory genes where a joint signal by phosphorylated NreC is derived from the two biochemically different stimuli nitrate and oxygen.

5.11 Outlook on further research on the NreABC system

This study shows that NreA is necessary for nitrate sensing in *S. carnosus* and that NreA modulates NreB phosphorylation according to the presence of nitrate. However, the exact location of interaction between NreA and NreB on a molecular level has not yet been identified. Future experiments will have to characterize the NreB/NreA interaction in detail in order to understand the mode of interaction and regulation on a molecular level. It has to be characterized and verified directly that NreA controls the kinase rather than the phosphatase activity of NreB and what the molecular basis for this regulation is. In addition, identification of the putative NreC-phosphatase domain in NreB will allow characterization of this activity and of its regulation. It will also be important to identify the mechanism for NreA activation and deactivation by nitrate. Comparisons between NreA structures with and without bound nitrate could give an insight on how nitrate effects NreA conformation. However, a nitrate-less NreA structure has yet to be solved.

Another approach for research is the search for NreABC homologs in other bacterial species. The homolactic fermentative *Lactobacillus plantarum* is an organism that features the NreABC system with an NreB-like protein that exhibits only two conserved cysteine residues instead of four (Unden *et al*., 2013). It would be interesting to identify if $NreB_{Lpl}$ also serves as a sensor for oxygen and if oxygen sensing is mediated by an Fe-S cluster or by a disulfide bond. *L. plantarum* also encodes NreA in the *nreABC* gene cluster. Since *L. plantarum* also contains genes for nitrate respiration, NreA is here probably correlated with nitrate metabolism as well.

6. References

Anantharaman, V., Koonin, E.V., and Aravind, L. (2001) Regulatory potential, phyletic distribution and evolution of ancient, intracellular small-molecule-binding domains. *J Mol Biol* **307**: 1271-92.

Aravind, L., and Ponting, C.P. (1997) The GAF domain: an evolutionary link between diverse phototransducing proteins. *Trends Biochem Sci* **22**: 458-459.

Ayora, S., Lindgren, P.E., and Götz, F. (1994) Biochemical properties of a novel metalloprotease from *Staphylococcus hyicus* subsp. *hyicus* involved in extracellular lipase processing. *J Bacteriol* **176**: 3218-3223.

Baikalov, I., Schröder, I., Kaczor-Grzeskowiak, M., Grzeskowiak, K., Gunsalus, R.P., and Dickerson, R.E. (1996) Structure of the *Escherichia coli* response regulator NarL. *Biochemistry* **35**: 11053-11061.

Beinert, H. (1983) Semi-micro method for analysis of labile sulfide and of labile sulfide plus sulfane sulfur in unusually stable iron-sulfur proteins. *Anal Biochem* **131**: 373-378.

Bertani, G. (1951) Studies on lysogenesis. I. The mode of phage liberation by lysogenic *Escherichia coli*. *J Bacteriol* **62**: 293-300.

Birck, C., Mourey, L., Gouet, P., Fabry, B., Schumacher, J., Rousseau, P., Kahn, D., and Samama, J.P. (1999) Conformational changes induced by phosphorylation of the FixJ receiver domain. *Structure* **7**: 1505-1515.

Blasco, F., Iobbi, C., Giordano, G., Chippaux, M., and Bonnefoy, V. (1989) Nitrate reductase of *Escherichia coli*: completion of the nucleotide sequence of the *nar* operon and reassessment of the role of the alpha and beta subunits in iron binding and electron transfer. *Mol Gen Genet* **218**: 249-256.

Blasco, F., Iobbi, C., Ratouchniak, J., Bonnefoy, V., and Chippaux, M. (1990) Nitrate reductases of *Escherichia coli:* sequence of the second nitrate reductase and comparison with that encoded by the *narGHJI* operon. *Mol Gen Genet* **222**: 104-111.

Blasco, F., Pommier, J., Augier, V., Chippaux, M., and Giordano, G. (1992) Involvement of the *narJ* or *narW* gene product in the formation of active nitrate reductase in *Escherichia coli*. *Mol Microbiol* **6**: 221-230.

Boudes, M., Lazar, N., Graille, M., Durand, D., Gaidenko, T.A., Stewart, V., and van Tilbeurgh, H. (2012) The structure of the NasR transcription antiterminator reveals a one-component system with a NIT nitrate receptor coupled to an ANTAR RNA-binding effector. *Mol Microbiol* **85**: 431-444.

Bradford, M.M. (1976) A rapid sensitive method for the quantitation of microgram quantities of protein utilizing the principle of protein-dye binding. *Anal Biochem* **72**: 248-254.

Browning, D.F., Cole, J.A., and Busby, S.J. (2000) Suppression of FNR-dependent transcription activation at the *Escherichia coli nir* promoter by Fis, IHF and

H-NS: modulation of transcription initiation by a complex nucleo-protein assembly. *Mol Microbiol* **37**: 1258-1269.

Brückner, R. (1992) A series of shuttle vectors for *Bacillus subtilis* and *Escherichia coli*. *Gene* **122**: 187-192.

Cavicchioli, R., Schröder, I., Constanti, M., and Gunsalus, R.P. (1995) The NarX and NarQ sensor-transmitter proteins of *Escherichia coli* each require two conserved histidines for nitrate-dependent signal transduction to NarL. *J Bacteriol* **177**: 2416-2424.

Cheung, J., and Hendrickson, W.A. (2009) Structural analysis of ligand stimulation of the histidine kinase NarX. *Structure* **17**: 190-201.

Chomczynski, P., and Sacchi, N. (1987) Single-step method of RNA isolation by acid guanidinium thiocyanate-phenol-chloroform extraction. *Anal. Biochem* **162**: 156-159.

Darwin, A.J., Li, J., and Stewart, V. (1996) Analysis of nitrate regulatory protein NarL-binding sites in the *fdnG* and *narG* operon control regions of *Escherichia coli* K-12. *Mol Microbiol* **20**: 621-632.

Deane-Drummond, C.E., and Glass, A.D. (1982) Nitrate Uptake into Barley (*Hordeum vulgare*) Plants: A New Approach Using $^{36}ClO_3^-$ as an Analog for NO_3^-. *Plant Physiol* **70**: 50-54.

Denis, K.S., Dias, F.M., and Rowe, J.J. (1990) Oxygen regulation of nitrate transport by diversion of electron flow in *Escherichia coli*. *J Biol Chem* **265**: 18095-18097.

Dower, W.J., Miller, J.F., and Ragsdale, C.W. (1988) High efficiency transformation of *E. coli* by high voltage electroporation. *Nucleic Acids Res* **16**: 6127-6145.

Drouault, S., Corthier, G., Ehrlich, S.D., and Renault, P. (2000) Expression of the *Staphylococcus hyicus* lipase in *Lactococcus lactis*. *Appl Environ Microbiol* **66**: 588-598.

Farinha, M.A., and Kropinski A.M. (1990) High efficiency electroporation of *Pseudomonas aeruginosa* using frozen cell suspensions. *FEMS Microbiol Lett* **58**: 221-225.

Fedtke, I., Kamps, A., Krismer, B., and Götz, F. (2002) The nitrate reductase and nitrite reductase operons and the *narT* gene of *Staphylococcus carnosus* are positively controlled by the novel two-component system NreBC. *J Bacteriol* **184**: 6624-6634.

Fish, W.W. (1988) Rapid colometric micromethod for the quantitation of complexed iron in biological samples. *Methods Enzymol* **158**: 357-364.

Gao, R., Mukhopadhyay, A., Fang, F., and Lynn, D.G. (2006) Constitutive activation of two-component response regulators: characterization of VirG activation in *Agrobacterium tumefaciens*. *J Bacteriol* **188**: 5204-5211.

Georgellis, D., Kwon, O., and Lin, E.C. (2001) Quinones as the redox signal for the *arc* two-component system of bacteria. *Science* **292**: 2314-2316.

Götz, F., and Schumacher, B. (1987) Improvements of protoplast transformation in *Staphylococcus carnosus*. *FEMS Microbiol Lett* **40**: 285-288.

Green, J., and Guest, J.R. (1993) Activation of FNR-dependent transcription by iron: an *in vitro* switch for FNR. *FEMS Microbiol Lett* **113**: 219-222.

Green, J., and Paget, M.S. (2004) Bacterial redox sensors. *Nat Rev Microbiol* **2**: 954-966.

Green, J., Bennett, B., Jordan, P., Ralph, E.T., Thomson, A.J., and Guest, J.R. (1996) Reconstitution of the [4Fe-4S] cluster in FNR and demonstration of the aerobic-anaerobic transcription switch *in vitro*. *Biochem J* **316**: 887-892.

Green, J., Trageser, M., Six, S., Unden, G., and Guest, J.R. (1991) Characterization of the FNR protein of *Escherichia coli*, an iron-binding transcriptional regulator. *Proc Biol Sci* **244**: 137-144.

Gunsalus, R.P. (1992) Control of electron flow in *Escherichia coli*: coordinated transcription of respiratory pathway genes. *J Bacteriol* **174**: 7069-7074.

Gunsalus, R.P., and Park, S.J. (1994) Aerobic-anaerobic gene regulation in *Escherichia coli*: control by the ArcAB and Fnr regulons. *Res Microbiol* **145**: 437-450.

Hammes, W.P. (2012) Metabolism of nitrate in fermented meats: the characteristic feature of a specific group of fermented foods. *Food Microbiol* **29**: 151-156.

Hanahan, D. (1983) Studies on transformation of *Escherichia coli* with plasmids. *J Mol Biol* **166**, 557-580.

Handel, S. (2013) Das Dreikomponentensystem NreABC - Dimerisierungs und Expressionstudien an *Staphylococcus carnosus* NreA sowie Characterisierung NreBC haltiger Firmicutes. Diplomarbeit am Institut für Mikrobiologie und Weinforschung, Johannes Gutenberg-Universität Mainz.

Hernandez, D., Dias, F.M., and Rowe, J.J. (1991) Nitrate transport and its regulation by O_2 in *Pseudomonas aeruginosa*. *Arch Biochem Biophys* **286**: 159-163.

Ho, Y.S., Burden, L.M., Hurley, J.H. (2000) Structure of the GAF domain, a ubiquitous signaling motif and a new class of cyclic GMP receptor. *EMBO J.* **19**: 5288-5299

Huynh, T.N., Noriega, C.E., and Stewart, V. (2010) Conserved mechanism for sensor phosphatase control of two-component signaling revealed in the nitrate sensor NarX. *Proc Natl Acad Sci U S A* **107**: 21140-21145.

Jordan, P.A., Thomson, A.J., Ralph, E.T., Guest, J.R., and Green, J. (1997) FNR is a direct oxygen sensor having a biphasic response curve. *FEBS Lett* **416**: 349-352.

Kalman, L.V., and Gunsalus, R.P. (1989) Identification of a second gene involved in global regulation of fumarate reductase and other nitrate-controlled genes for anaerobic respiration in *Escherichia coli*. *J Bacteriol* **171**: 3810-3816

Kamps, A., Achebach, S., Fedtke, I., Unden, G., and Götz, F. (2004) Staphylococcal NreB: an O_2-sensing histidine protein kinase with an O_2-labile iron-sulphur cluster of the FNR type. *Mol Microbiol* **52**: 713-723.

Karimova, G., Pidoux, J., Ullmann, A., and Ladant, D. (1998) A bacterial two-hybrid system based on a reconstituted signal transduction pathway. *Proc Natl Acad Sci U S A* **95**: 5752-5756.

Karimova, G., Dautin, N., and Ladant, D. (2005) Interaction network among *Escherichia coli* membrane proteins involved in cell division as revealed by bacterial two-hybrid analysis. *J Bactoriol* **187**: 2233-2243.

Khoroshilova, N., Popescu, C., Münck, E., Beinert, H., and Kiley, P.J. (1997) Iron-sulfur cluster disassembly in the FNR protein of *Escherichia coli* by O_2: [4Fe-4S] to [2Fe-2S] conversion with loss of biological activity. *Proc Natl Acad Sci U S A* **94**: 6087-6092.

Kiley, P.J., and Beinert, H. (1998) Oxygen sensing by the global regulator, FNR: the role of the iron-sulfur cluster. *FEMS Microbiol Rev* **22**: 341-352.

King, T:E., and Morris, R.O. (1967) Determination of acid-labile sulfide and sulfhydryl groups. *Methods Enzymol* **10**: 634-641.

Koch-Singenstreu, M. (2013) Dissertation am Institut für Mikrobiologie und Weinforschung, Johannes Gutenberg-Universität Mainz.

Koropatkin, N.M., Pakrasi, H.B., and Smith, T.J. (2006) Atomic structure of a nitrate-binding protein crucial for photosynthetic productivity. *Proc Natl Acad Sci U S A* **103**: 9820-9825.

Krell, T., Lacal, J., Busch, A., Silva-Jiménez, H., Guazzaroni, M.E., and Ramos, J.L. (2010) Bacterial sensor kinases: diversity in the recognition of environmental signals. *Annu Rev Microbiol* **64**: 539-559.

Kretzschmar, A.-K. (2013) Regulation des Nitrattransporters under der Nitratreduktase von *Staphylococcus carnosus* durch NreBC in Abhängigkeit von Sauerstoff und Nitrat. Masterarbeit am Institut für Mikrobiologie und Weinforschung, Johannes Gutenberg-Universität Mainz.

Kucera, I. (2006) Interference of chlorate and chlorite with nitrate reduction in resting cells of *Paracoccus denitrificans*. *Microbiology* **152**: 3529-3534.

Laemmli, U.K. (1970) Cleavage of structural proteins during the assembly of the head of bacteriophage T4. *Nature* **227**: 680-685.

Lamberg, K.E., and Kiley, P.J. (2000) FNR-dependent activation of the class II *dmsA* and *narG* promoters of *Escherichia coli* requires FNR-activating regions 1 and 3. *Mol Microbiol* **38**: 817-827.

Lazazzera, B.A., Beinert, H., Khoroshilova, N., Kennedy, M.C., and Kiley, P.J. (1996) DNA binding and dimerization of the Fe-S-containing FNR protein from *Escherichia coli* are regulated by oxygen. *J Biol Chem* **271**: 2762-2768.

Li, G., and Zhang, X.C. (2004) GTP hydrolysis mechanism of Ras-like GTPases. *J Mol Biol* **340**: 921-932.

Löfblom, J., Kronqvist, N., Uhlén, M., Ståhl, S., and Wernérus, H. (2007) Optimization of electroporation-mediated transformation: *Staphylococcus carnosus* as model organism. *J Appl Microbiol* **102**: 736-747.

Martinez, S.E., Beavo, J.A., and Hol, W.G. (2002) GAF domains: two-billion-year-old molecular switches that bind cyclic nucleotides. *Mol Interv* **2**: 317-23.

Mascher, T., Helmann, J.D., and Unden, G. (2006) Stimulus perception in bacterial signal-transducing histidine kinases. *Microbiol Mol Biol Rev* **70**: 910-938.

McLaughlin, K.J., Strain-Damerell, C.M., Xie, K., Brekasis, D., Soares, A.S., Pa-

get, M.S., and Kielkopf, C.L. (2010) Structural basis for NADH/NAD^+ redox sensing by a Rex family repressor. *Mol Cell* **38**: 563-575.

Melville, S.B., and Gunsalus, R.P. (1990) Mutations in *fnr* that alter anaerobic regulation of electron transport-associated genes in *Escherichia coli*. *J Biol Chem* **265**: 18733-18736.

Melville, S.B., Gunsalus, R.P. (1996) Isolation of an oxygen-sensitive FNR protein of *Escherichia coli*: interaction at activator and repressor sites of FNR-controlled genes. *Proc Natl Acad Sci U S A* **93**: 1226-1231.

Meng, W., Green, J., and Guest, J.R. (1997) FNR-dependent repression of *ndh* gene expression requires two upstream FNR-binging sites. *Microbiology* **143**: 1521-1532.

Mitra, R., Das, H.K., and Dixit, A. (2005) Identification of a positive transcription regulatory element within the coding region of the *nifLA* operon in *Azotobacter vinelandii*. *Appl Environ Microbiol* **71**: 3716-3724.

Müllner, M. (2008) Biochemische Charakterisierung des O_2-Sensors NreB aus *Staphylococcus carnosus*. Dissertation am Institut für Mikrobiologie und Weinforschung, Johannes Gutenberg-Universität Mainz.

Müllner, M., Hammel, O., Mienert, B., Schlag, S., Bill, E., and Unden, G. (2008) A PAS domain with an oxygen labile $[4Fe\text{-}4S]^{2+}$ cluster in the oxygen sensor kinase NreB of *Staphylococcus carnosus*. *Biochemistry* **47**: 13921-13932.

Neubauer, H, and Götz, F. (1996) Physiology and interaction of nitrate and nitrite reduction in *Staphylococcus carnosus*. *J Bacteriol* **178**: 2005-2009.

Niemann, V., Koch-Singenstreu, M., Nilkens, S., Götz, F., Unden, G., and Stehle, T. (2013) The NreA protein functions as a nitrate receptor in the staphylococcal nitrate regulation system. (Submitted to *Journal of Molecular Biology*, 09/2013)

Nilkens, S., Koch-Singenstreu, M., Niemann, V., Götz, F., Stehle, T., Unden, G. (2013) Nitrate/oxygen co-sensing by an NreA/NreB sensor complex of *Staphylococcus carnosus*. (Submitted to *Molecular Microbiology*, 09/2013)

Pantel, I., Lindgren, P.E., Neubauer, H., and Götz, F. (1998) Identification and characterization of the *Staphylococcus carnosus* nitrate reductase operon. *Mol Gen Genet* **259**: 105-114.

Partch, C.L., and Gardner, K.H. (2010) Coactivator recruitment: a new role for PAS domains in transcriptional regulation by the bHLH-PAS family. *J Cell Physiol* **223**: 553-557.

Pérez-Roger, I., García-Sogo, M., Navarro-Aviñó, J.P., López-Acedo, C., Macián, F., and Armengod, M.E. (1991) Positive and negative regulatory elements in the *dnaA-dnaN-recF* operon of *Escherichia coli*. *Biochimie* **73**: 329-334.

Peschel, A., Augustin, J., Kupke, T., Stevanovic, S., and Götz, F. (1993) Regulation of epidermin biosynthetic genes by EpiQ. *Mol Microbiol* **9**: 31-39.

Ponting, C.P., and Aravind, L. (1997) PAS: a multifunctional domain family comes to light. *Curr Biol* **7**: 674-677.

Rabin, R.S., and Stewart, V. (1993) Dual response regulators (NarL and NarP) interact with dual sensors (NarX and NarQ) to control nitrate- and nitrite-

regulated gene expression in *Escherichia coli* K-12. *J Bacteriol* **175**: 3259-3268.

Razeto, A., Ramakrishnan. V., Litterst, C.M., Giller, K., Griesinger, C., Carlomagno, T., Lakomek, N., Heimburg, T., Lodrini, M., Pfitzner, E., and Becker, S. (2004) Structure of the NCoA-1/SRC-1 PAS-B domain bound to the LXXLL motif of the STAT6 transactivation domain. *J Mol Biol* **336**: 319-329.

Reddy, D., Lancaster, J.R. Jr, and Cornforth, D.P. (1983) Nitrite inhibition of *Clostridium botulinum*: electron spin resonance detection of iron-nitric oxide complexes. *Science* **221**: 769-770.

Reinhart, F. (2010) The Oxygen Sensors FNR from Escherichia coli and NreABC from Staphylococcus carnosus. Dissertation am Institut für Mikrobiologie und Weinforschung, Johannes Gutenberg-Universität Mainz.

Reinhart, F., Huber, A., Thiele, R., and Unden, G. (2010) Response of the oxygen sensor NreB to air *in vivo*: Fe-S-containing NreB and apo-NreB in aerobically and anaerobically growing *Staphylococcus carnosus*. *J Bacteriol* **192**: 86-93.

Rosenstein, R., Nerz, C., Biswas, L., Resch, A., Raddatz, G., Schuster, S.C., and Götz, F. (2009) Genome analysis of the meat starter culture bacterium *Staphylococcus carnosus* TM300. *Appl Environ Microbiol* **75**: 811-822.

Rosenstein, R., Peschel, A., Wieland, B., and Götz, F. (1992) Expression and regulation of the antimonite, arsenite, and arsenate resistance operon of *Staphylococcus xylosus* plasmid pSX267. *J Bacteriol* **174**: 3676-3683.

Sambrook, J., and Russell, D.W. (2001) Molecular Cloning: A Laboratory Manual, 3rd edn, vol. 3. New York: Cold Spring Harbor Laboratory Press.

Sasarman, A., Purvis, P., and Portelance, V. (1974) Role of menaquinone in nitrate respiration in *Staphylococcus aureus*. *J Bacteriol* **117**: 911-913.

Schlag, S. (2008) Dissimilatory nitrate and nitrite reduction in staphylococci: regulation and implication in biofilm formation. Dissertation. Eberhard Karls Universität Tübingen.

Schlag, S., Fuchs, S., Nerz, C., Gaupp, R., Engelmann, S., Liebeke, M., Lalk, M., Hecker, M., and Götz, F. (2008) Characterization of the oxygen-responsive NreABC regulon of *Staphylococcus aureus*. *J Bacteriol* **190**: 7847-7858.

Schleifer, K.H., and Fischer, U. (1982) Description of a new species of the genus *Staphylococcus*: *Staphylococcus carnosus. Int J Syst Evo Microbiol* **32**: 153-156.

Schröder, I., Wolin, C.D., Cavicchioli, R., and Gunsalus, R.P. (1994) Phosphorylation and dephosphorylation of the NarQ, NarX, and NarL proteins of the nitrate-dependent two-component regulatory system of *Eschericha coli*. *J Bacteriol* **176**: 4985-4992.

Schultz, J., Milpetz, F., Bork, P., and Ponting, C.P. (1998) SMART, a simple modular architecture research tool: identification of signaling domains. *Proc Natl Acad Sci U S A* **95**: 5857-5864.

Siegel, L.M. (1965) A Direct Microdetermination for Sulfide. *Anal Biochem* **11**: 126-132.

Six, S., Trageser, M., Kojro, E., Farenholz, F., and Unden, G. (1996) Reactivity of the N-terminal cysteine residues in active and inactive forms of FNR, and O_2-responsive, Fe containing transcriptional regulator of *Escherichia coli*. *J Inorg Biochem* **62**: 89-102.

Sohaskey, C.D. (2005) Regulation of nitrate reductase activity in *Mycobacterium tuberculosis* by oxygen and nitric oxide. *Microbiology* **151**: 3803-3810.

Stewart, V. (1982) Requirement of Fnr and NarL functions for nitrate reductase expression in *Escherichia coli* K-12. *J Bacteriol* **151**: 1320-1325.

Stock, A.M., Robinson, V.L., and Goudreau, P.N. (2000) Two-component signal transduction. *Annu Rev Biochem* **69**: 183-215.

Stock, J.B., Ninfa, A.J., Stock. A.M. (1989) Protein phosphorylation and regulation of adaptive responses in bacteria. *Microbiol Rev* **53**: 450-490.

Stookey, L.L (1970) Ferrozine-a new spectrophotometric reagent for iron. *Anal Chem* **42**: 779-781.

Sun, F., Ji, Q., Jones, M.B., Deng, X., Liang, H., Frank, B., Telser, J., Peterson, S.N., Bae, T., and He, C. (2012) AirSR, a [2Fe-2S] cluster-containing two-component system, mediates global oxygen sensing and redox signaling in *Staphylococcus aureus*. *J Am Chem Soc* **134**: 305-314.

Taylor, B.L., and Zhulin, I.B. (1999) PAS domains: internal sensors of oxygen, redox potential, and light. *Microbiol Mol Biol Rev* **63**: 479-506.

Unden, G., and Schirawski, J. (1997) The oxygen-responsive transcriptional regulator FNR of *Escherichia coli*: the search for signals and reactions. *Mol Microbiol* **25**: 205-210.

Unden, G., Becker, S., Bongaerts, J., Holighaus, G., Schirawski, J., and Six, S. (1995) O_2-sensing and O_2-dependent gene regulation in facultatively anaerobic bacteria. *Arch Microbiol* **164**: 81-90.

Unden, G., Nilkens, S., and Singenstreu, M. (2013) Bacterial sensor kinases using Fe-S cluster binding PAS or GAF domains for O_2 sensing. *Dalton Trans* **42**: 3082-3087.

van Oort, M.G., Deveer, A.M., Dijkman, R., Tjeenk, M.L., Verheij, H.M., de Haas, G.H., Wenzig, E., and Götz, F. (1989) Purification and substrate specificity of *Staphylococcus hyicus* lipase. *Biochemistry* **28**: 9278-9285.

Wieland, K.P., Wieland, B., and Götz, F. (1995) A promoter-screening plasmid and xylose-inducible, glucose-repressible expression vectors for *Staphylococcus carnosus*. *Gene* **158**: 91-96.

Willett, J.W., and Kirby (2012) Genetic and biochemical dissection of a HisKA domain identifies residues required exclusively for kinase and phosphatase activities. *PLoS Genet* **8**: 1003084.

Williams, S.B., and Stewart, V. (1997) Discrimination between structurally related ligands nitrate and nitrite controls autokinase activity of the NarX transmembrane signal transducer of *Escherichia coli* K-12. *Mol Microbiol* **26**: 911-925.

Witan, J., Monzel, C., Scheu, P.D., and Unden, G. (2012) The sensor kinase DcuS of *Escherichia coli*: two stimulus input sites and a merged signal pathway in

the DctA/DcuS sensor unit. *Biol Chem* **393**: 1291-1297.

Wu, H., Tyson, K.L., Cole, J.A., and Busby, S.J. (1998) Regulation of transcription initiation at the *Escherichia coli nir* operon promoter: a new mechanism to account for co-dependence on two transcription factors. *Mol Microbiol* **27**: 493-505.

Yan, M., Yu, C., Yang, J., Ji, Y. (2011) The essential two-component system YhcSR is involved in regulation of the nitrate respiratory pathway of *Staphylococcus aureus*. *J Bacteriol* **193**: 1799-1805.

Yanisch-Perron, C., Vieira, J., and Messing, J. (1985) Improved M13 phage cloning vectors and host strains: nucleotide sequences of the M13mp18 and pUC19 vectors. *Gene* **33**: 103-119.

Zell, C., Resch, M., Rosenstein, R., Albrecht, T., Hertel, C., and Götz, F. (2008) Characterization of toxin production of coagulase-negative staphylococci isolated from food and starter cultures. *Int J Food Microbiol* **127**: 246-251.

Zhao, R., Collins, E.J., Bourret, R.B., Silversmith, R.E. (2002) Structure and catalytic mechanism of the *E. coli* chemotaxis phosphatase Chez. *Nat Struct Biol* **9**: 570-575.

Zhulin, I.B., Taylor, B.L., and Dixon, R. (1997) PAS domain S-boxes in Archaea, Bacteria and sensors for oxygen and redox. *Trends Biochem Sci* **22**: 331-333.

Zoraghi, R., Corbin, J.D., and Francis, S.H. (2004) Properties and functions of GAF domains in cyclic nucleotide phosphodiesterases and other proteins. *Mol Pharmacol* **65**: 267-278.

7. Publications

Papers:

Nilkens, S., Koch-Singenstreu, M., Niemann, V., Götz, F., Unden, G. (2013) Nitrate/oxygen co-sensing by an NreA/NreB sensor complex of *Staphylococcus carnosus*. (Submitted to *Molecular Microbiology* 09/2013; Manuscript in supplement)

The data of the manuscript are predominantly based on this dissertation. The manuscript was essentially written by me, and the parts that are based on my work were, in agreement with my supervisor, adopted for this thesis. This refers to the experimental procedures and the result section.

Niemann, V., Koch-Singenstreu, M., Nilkens, S., Götz, F., Unden, G., Stehle, T. (2013) The NreA protein functions as a nitrate receptor in the staphylococcal nitrate regulation system. (Submitted to *Journal of Molecular Biology* 09/2013)

Unden, G., Nilkens, S., Singenstreu, M. (2013) Bacterial sensor kinases using Fe-S cluster binding PAS or GAF domains for O_2 sensing. *Dalton Trans* **42**: 3082-3087.

Talks:

Nilkens, S., Singenstreu, M., Unden, G. (2011) The NreABC Three-Component System of *Staphylococcus carnosus*. 7th European Workshop on Bacterial Respiratory Chains, Höör, Lund, Sweden

Nilkens, S., Singenstreu, M., Niemann, V., Stehle, T., Götz, F., Unden, G. (2012) The Three Component System NreABC Combines Oxygen and Nitrate Sensing in *Staphylococcus carnosus*. 29. Symposium "Mechanisms of Gen-regulation", Wartaweil, Munich.

Nilkens, S., Singenstreu, M., Unden, G. (2013) Sauerstoffsensoren und Signalverarbeitung in Bakterien. Seminar Advanced Modules „Signalleitung und Transport“ Universität des Saarlandes.

Posters:

Nilkens, S., Singenstreu, M., Reinhart, F., Unden, G. (2010) Response of the tri-component system NreABC of *Staphylococcus carnosus* to oxygen and nitrate. 28. Symposium „Mechanisms of Genregulation", Neustadt an der Weinstraße.

Nilkens, S., Singenstreu, M., Unden, G. (2013) Combined Oxygen and Nitrate Sensing by the *Staphylococcus carnosus* NreAB Sensor Complex. International Conference on Microbiology 2013 (VAAM) Bremen.

8. Danksagung

9. Lebenslauf

10. Erklärung

Hiermit erkläre ich, dass die vorliegende Dissertation von mir selbst verfasst wurde und ich keine anderen als die angegebenen Quellen und Hilfsmittel verwendet habe. Das im Anhang beigefügte Manuskript wurde hauptsächlich von mir verfasst und in Absprache mit meinem Betreuer wurden die Teile, die auf meiner Arbeit basieren, in dieser Dissertation übernommen. Dies bezieht sich auf die Beschreibung der experimentellen Durchführung und auf den Ergebnisteil.

Mainz, September 2013

11. Anhang

11.1 Manuskript: **Nitrate/oxygen co-sensing by an NreA/NreB sensor complex of *Staphylococcus carnosus*.**
(Eingereicht bei Molecular Microbiology 09/2012)